FUNCTIONAL ANALYSIS OF *SOX11* AND *NF1* IN SENSORY NEURON DEVELOPMENT AND PLASTICITY

APPROVED BY SUPERVISORY COMMITTEE

Luis F. Parada Ph.D.	**Advisor**
Stephen C. Cannon M.D., Ph.D.	**Committee Chair**
Jane E. Johnson Ph.D.	
Shuxin Li M.D., Ph.D.	

Dedicated to My Grandma, Shuzhen Chen,
My Parents, Naiwei Shen and Shikai Lin,
My Husband, Chao Zhu
and My Best Friend, Wei Sun

ACKNOWLEDGEMENTS

I would like to give my dearest thanks to my mentor, Dr. Luis Parada, who provides me the opportunity to work in such a great laboratory. When I first joined his lab, I hardly knew anything about biological research. It was his patient guidance which walked me through all the difficulties to become a qualified scientific researcher. His enthusiasm and insight into biology, his broad view of our research field and his kindness towards other people set excellent examples for both my work and life.

Dr. Lei Lei and Dr. Mario Romero are two terrific scientists and collaborators of several experiments in my thesis research. From the very first day I met them, they have been providing me unselfish technical support as well as theoretical guidance. Without their help, I could not be where I am today.

I also want to thank my colleagues and close friends: Dr. Douglas Benson, Jian Chen, Yanjiao Li, Wei Zhang and Dr. Jing Zhou for their helpful discussion and fun in everyday life. It is lucky for me to live and work in such a friendly environment. Sincere thanks will also be given to everybody in Parada lab. The past five years will be the most beautiful memory in my life, wherever I am, whatever I do in the future.

Dr. Stephen Cannon, Dr. Jane Johnson and Dr. Shuxin Li are my thesis committee members. I really appreciate their valuable advice on my projects and thesis.

Special thanks to Dr. Wei Sun, my best friend and teacher in China, who has inspired me every time I was down.

Last but not least, I thank with my dearest love to my family: my grandma, my parents and my husband, who are always with me no matter what happen.

FUNCTIONAL ANALYSIS OF *SOX11* AND *NF1* IN SENSORY NEURON DEVELOPMENT AND PLASTICITY

By

LU LIN

DISSERTATION

Presented to the Faculty of the Graduate School of Biomedical Sciences
The University of Texas Southwestern Medical Center at Dallas
In Partial Fulfillment of the Requirements
For the Degree of

DOCTOR OF PHILOSOPHY

The University of Texas Southwestern Medical Center at Dallas
Dallas, Texas
August, 2008

FUNCTIONAL ANALYSIS OF *SOX11* AND *NF1* IN SENSORY NEURON DEVELOPMENT AND PLASTICITY

Lu Lin Ph.D.

The University of Texas Southwestern Medical Center at Dallas, 2008

Supervising Professor: **Luis F. Parada, Ph.D.**

Development of sensory neurons is controlled by both cell-extrinsic and cell-intrinsic factors. The transcription factor Sox11 is abundantly expressed in embryonic sensory neurons. In the first part of this thesis, by using a *Sox11*-/- mouse model, I show that the loss of *Sox11* results in increased cell death in embryonic sensory ganglia, which leads to a significant neuronal loss around birth. The ablation of *Sox11* also leads to cell-death-independent axonal growth defects both *in vivo* and *in vitro*. Furthermore, I demonstrate that *Sox11*-deficient MEFs exhibit decreased level of phospho-AKT compared to controls. These data suggest that Sox11 is required for multiple key steps of sensory neuron development, probably through regulating the expression of component(s) of the signaling pathways downstream of growth factors.

Adult sensory neurons exhibit various degrees of plasticity following different types of injury. Neurofibromin, the protein encoded by the tumor suppressor gene *Nf1*, functions as a negative regulator of Ras and its two major downstream pathways: MEK-ERK and PI3K-Akt pathway. *Nf1*-/- embryonic sensory neurons survive without neurotrophin support attributed to enhanced PI3K activity in the absence of *Nf1*. In the second part of this thesis, by using mice with *Nf1* specifically deleted in neurons (*Nf1*-SynI-CKO), I demonstrate that *Nf1*-/- adult sensory neurons exhibit enhanced neurite outgrowth *in vitro*. After dorsal root injury, spontaneous functional recovery and increased axonal sprouting from uninjured sensory neurons are observed in *Nf1*-SynI-CKO mice compared to permanent sensory deficits in controls. These appear to be mediated both by cell autonomous capacity of spared *Nf1*-/- DRG neurons and by non-cell autonomous contribution from *Nf1*-/- neurons in the spinal cord, as suggested by

co-culture experiments. To further confirm whether the spinal cord or DRG neurons contribute to functional recovery in *Nf1*-SynI-CKO mice, I generated other mutants with *Nf1* deleted more specifically and completely in DRG (*Nf1*-Isl1-CKO). In the third part of this thesis, I discuss some unanticipated results due to Cre expression in the gastrointestinal tract. *Nf1*-Isl1-CKO mice develop gastric epithelium hyperplasia and inflammation with increased proliferation and apoptosis. These phenotypes seem to be attributed to the loss of *Nf1* in non-gastric epithelial cells.

TABLE OF CONTENTS

List of Publications

1. Lei L, Zhou J, **Lin L**, Parada LF. Brn3a and Klf7 cooperate to control TrkA expression in sensory neurons. Dev Biol. 2006 Dec 15; 300(2):758-69.

2. Romero MI*, **Lin L***, Lush ME, Lei L, Parada LF, Zhu Y. Deletion of Nf1 in neurons induces increased axon collateral branching after dorsal root injury. J Neurosci. 2007 Feb 21; 27(8): 2124-34. (*contributed equally)

3. Chen J, Kwon C, **Lin L**, Li Y, Parada LF. Inducible site-specific recombination in neural stem/progenitor cells. Genesis, in revision.

4. **Lin L**, Wang Y, Wang J, Wegner M, Parada LF, Lei L. Sox11 regulates survival and axon growth of embryonic sensory neurons. In preparation.

5. **Lin L**, Chen J, Parada LF. *Nf1* deficient mice develop gastric hyperplasia. In preparation.

List of Figures

List of Tables

List of Abbreviations

ANOVA	analysis of variance between groups
BAF	BOC-Asp(OMe)-FMK
***Bax*+/-**	*Bax* heterozygous mutant
***Bax*-/-**	*Bax* homozygous mutant
BDNF	brain-derived neurotrophic factor
bHLH	basic helix-loop-helix
BrdU	2-bromo-5'-deoxyuridine
CagA	cytotoxin-associated antigen A
CB	cerebellum
CGRP	calcitonin gene-related peptide
CKO	conditional knockout
CNS	central nervous system
CSPGs	chondroitin sulphate proteoglycans
CTB	cholera toxin β-subunit
CTX	cerebral cortex
DIV	day *in vitro*
DMEM	Dulbecco's Modified Eagle's Medium
DREZ	dorsal root entry zone
DRG	dorsal root ganglia
E12.5	embryonic day 12.5
ERK	extracellular-regulated kinase
FBS	fetal bovine serum
GAP	GTPase-activating protein
GDNF	glial cell line derived neurotrophic factor
GEFs	guanine-nucleotide exchange factors
GI	gastrointestinal
GRD	GAP-related domain

GSK3β	glycogen synthase kinase 3β
HGF	hepatocyte growth factor
HMG	high mobility group
IFP	inflammatory fibroid polyps
IGF-1	insulin-like growth factor-1
IP	intraperitoneally
KitL	Kit ligand
Klf	Kruppel-like zinc finger transcription factor
LCB	lateral cutaneous branch of spinal nerves
MAG	myelin-associated glycoprotein
MAI	myelin-associated inhibitors
MEF	mouse embryonic fibroblast
MEK	mitogen activated protein kinase kinase
NCC	neural crest cell
NGF	nerve growth factor
NFATc1	nuclear factor of activated T cells
NF1	neurofibromatosis type 1
Nf1	neurofibromatosis type 1 gene
***Nf1*+/-**	*Nf1* heterozygous mutant
***Nf1*-/-**	homozygous mutant
***Nf1*-Isl1-CKO**	*Nf1* Islet 1-Cre conditional knockout
***Nf1*-Prph1-CKO**	*Nf1* Peripherin 1-Cre conditional knockout
***Nf1*-SynI-CKO**	*Nf1* Synapsin I-Cre conditional knockout
Ngn1	neurogenin 1
Ngn2	neurogenin 2
NT3	neurotrophin-3
NT4	neurotrophin-4
NTF	neurotrophic factor
OMgp	oligodendrocyte-myelin glycoprotein
ONB	ophthalmic branch of the trigeminal nerve
P0	postnatal day 0

PAS	periodic acid-Schiff
PBS	phosphate-buffered saline
PCNA	proliferating cell nuclear antigen
PFA	paraformaldehyde
PI	propidium iodide
PI3K	phosphatidylinositol-3-kinase
PNS	peripheral nervous system
PTP	protein tyrosine phosphatase
R26;Prph1	Rosa26;Peripherin1-Cre
R26;Isl1	Rosa26;Islet1-Cre
SC	spinal cord
SH2	SRC Homology 2
SHP2	SH2-domain-containing protein tyrosine phosphatase
SMA	smooth muscle actin
SOX	sry-related box
Sox11+/-	mice with one *Sox11* allele replaced by *lacZ*
Sox11-/-	*Sox11* homozygous null mutant
TFF1	trefoil factor 1
TG	trigeminal ganglia
TGFβ	transforming growth factor-beta
Trk	tyrosine receptor kinase
TSG	tumor suppressor gene
WT	wild type

Chapter I

Introduction

I . Development of Neural Crest Cells and Sensory Neurons

Sensory Neurons and Neural Crest Cells

Sensory ganglia are clusters of primary neurons in the peripheral nervous system (PNS), through which sensory information is relayed to the central nervous system (CNS) for further processing. Somatosensory information of trunk and limb areas is transduced to the spinal cord through sensory neurons residing in the dorsal root ganglia (DRG) (Scott, 1992); while sensory information from the face is relayed to the brain stem by sensory neurons located in the trigeminal ganglia (TG) (Waite, 1995).

DRG and some TG neurons are derived from neural crest cells (NCCs) through complicated developmental processes (Marmigere and Ernfors, 2007). As early as E8.5 in mouse, NCCs begin to leave the dorsal neural tube and migrate ventrally to form the DRG (Serbedzija et al., 1990). Neurogenesis in the DRG then happens in three waves, which generate large-diameter mechanoceptive and proprioceptive neurons and subsequently small-diameter nociceptive neurons (Frank and Sanes, 1991; Maro et al., 2004). At a later time point, sensory neuron subtype specification occurs within the sensory ganglia. Different subtypes of sensory neurons express different markers and their projections into the spinal cord are specified (Fig. 1.1). In addition, cell proliferation, cell survival and axonal growth are also important aspects of the developmental processes of sensory neurons. Regulation of these processes by different extrinsic and intrinsic factors is summarized in Table 1.1 and will be discussed in more detail in the following sections.

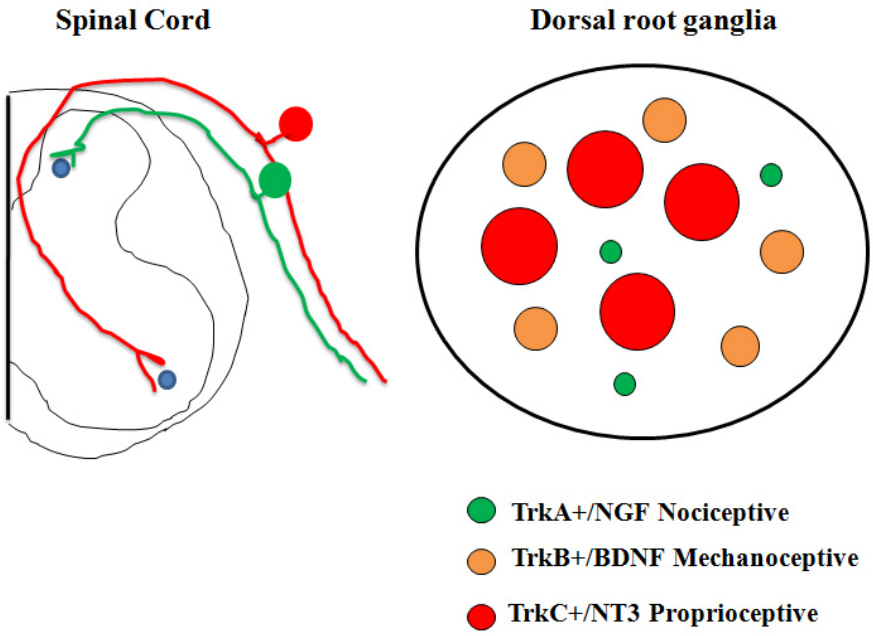

Fig.1.1. Different subtypes of neurons in DRG and their projections into the spinal cord (modified from (Chen et al., 2006a)).

Developmental process	**Genes or Pathways Involved**	
Neurogenesis	*Ngn1, Ngn2, Sox10*	
Neuronal subtype specification	**Nociceptive**	*TrkA, Klf7, Runx1, Brn3a*
	Mechanoceptive	*TrkB, Brn3a*
	Proprioceptive	*TrkC, Runx3, Brn3a*
Survival	*Bax, CREB, TrkA/TrkB/TrkC*, PI3K pathway	
Axonal growth	*Sema3a, NGF/BDNF/NT3, Eph/Ephrin*, PI3K and MAPK pathways	

Table 1.1. Genes and pathways involved in sensory neuron development (summarized from (Marmigere and Ernfors, 2007)).

Neurotrophins and Sensory Neuron Development

Neurotrophic factors and their receptors regulate proliferation, cell fate selection, axonal growth, and survival of sensory neurons (Bibel and Barde, 2000; Huang and Reichardt, 2001; Huang and Reichardt, 2003; Parada et al., 1992). Tyrosine receptor kinases (Trks) are receptors for the nerve growth factor (NGF) family of neurotrophins: TrkA binds NGF, TrkB binds brain-derived neurotrophic factor (BDNF) and neurotrophin-4 (NT4), and TrkC binds neurotrophin-3 (NT3). TrkA, TrkB and TrkC are required for the survival of nociceptive, mechanoreceptive, and proprioceptive sensory neurons, respectively (Huang and Reichardt, 2001). Ret, a member of the receptor complex for glial cell line derived neurotrophic factor (GDNF) family proteins, defines an additional subpopulation of sensory neurons (Baudet et al., 2000; Molliver et al., 1997). Different signaling pathways can be activated by neurotrophins, such as the mitogen activated protein kinase kinase (MEK)-extracellular signal regulated kinase (ERK) pathway and the phosphatidyl inositol 3 kinase (PI3K)-Akt pathway (Huang and Reichardt, 2001; Huang and Reichardt, 2003). Both pharmacological and genetic methods disrupting these pathways revealed their various functions in the developmental process of sensory neurons. For example, the MEK-ERK pathway was shown to be important for NGF-induced neurite outgrowth but not survival of embryonic sensory neurons both *in vitro* and *in vivo* (Markus et al., 2002a; Zhong et al., 2007); while the PI3K-Akt pathway is necessary for both survival and neurite extension of these neurons (Atwal et al., 2000; Vogel et al., 2000). Furthermore, the MEK-ERK and PI3K-Akt pathways can respectively regulate axonal elongation and distal branching of embryonic DRG neurons when neuronal death was prevented (Markus et al., 2002b).

Transcription Factors and Sensory Neuron Development

On the other hand, several transcriptional factors have been shown to play important cell-intrinsic roles in various stages of sensory neuron development (Marmigere and Ernfors, 2007). The basic helix-loop-helix (bHLH) transcription factors neurogenin 1 (Ngn1) and neurogenin 2 (Ngn2) are required for neurogenesis and the specification of peripheral sensory neurons (Fode et al., 1998; Ma et al., 1998; Ma et al., 1999). Kruppel-

like zinc finger transcription factor Klf7 and POU domain transcription factor Brn3a are required for the survival of sensory neurons through regulating the expression of Trk receptors (Eng et al., 2001; Huang et al., 1999; Lei et al., 2005; Lei et al., 2006; Ma et al., 2003). Brn3a also regulates axonal growth and target innervations of sensory neurons independent of Trks (Eng et al., 2001). Runx family transcription factors play important roles in sensory neuron subtype specification and diversification. Runx1 is required specifically for the development of TrkA positive nociceptive neurons, while Runx3 is important for the development of TrkC positive proprioceptive neurons (Chen et al., 2006b; Kramer et al., 2006; Levanon et al., 2002). Loss of *CREB* results in cell death and impaired axonal growth of all subtypes of sensory neurons (Lonze et al., 2002). In addition, ETS-domain transcription factors ER81 and PEA3, paired homeodomain transcription factor DRG11, and Runx3 control the connection between sensory neurons and their central targets (Chen et al., 2006a; Chen et al., 2001; Lin et al., 1998).

II. *Nf1* and Neural Crest Development

Nf1 Gene and Neurofibromatosis Type 1

Neurofibromatosis type 1 (NF1) is a common inherited neurological disorder which happens in about 1 of 3500 newborns worldwide. Most NF1 patients have benign tumors along peripheral and optic nerves (neurofibromas and gliomas) and abnormal distribution of melanocytes (cafe-au-lait spots). Other symptoms include macrocephaly, short stature and learning disabilities (Riccardi, 1999).

The disorder is caused by either an inherited or a new mutation in the *Nf1* gene, which was cloned in 1990 (Cawthon et al., 1990; Wallace et al., 1990). The human *Nf1* gene is located within chromosome 17. It occupies about 335 kb of genomic DNA and contains 60 exons (Li et al., 1995). The gene product, neurofibromin, is a cytoplasmic protein with a predicted size of 2818 amino acids (Buchberg et al., 1990). Neurofibromin shares a region of similarity with members of the Ras GTPase-activating protein (GAP) family including mammalian p120RasGAP protein, the yeast IRA1 and IRA2 (Xu et al., 1990b) and Drosophila GAP1 (Gaul et al., 1992). This shared region is thus called GAP-related domain (GRD) (Cichowski and Jacks, 2001).

Neurofibromin and Ras Signaling Pathways

Ras is a small G-protein involved in various cellular processes and exists in two forms: an active GTP-bound form and an inactive GDP-bound form. Guanine-nucleotide exchange factors (GEFs) can promote GTP binding and the activation of Ras, whereas GAPs can dramatically enhance the rate of GTP hydrolysis and thus are important negative regulators of Ras signaling pathways (Donovan et al., 2002).

Two major pathways downstream of Ras are the MEK/ERK pathway and the PI3K/Akt pathway. They play important roles in multiple cellular processes such as proliferation, differentiation, survival and neurite extension (Huang and Reichardt, 2001) (see previous discussion). Other effectors of Ras include RalGEFs, PLCε and so on, whose functions are still uncertain (Zhu and Parada, 2001a) (Fig. 1.2).

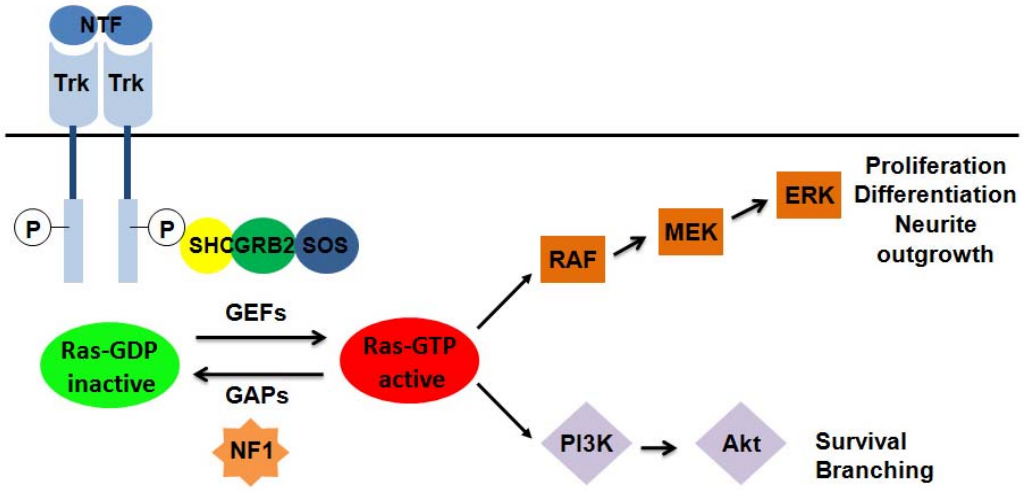

Fig.1.2. Neurofibromin and related signaling pathways (Modified from (Zhu and Parada, 2001a)). Two major signaling pathways downstream of Ras are MEK/ERK pathway and PI3K/Akt pathway. They are important for proliferation, differentiation, survival, neurite growth and branching of sensory neurons. Neurofibromin functions as a negative regulator of Ras-signaling pathways. Deletion of *Nf1* results in activation of effectors downstream of Ras.

Neurofibromin can function as a Ras-GAP both *in vitro* and *in vivo* (Martin et al., 1990; Xu et al., 1990a). In Drosophila, mutation of *Nf1* also inhibits the cAMP/PKA

signaling pathway and subsequently affects growth and learning (Guo et al., 1997; The et al., 1997). It is possible that the Ras and PKA pathways may converge on the MEK-ERK signaling cascade and activate targeting transcription factors. However, interactions between neurofibromin and cAMP/PKA pathway need to be further investigated in vertebrate models (Zhu and Parada, 2001b).

Functions of *Nf1* in Sensory Neurons and Other Cell Types

Nf1 has cell-autonomous effects in various cell types. For example, homozygous *Nf1* mutant (*Nf1-/-*) embryonic sensory neurons can survive in the absence of neurotrophic support (Vogel et al., 1995). Heterozygous *Nf1* mutant (*Nf1+/-*) astrocytes exhibit increased proliferation compared to controls (Bajenaru et al., 2001). The loss of *Nf1* also induces senescence in human fibroblasts but immortalizes mouse embryonic fibroblasts (MEFs) (Courtois-Cox et al., 2006).

On the other hand, *Nf1* deficiency also results in paracrine effects of several cell types. For example, *Nf1-/-* Schwann cells secrete Kit ligand (KitL), which stimulates mast cell migration (Yang et al., 2003), and *Nf1+/-* mast cells can secrete increased amount of transforming growth factor-beta (TGFβ) (Yang et al., 2006), the interaction of these two cell types are important for the development of neurofibroma. It was also reported that *Nf1+/-* microglia can secrete paracrine factors such as insulin-like growth factor-1 (IGF-1) and hepatocyte growth factor (HGF) to stimulate growth of *Nf1-/-* astrocytes (Daginakatte and Gutmann, 2007).

III. Neurofibromatosis type 1 and Gastrointestinal Manifestations

Gastrointestinal Manifestations in NF1 patients

As mentioned earlier, major clinical features of NF1 are cafe-au-lait spots and benign tumors of peripheral and optic nerves. Less penetrant manifestations include pathologies involving the skin, bones, endocrine organs and blood vessels (Le and Parada, 2007). Gastrointestinal (GI) tract can also be affected in these patients. Gastric tumors were reported in about 2 to 25 percent of NF1 patients with various tumor locations and tumor types (Petersen and Ferguson, 1984; Riccardi, 1981; Rutgeerts et al., 1981; Uflacker et al., 1985), including those of epithelial origin (adenoma and

adenocarcinoma), stromal origin (gastrointestinal stromal tumor) and others. In rare cases, GI tumors can even cause gastric outlet obstruction in NF1 patients (Bakker et al., 2005). Non-neoplastic lesions such as inflammatory fibroid polyps (IFP) were seen in GI tract of patients with NF1 as well (Ng et al., 2004). However, the etiological mechanisms of GI lesions in NF1 patients have not been studied yet.

Mouse Models for Gastric Hyperplasia and Gastric Tumor

Gastric cancer is the second most prevalent tumor in the world and the second most common cause of global cancer death (Hatakeyama, 2004; Ushijima and Sasako, 2004). Different rodent models have been developed to study the pathogenic mechanisms of GI tumors. These models can be classified into three categories: (a) Mice infected with Helicobacter pylori: chronic infection with Helicobacter in C57BL/6 mice results in hyperplasia, inflammation and metaplasia in gastric epithelium (Goldenring and Nomura, 2006); (b) Mice with disturbed levels of gastrin, a hormone which can stimulate acid secretion in stomach: both gastrin-overexpressing and gastrin-deficient mice develop gastric tumor (Wang et al., 2000; Zavros et al., 2005); (c) Mice with genetic modification. The targeted genes in mice developing gastric hyperplasia include ion transporters (H/K-ATPase b subunit, Na/K exchanger2, Kvlqt1 channel) (Lee et al., 2000; Scarff et al., 1999; Schultheis et al., 1998), signal transducers (TGFα, sonic hedgehog) (Ramalho-Santos et al., 2000; Sharp et al., 1995), transcription factors (Fox1, NF-kB) (Ishikawa et al., 1997; Kaestner et al., 1997), cell adhesion molecules (Li et al., 2000; Saitou et al., 2000) and others (Gut et al., 2002). Moreover, gastric cancers are observed in mice deficient for trefoil factor 1 (*TFF1*) (Lefebvre et al., 1996), in mice with deficiency in *Smad4* and *Runx3* which are factors involved in TGFβ signaling (Li et al., 2002; Xu et al., 2000) and in mice with point mutation of IL-6 cytokine co-receptor *gp130* (Tebbutt et al., 2002).

In the last mouse model, the SRC homology 2 (SH2)-domain-containing protein tyrosine phosphatase (PTP) - SHP2 binding site on gp130 was mutated, resulting in impairment of IL-6 dependent SHP2-Ras-ERK activation, whereas STAT3 activation remains normal. Furthermore; STAT3 was shown to be required for the gastric phenotypes in this mouse model (Jenkins et al., 2005). It is therefore proposed that under

normal physiological conditions, a reciprocal regulation between SHP2-Ras-ERK and STAT3 pathways exists downstream of cytokine signaling inside gastric epithelial cells, and the dysregulation of the STAT3 pathway seems to be responsible for gastric cancer development.

On the other hand, activation of the Ras-ERK pathway is also involved in gastric cancer, especially in the pathological mechanisms of Helicobacter pylori infections, which is demonstrated to be the major etiological factor of gastric cancer in human (Macarthur et al., 2004). The bacteria carry the cytotoxin-associated antigen A (*CagA*) gene, whose encoded protein is injected into the gastric epithelial cells by the bacteria. Once injected, CagA undergoes tyrosine phosphorylation inside the cells and binds to SHP2, resulting in Ras-MEK-ERK pathway activation and the following pathological changes (Hatakeyama, 2004).

One hypothesis to make these two theories consistent is that CagA can sequester and reduce the intracellular pool of SHP2, thereby relieving the inhibition from SHP2 and activating the STAT3 pathways (Giraud et al., 2007). However, we cannot exclude the possibility that the Ras-MEK-ERK pathway plays some role in this process that is independent of SHP2.

Chapter II

Sox11 Regulates Survival and Axonal Growth of Embryonic Sensory Neurons

Abstract

In vertebrates, the somatosensory neurons transduce various stimuli including temperature, pain and touch from the periphery to the spinal cord and then the information is relayed to higher centers in the brain. Development of sensory neurons is controlled by various cell-extrinsic factors including growth factors and cell-intrinsic factors including transcription factors. One member of the Sox family of transcription factors, Sox11, is expressed at high level in embryonic sensory ganglia. Here, using a *Sox11*-/- mouse model, we show that the loss of *Sox11* results in increased cell death in embryonic sensory ganglia, which leads to a significant neuronal loss around birth. The ablation of *Sox11* also leads to axonal growth defects both *in vivo* and *in vitro*, and the defects cannot be rescued by blocking cell death. Therefore, Sox11 regulates multiple key steps of sensory neuron development. Furthermore, we demonstrate that *Sox11* deficient MEFs exhibit decreased levels of phospho-AKT compared to controls, suggesting Sox11 may regulate the expression of component(s) of the signaling pathways downstream of growth factors.

Introduction

Sensory ganglia are neural crest derived clusters of primary neurons in the PNS, through which sensory information is relayed to the CNS for further processing. Somatosensory information from trunk and limbs is transduced to the spinal cord through sensory neurons residing in the DRG (Scott, 1992); while facial sensory information is relayed to the brain stem by TG sensory neurons (Waite, 1995).

Neurotrophic factors and their downstream MEK-ERK and PI3K-Akt signaling pathways regulate proliferation, cell fate selection, axonal growth, and survival of sensory neurons (Atwal et al., 2000; Bibel and Barde, 2000; Huang and Reichardt, 2001; Huang and Reichardt, 2003; Markus et al., 2002a; Markus et al., 2002b; Parada et al., 1992; Vogel et al., 2000; Zhong et al., 2007). Several transcription factors including Ngn1, Ngn2, Klf7, Brn3a, Runx1, Runx3, CREB et al, play important cell-intrinsic roles in various stages of sensory neuron development through Trk dependent or independent manner (Chen et al., 2006b; Eng et al., 2001; Fode et al., 1998; Huang et al., 1999; Kramer et al., 2006; Lei et al., 2005; Lei et al., 2006; Levanon et al., 2002; Lonze et al., 2002; Ma et al., 2003; Ma et al., 1998; Ma et al., 1999)

The Sry-related box (*Sox*) genes encode a group of transcription factors with a high mobility group (HMG)-type DNA binding domain (Bowles et al., 2000; Kamachi et al., 2000; Schepers et al., 2002). Multiple Sox transcription factors are involved in the specification and maintenance of neural progenitor identity in CNS and PNS (Pevny and Placzek, 2005; Wegner and Stolt, 2005). Among them, Sox9 and Sox10 have specific functions in murine NCC development (Cheung and Briscoe, 2003; Kim et al., 2003). They both inhibit or delay neuronal differentiation and preserve glial potential of NCC progenitors. Another member of Sox family, Sox11, is widely expressed in both CNS and PNS starting from early embryonic stages (Hargrave et al., 1997; Kuhlbrodt et al., 1998). Expression of Sox11 is abundant in embryonic but at very low level in adult sensory ganglia (Tanabe et al., 2003). After peripheral nerve injury, *Sox11* mRNA is up-regulated in adult DRG (Tanabe et al., 2003). *In vitro* culture suggests that Sox11 is necessary for survival and axonal growth of adult sensory neurons (Jankowski et al., 2006). However, the *in vivo* function of Sox11 in the developmental processes of sensory neurons has not been reported.

In this study, we investigate the role of Sox11 in embryonic sensory neuron development using *Sox11* null (*Sox11-/-*) mice in which the exon encoding the entire *Sox11* open reading frame was replaced by a nuclear localized β-galactosidase (*lacZ*) reporter gene (Sock et al., 2004). We demonstrate that Sox11 is expressed in embryonic sensory neurons in both DRG and TG. Our data show that the ablation of *Sox11* results in increased cell death and causes the reduction of all sensory neuron subtypes in DRG and TG. The ablation of *Sox11* also leads to defects in axonal growth of sensory neurons both *in vivo* and *in vitro* in a cell-death-independent way. Therefore, our data establish Sox11 as a novel key regulator of sensory neuron development.

Materials and Methods

Breeding and Genotyping of *Sox11*-/- and *Sox11*-/-; *Bax*-/- Mice

Mice were housed and maintained according to the IACUC guidelines of University of Texas Southwestern Medical Center and Arizona State University. *Sox11*$^{+/lacZ}$ knock-in mice, which were referred to as *Sox11*+/- mice, were mated to generate *Sox11*-/- embryos (Sock et al., 2004). *Sox11*+/- mice were crossed with *Bax*+/− mice to generate *Sox11*+/-;*Bax*+/- mice and then *Sox11*+/-;*Bax*+/- mice were mated to generate *Sox11*-/-;*Bax*-/- embryos. Timed pregnant female mice were sacrificed to collect embryos at different developmental stages. Genotyping of the *Sox11* and *Bax* mutant mice was done by PCR as previously described (Ma et al., 2003; Sock et al., 2004).

Nissl Staining and Cell Counts

For embryonic day 18.5 (E18.5) and postnatal day 0 (P0) cell counts, tissues were fixed in 4% paraformaldehyde (PFA) overnight, protected in 30% sucrose until sunk and then embedded in OCT. For E18.5 DRG, trunk transverse sections were cut continuously at 14 μm using a cryostat machine (Leica), collected directly on Superfrost (+) slides (Fisher) and kept in a -80 °C freezer before use. For P0 TG, head sagittal sections were cut serially at 14 μm using a cryostat, collected onto Superfrost(+) slides, and kept in a -80 °C freezer before use. For E12.5 DRG and TG counts, tissues were fixed in 4% PFA, processed and embedded in paraffin and 5 μm sagittal sections were made. Sections were stained with 0.5% cresyl violet and cell counting was performed as described previously (Lei et al., 2005). Briefly, pictures were taken every 140 μm for P0 TG, every 14 μm for E18.5 DRG, every 150 μm for E12.5 TG and every 30 μm for E12.5 cervical DRG, respectively, and cells with visible nucleoli were counted as neurons. For P0 TG, the total number of neurons was calculated by multiplying the sum by 10. For E18.5 DRG, the sum was reported as the total number of neurons. For E12.5 TG and DRG, the total number of neurons was calculated by multiplying the sum by 30 or 6, respectively.

Immunohistochemistry

Whole-mount neurofilament immunostaining was performed using the 2H3 hybridoma supernatant (Developmental Studies Hybridoma Bank, 1:70) as previously

described (Lonze et al., 2002). For DRG explant immunostaining, the 2H3 hybridoma supernatant was diluted 1:10 in blocking solution (5% normal donkey serum in PBS plus 0.3% Triton X-100) and incubated overnight at 4°C. Frozen sections were processed for immunofluorescent staining as previously described (Lei et al., 2006). Primary antibodies included TrkA (rabbit, L.F. Reichardt, UCSF, 1:500), TrkB (chick, L.F. Reichardt, UCSF, 1:500), TrkC (goat, L.F. Reichardt, UCSF, 1:500), Ret (rabbit, IBL, 1:50), p75 (rabbit, L.F. Reichardt, UCSF, 1:5000) and Tuj1 (mouse, Covance, 1:500). Immunofluorescent staining on paraffin sections was carried out by incubating with primary antibodies in 2% normal goat serum overnight at 4 °C after antigen retrieval. Primary antibodies included lacZ (rabbit, ICN, 1:500), Tuj1 (mouse, Covance, 1:500) and BrdU (mouse, Dako, 1:100). Immunofluorescence was visualized after 1 hour incubation with appropriate Cy2-, Cy3-, or Cy5-conjugated secondary antibodies (Jackson Labs, 1:200) at room temperature. DAPI (Fluka, 1 μg/ml) was added together with the secondary antibodies to stain nuclei. The immunostaining was visualized using a Nikon Eclipse TE2000-U fluorescence microscope or a Zeiss 510 confocal microscope. Digital images were captured using a Photometrics CoolSnap CCD camera (Roper Scientific) and analyzed using the Metamorph software (Universal Imaging).

Cell Proliferation

Pregnant female mice were injected intraperitoneally (IP) with 100 μg/g of body weight 2-bromo-5'-deoxyuridine (BrdU, Sigma) 2 hours before sacrifice. Embryos were collected and 14 μm transverse cryostat sections were made. Anti-BrdU staining was performed using a standard procedure with anti-BrdU-Alexa488 (mouse, Molecular Probes, 1:500) (Lei et al., 2005). The numbers of BrdU positive cells in TG (every tenth section) and C1/C2 DRG (every section) were counted.

Apoptosis

Paraffin sections were deparaffinized and rehydrated. After antigen retrieval, sections were incubated with an antibody against cleaved Caspase-3 (rabbit, Cell Signaling Technology, 1:400). The visualization of primary antibodies was performed with a horseradish peroxidase system (Vectastain ABC kit, Vector). Digital images were

captured with a CCD camera under a light microscope (Olympus). Cleaved Caspase-3 positive cells were counted in at least 10 sections for each TG or DRG.

Dissociated DRG Neuron Culture

Dissociated DRG neuron culture was carried out as described previously (Lei et al., 2005). Briefly, DRG were isolated from E13.5 embryos and dissociated by trypsin. Neurons were cultured in Neurobasal media (Gibco) containing NGF (NGF-7S, Sigma, 10 ng/ml) on poly-D-ornithine and laminin (Sigma)-coated chamber slides (Nalge Nunc). Cells were fixed with 4% PFA at 6 hours, 24 hours, 48 hours, and 72 hours, respectively, after plating and stained with 2H3 antibody (1:50). The percentage of neuronal survival was calculated by dividing the neuron number at 24 hours, 48 hours, and 72 hours, respectively, by the numbers at 6 hours. The values for the mutants were normalized against the values for the wild-type neurons, which were set at 100%.

DRG Explants Culture

DRG explants culture was performed as described previously (Lonze et al., 2002). Briefly, DRG explants were removed from E13.5 embryos and grown on chamber slides coated with poly-D-ornithine and laminin in Neurobasal medium containing NGF (10 ng/ml) with or without the caspase inhibitor BOC-Asp(OMe)-FMK (BAF, Enzyme Systems, 50 μM). After 30 hours, ganglia were fixed and immunostained with 2H3 antibody (1:50). Axon lengths were quantified as described previously (Fitzli et al., 2000). For each ganglion, the 20 longest axons were measured using Metamorph software (Universal Imaging). Only ganglia with visible axonal processes after 1 day *in vitro* (DIV) were scored.

Preparation and Culture of MEFs

MEFs were prepared as described previously (Lu et al., 2006). Briefly, brain and internal organs were removed from E12.5 control and *Sox11-/-* embryos. The remaining tissues were subjected to trypsin digestion and triturated to single cell suspension. The cells were then cultured in Dulbecco's Modified Eagle's Medium **(**DMEM, Hyclone) supplemented with 10% fetal bovine serum (FBS), penicillin and streptomycin. For

serum withdrawal experiments, regular culture media were replaced by DMEM for 24 hours. MEFs of 2-3 passages were used for the experiments.

Western Blots

Mouse embryonic DRGs and MEF cells were extracted and subjected to Western blots as described previously (Romero et al., 2007). Briefly, freshly dissected DRG tissues or MEF cells were quickly rinsed with ice-cold 1X PBS twice and then homogenized in RIPA buffer (50 mM Tris-HCl, PH 7.4, 1% NP-40, 0.25% Na-deoxycholate, 150 mM NaCl, phosphatase inhibitor cocktail (Upstate, 1:100), and the protease inhibitor cocktail (Complete Mini, Roche, 1 tablet/10 ml)). The solutions were incubated on ice for 30 minutes and centrifuged at 14,000 rpm for 20 min at 4 °C. Supernatants were collected and protein concentrations were determined by the BCA Protein Assay Kit (Pierce). 10 μg (for DRG tissues) or 20 μg (for MEFs) of proteins were loaded into each well and separated by 10% SDS-PAGE gels. Proteins were then transferred to nitrocellulose membranes for blotting. Primary antibodies included phospho-p44/42 MAPK (P-ERK, rabbit, Cell Signaling Technology, 1:1000), p44/42 MAPK (ERK, rabbit, Cell Signaling Technology, 1:1000), phospho-AKT (P-Akt, rabbit, Cell Signaling Technology, 1:1000), AKT (rabbit, Cell Signaling Technology, 1:1000), GAPDH (rabbit, Abcam, 1:1000) and acetylated tubulin (mouse, Sigma, 1:1000). HRP-conjugated secondary antibodies were used (1:5000, Santa Cruz Biotechnology). Immunoreactivity was detected with the ChemiGlow reagent (Alpha Innotech), and the densitometry analysis was performed with the KODAK 1D Image Analysis Software.

Statistics

All cell counts and measurements were performed in a genotype-blind manner. Statistical analysis was done using Student's *t*-test with p values ≤ 0.05 as being statistically significant. *= $p \leq 0.05$; **= $p \leq 0.01$; ***= $p \leq 0.001$. Error bar, SEM.

Results

Sox11 is Expressed in Embryonic TG and DRG Neurons

Previous reports showed that *Sox11* mRNA is widely expressed in the developing CNS and PNS (http://www.stjudebgem.org) (Hargrave et al., 1997; Kuhlbrodt et al., 1998). The expression of Sox11 is evident in DRG and TG as early as E11.5 (Hargrave et al., 1997). To characterize the expression pattern of Sox11 in sensory ganglia during development, we took advantage of *Sox11*+/- embryos, in which the complete open reading frame of *Sox11* was replaced with a *lacZ* reporter gene and the lacZ expression reflects the endogenous Sox11 expression patterns (Sock et al., 2004).

In mice, NCCs start to detach from the dorsal neural tube at E8.5 and migrate ventrally to form DRG (Marmigere and Ernfors, 2007). p75, the low-affinity neurotrophin receptor, has been used as a marker for the migrating NCCs (Bannerman and Pleasure, 1993; Farinas et al., 1996; Stemple and Anderson, 1992). We first performed X-gal staining followed by immunohistochemical staining on cross sections of E9.5 *Sox11*+/- embryos, and found β-gal signals were co-localized with p75, suggesting Sox11 is expressed in migrating NCCs (Fig. 2.1A and 2.1B).

To examine whether Sox11 expression in sensory ganglia is restricted to neurons, we performed immunofluorescent staining on DRG and TG sections from *Sox11*+/- embryos and found that the majority of lacZ positive cells in DRG and TG co-expressed Tuj1, a neuronal marker, at E11.5 (Fig. 2.1C-2.1H), while a small percentage of Tuj1 positive neurons were lacZ negative, thus not expressing Sox11 (arrowheads in insets of Fig. 2.1). We also performed the same staining on E11.5 *Sox11*-/- sensory ganglia and found that the percentage of lacZ/Tuj1 double positive cells in total Tuj1 positive cells increased in *Sox11*-/- DRG and TG, while the percentage of lacZ/Tuj1 double positive cells in total lacZ positive cells in sensory ganglia remained the same in the absence of *Sox11* compared to *Sox11*+/- (Table 2.1, see discussion). Similar results were also observed in E13.5 sensory ganglia (Table 2.1).

We also examined whether Sox11 is expressed in sensory ganglia prior to neurogenesis. Neurogenesis in sensory ganglia occurs in distinctive waves both during neural progenitor cell migration and after the initial formation of ganglia (Marmigere and Ernfors, 2007). We pulsed pregnant females with the thymidine analog BrdU at E11.5,

when neurogenesis in TG and DRG is readily detectable, and examined *Sox11*+/- embryos. We found no co-localization of BrdU and lacZ in TG and DRG, indicating that Sox11 transcription is present only in progenitors or neurons once they have exited the cell cycle (Fig. 2.1I-2.1N).

Taken together, these data demonstrate that Sox11 is expressed primarily in embryonic sensory neurons.

			Tuj1+lacZ+ (No. of cells)	Tuj1+ (No. of cells)	lacZ+ (No. of cells)	Percentage of Tuj1+lacZ+/Tuj1+	Percentage of Tuj1+lacZ+/lacZ+
Sox11+/-	E11.5	TG	78	251	78	31.1%	100%
		DRG	371	693	374	53.5%	99.2%
	E13.5	TG	375	566	376	66.3%	99.7%
		DRG	N.D.	N.D.	N.D.	N.D.	N.D.
Sox11-/-	E11.5	TG	510	551	510	92.6%	100%
		DRG	139	161	139	86.3%	100%
	E13.5	TG	674	714	681	94.4%	99%
		DRG	603	660	609	91.4%	99%

Table 2.1. Summary of Tuj1 and lacZ double labeling in embryonic sensory ganglia. DRG and TG sections from E11.5, E13.5 *Sox11*+/- and *Sox11*-/- embryos were subjected to immunofluorescent staining for Tuj1 and lacZ. The number of Tuj1 positive, lacZ positive and Tuj1/lacZ double positive cells was counted. The percentage of Tuj1/lacZ double positive cells as of Tuj1 positive indicated the percentage of neurons that express Sox11; while the percentage of Tuj1/lacZ double positive cells as of lacZ positive indicated the percentage of Sox11-expressing cells that are neurons, respectively. N.D.: not determined. The data demonstrated that the majority of Sox11-expressing cells are neurons in embryonic sensory ganglia.

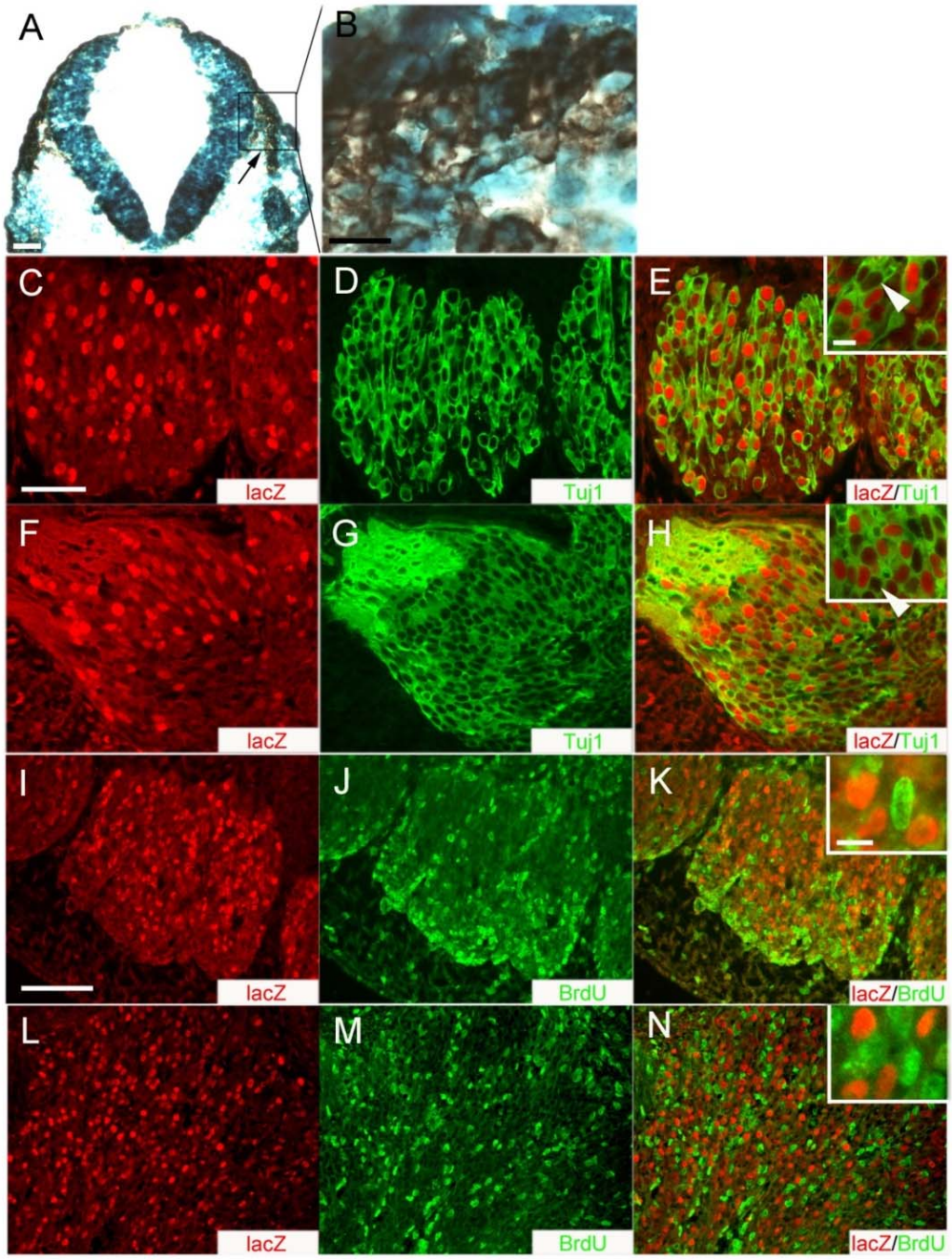

Fig. 2.1. Sox11 is expressed in migrating NCCs and embryonic sensory neurons. (A-B) Transverse sections from E9.5 *Sox11*+/- embryos were subjected to X-gal staining followed by immunohistochemical staining using antibodies against p75. Co-localization of β-gal (blue) and p75 (brown) signals can be observed in the migrating NCCs (arrow in A, higher magnification in B). (C-H) Tuj1 (green) and lacZ (red) double labeling of DRG (C-E) and TG (F-H) sections from E11.5 *Sox11*+/- embryos showed that the majority of lacZ positive cells were also Tuj1 positive

(E and H), thus are neurons. Some Tuj1 positive neurons were negative for lacZ (arrowheads in E and H). (I-N) BrdU (green) and lacZ (red) double labeling of E11.5 DRG (I-K) and TG (L-N) sections showed that lacZ positive cells were not positive for BrdU, thus are not proliferating progenitors. Insets depict higher magnification images, showing the co-localization of lacZ and Tuj1 signals in most cells (insets in E and H), and the non-overlapping lacZ and BrdU signals (insets in K and N). Scale bars = 100 μm in A and I-N; 20 μm in B; 50 μm in C-H and 10 μm in insets.

Different Subtypes of Sensory Neurons are Depleted in *Sox11*-/- Mice

To investigate the impact of the ablation of *Sox11* on sensory neuron development, we first performed Nissl staining and counted neurons in sensory ganglia at P0, when *Sox11*-/- mice die of major congenital heart and lung defects (Sock et al., 2004). We found that the number of trigeminal neurons in *Sox11*-/- mice dramatically decreased compared to controls (Fig. 2.2L and 2.2K). To find out whether this neuronal loss is cell-subtype-specific, we performed immunostaining using antibodies against neurotrophin receptors TrkA, TrkB, TrkC, and Ret (Fig. 2.2A-2.2J). Similar percentage of decrease was observed in all four subtypes of sensory neurons in *Sox11*-/- TG compared to controls (Fig. 2.2M), suggesting that the loss of *Sox11* leads to death of all subtypes of sensory neurons. Significant loss of DRG neurons was also present in E18.5 *Sox11*-/- embryos at several cervical levels compared to controls (Fig. 2.3I-2.3K). Similar to TG, all sub-populations of DRG neurons, based on the expression of Trk receptors and Ret, were reduced at a comparable proportion (Fig. 2.3A-2.3H). Taken together, these data suggest that Sox11 is required for the survival of all subtype of sensory neurons *in vivo*.

We then examined neuronal number in sensory ganglia at an earlier time point. No significant difference in the number of neurons was observed in E12.5 *Sox11*-/- TG (Fig. 2.4M) or DRG (Fig. 2.4N) compared to controls as revealed by Nissl staining. Furthermore, the percentage of different subtypes of sensory neurons (TrkA, TrkB, TrkC, and Ret positive, respectively) did not change in *Sox11*-/- TG (Fig. 2.4), suggesting that the loss of *Sox11* does not affect the formation of major sensory neuron subtypes during early development.

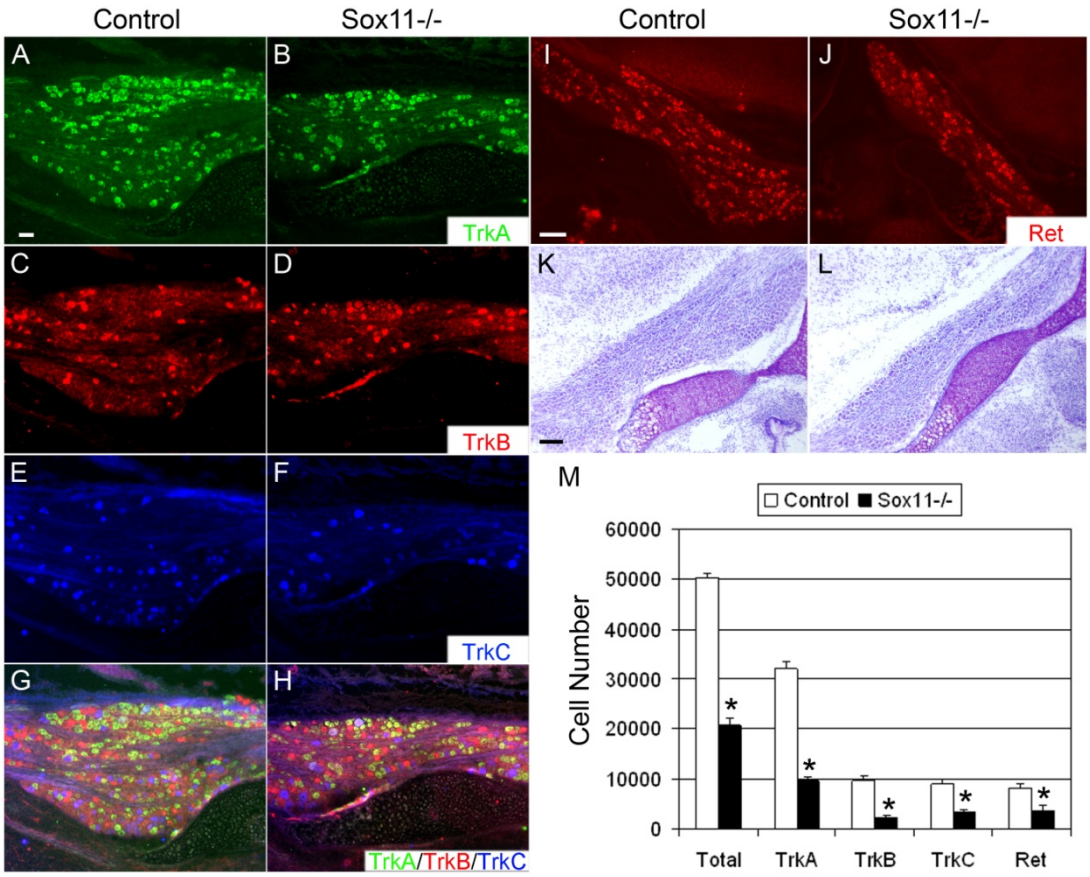

Fig. 2.2. Different types of sensory neurons are lost in P0 *Sox11*-/- TG (in collaboration with Dr. Lei Lei). Nissl staining revealed that at P0, the total neuronal number decreased by about 60% in *Sox11*-/- TG (L) compared to control (K, M, N=4 for each genotype). The neuronal loss in *Sox11*-/- TG was not restricted to any subtype as shown by immunostaining using antibodies for neurotrophic receptors: TrkA (A and B), TrkB (C and D), TrkC (E and F) and Ret (I and J). The number of each type of sensory neurons in *Sox11*-/- TG all decreased at a similar proportion (M, N=2 for each genotype). Student's t-test. Data represents mean +/- SEM. *=$p<0.05$. Scale bars = 50 µm in A-H and 100 µm in I-L.

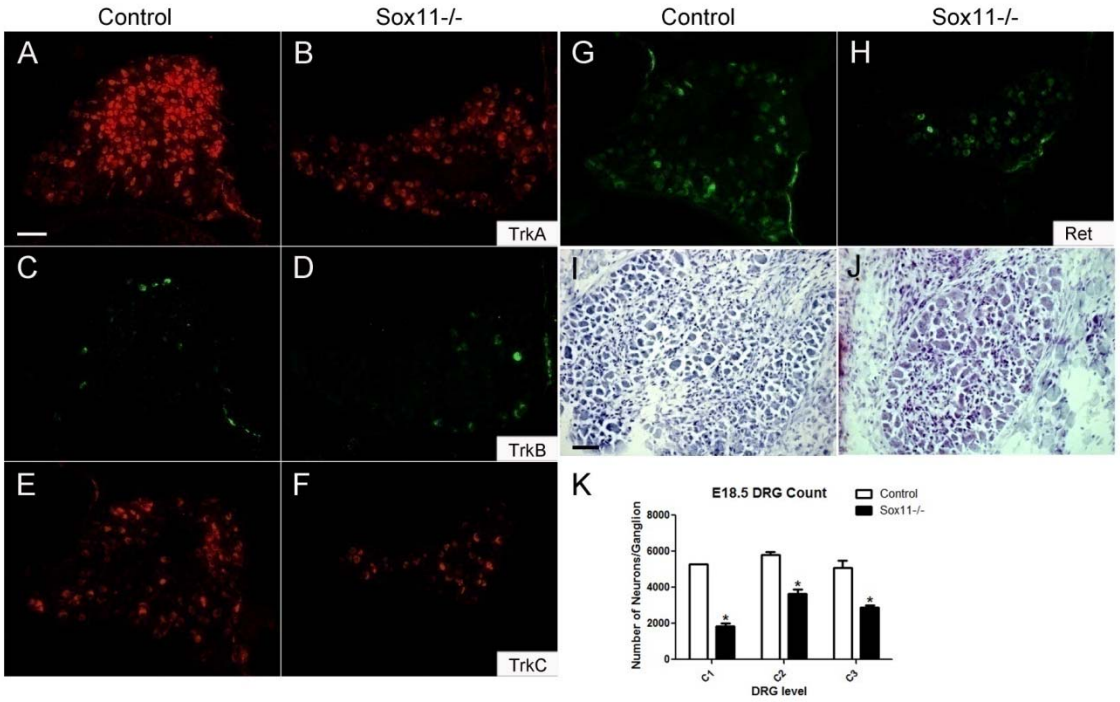

Fig. 2.3. Loss of different subtypes of sensory neurons in E18.5 *Sox11*-/- DRG (in collaboration with Dr. Lei Lei). Nissl staining revealed that at E18.5, a significant decrease of neuronal number was observed in *Sox11*-/- DRG (J) compared to control (I) at several levels (K, cervical 1-3, N=2 for each genotype at each cervical level examined). Immunofluorescent staining for different markers revealed that at this time point, all subtypes of sensory neurons at the cervical level were reduced in *Sox11*-/- DRG compared to control: 67.6% for TrkA (A and B), 78.8% for TrkB (C and D), 79.2% for TrkC (E and F), and 70.2% for Ret (G and H), respectively (≥11 sections were counted for each marker). Percentage was calculated by dividing the number of specific marker positive cells in *Sox11*-/- by that in the control. Student's t-test. Data represents mean +/- SEM. *=$p<0.05$. Scale bars = 100 μm.

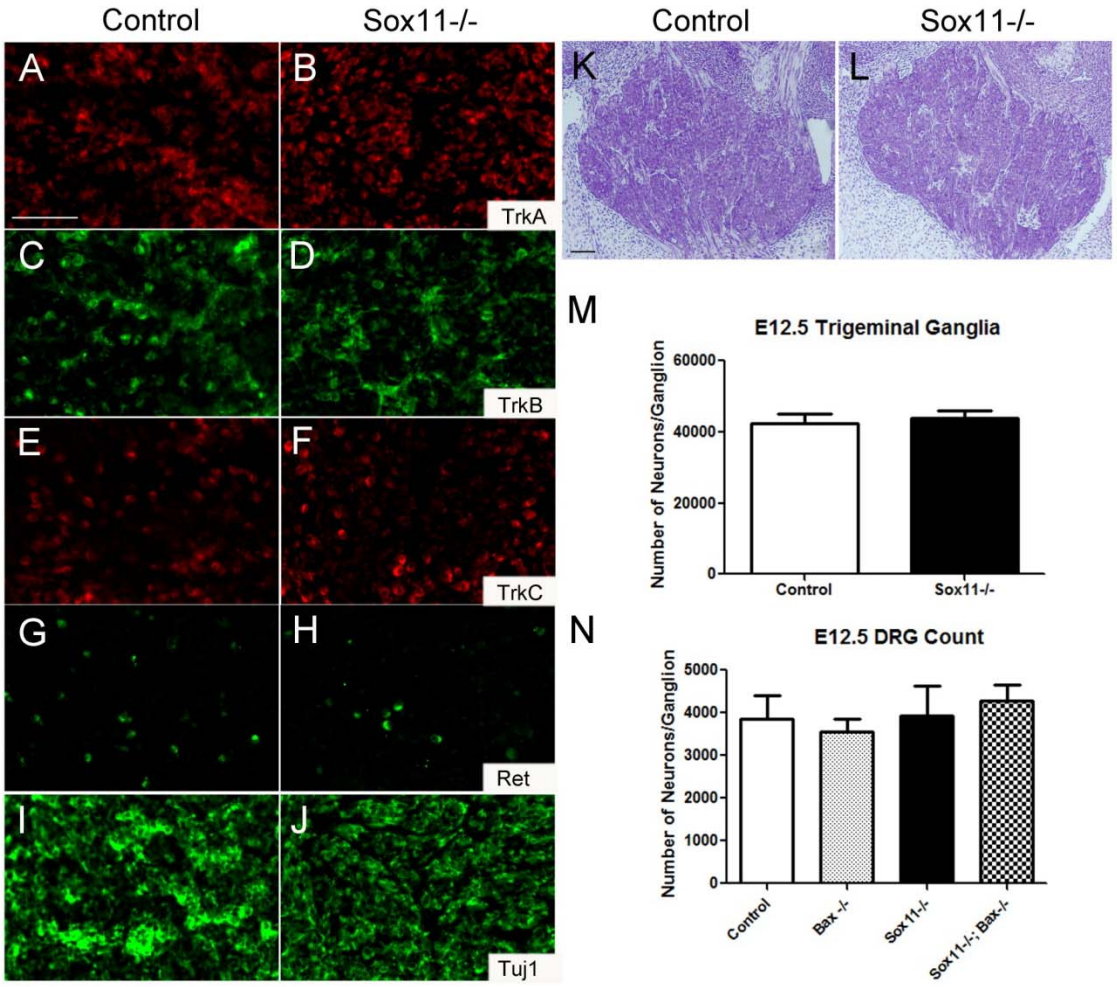

Fig. 2.4. The loss of *Sox11* does not affect the acquisition of major sensory neuron subtypes revealed by neurotrophic receptor expression in E12.5 sensory ganglia. Nissl staining revealed that at E12.5, the total neuronal number did not change in *Sox11*-/- TG (L) compared to control (K and M, N=2 for each genotype). The number of DRG neurons in *Sox11*-/- was also comparable to controls. There was no significant change of neuronal number in *Bax*-/- or *Sox11*-/-;*Bax*-/- DRG compared to control or *Sox11*-/- (N, N=2 for *Bax*-/-, N=6 for the other three genotypes). Adjacent sections from control (A, C, E, G, I) and *Sox11*-/- (B, D, F, H, J) E12.5 TG were subjected to immunostaining using antibodies for TrkA (A and B), TrkB (C and D), TrkC (E and F), Ret (G and H) and Tuj1 (I and J). The percentage of different sub-types of neurons was comparable between control and *Sox11*-/- (TrkA+: 80.8% vs. 81.7%; TrkB+: 14.9% vs. 12.3%; TrkC+: 25.5% vs. 20.6% and Ret+: 9.6% vs. 8.5%). The numbers of specific marker positive cells were counted and the percentages were calculated by dividing that by the total number of

Tuj1 positive cells within the same section. 1458 and 2010 Tuj1 positive cells were counted in control and *Sox11-/-*, respectively. Student's t-test. Data represents mean +/- SEM. Scale bars = 50 μm in A-J and 100 μm in K and L.

The Loss of *Sox11* does not Affect NCC Migration or Cell Proliferation in Sensory Ganglia

To understand the mechanism of sensory neuronal loss in the absence of *Sox11*, we first compared the migration of NCC in control and *Sox11-/-* embryos by using p75 immnuofluorescent staining on E9.5 tissues, and found no obvious difference (Fig. 2.5A and 2.5B). These results suggest that the loss of *Sox11* does not affect NCC migration.

We also examined whether cell proliferation in sensory ganglia was impaired in the absence of Sox11. The number of BrdU positive cells in E11.5 DRG and TG were counted, but no significant difference was detected between *Sox11*-/- and controls (Fig. 2.5C-2.5G), consistent with the finding that lacZ and BrdU did not co-localize in sensory ganglia at this time point (Fig. 2.1I-2.1N). Therefore, Sox11 is not required for proliferation of neural progenitors in sensory ganglia during the peak of neurogenesis.

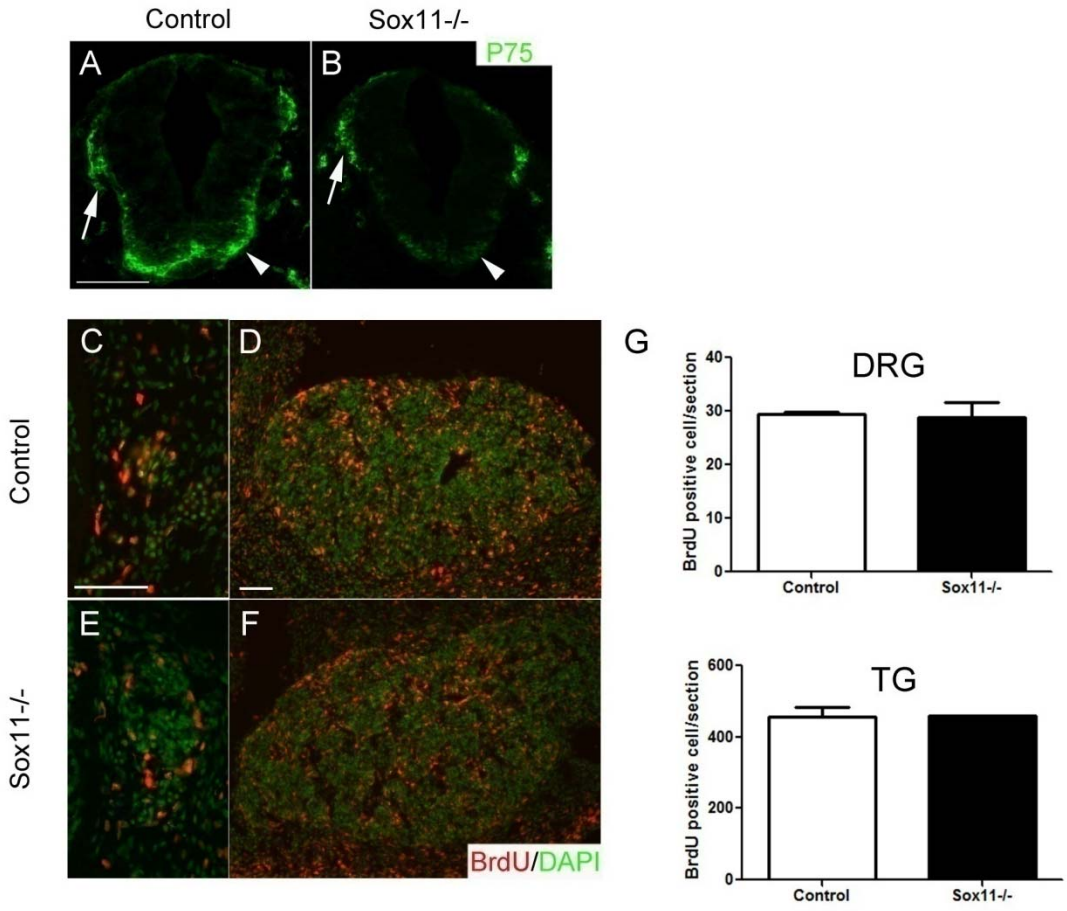

Fig. 2.5. The loss of *Sox11* does not affect migration of neural crest cells or cell proliferation in sensory ganglia (in collaboration with Dr. Lei Lei). (A-B) p75 staining (green) of E9.5 control (A) and *Sox11-/-* (B) transverse sections revealed no significant difference in the migrating neural crest cells (arrows). Arrowheads indicate ventral neural tube. (C-G) DRG (C and E) and TG (D and F) sections from control (C and D) and *Sox11-/-* (E and F) E11.5 embryos were subjected to BrdU immunostaining (red, BrdU; green, DAPI). The number of BrdU positive cells did not change in *Sox11-/-* DRG or TG compared to controls (G, N=2 for each genotype), indicating that proliferation of neural crest cell progenitors at this time point is not affected by the loss of *Sox11*. Student's t-test. Data represents mean +/- SEM. Scale bars = 100 μm in A, B, D and F; 50 μm in C and E.

The Loss of Sox11 Causes Increased Cell Death in Sensory Ganglia

We then examined whether *Sox11-/-* sensory neurons had increased apoptosis. At E12.5, a significant increase of cleaved Caspase-3 positive cells was detected in *Sox11-/-* DRG (Fig. 2.6B) and TG (Fig. 2.6F) compared to controls (Fig. 2.6A and 2.6E, respectively). At E13.5, increased cell death was only observed in *Sox11-/-* DRG ($p=0.06$), while there was no difference in cell death between *Sox11-/-* and control TG (Fig. 2.6C and 2.6G). Taken together, these data demonstrate that the loss of *Sox11* results in increased cell death in embryonic sensory ganglia.

To examine whether the increased cell death in the absence of Sox11 depends on the pro-apoptotic gene *Bax* (White et al., 1998), we then crossed *Bax-/-* with *Sox11-/-* mice and examined the number of cleaved Caspase 3-positive cells in DRG and TG from *Sox11-/-;Bax-/-* embryos. Our results revealed that compared to *Sox11-/-*, DRG (Fig. 2.6D) and TG (Fig. 2.6H) from *Sox11-/-;Bax-/-* embryos had significantly decreased number of cleaved Caspase 3-positive cells, suggesting that the loss of *Bax* rescues *Sox11-/-* sensory neurons from apoptosis *in vivo*.

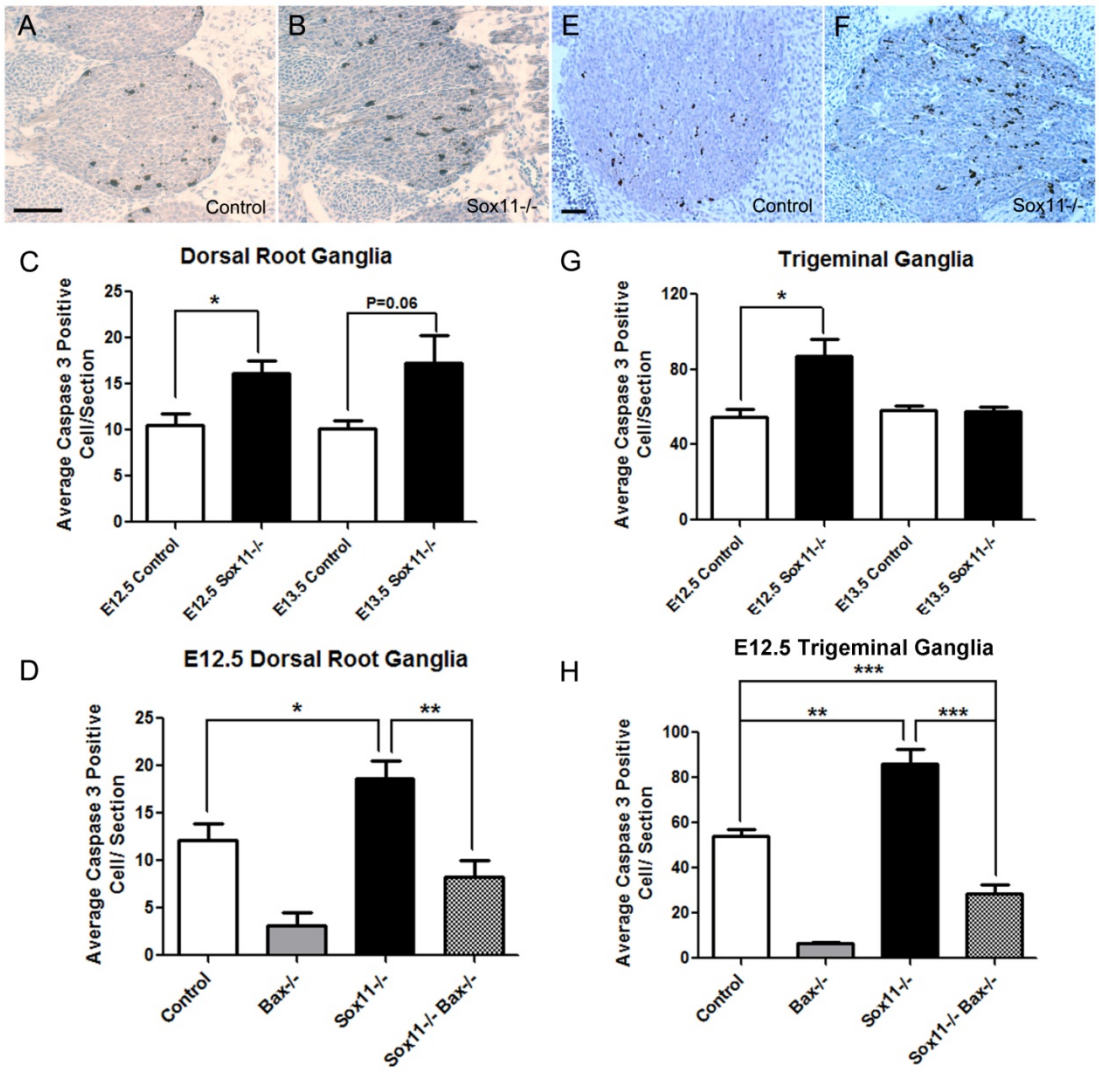

Fig. 2.6. Increased cell death in *Sox11*-/- sensory ganglia. DRG (A, B) and TG (E, F) sections from control (A, E), *Sox11*-/- (B, F), *Bax*-/- and *Sox11*-/-;*Bax*-/- embryos were subjected to cleaved Caspase 3 staining. At E12.5, there was a significant increase of Caspase 3-positive cells in *Sox11*-/- DRG and TG (B and F, respectively) compared to controls (A and E, respectively). At E13.5, there was also an increase of Caspase 3-positive cells in *Sox11*-/- DRG (C, p=0.06), but no difference was observed in TG at this time point (G). At E12.5, significant decrease of Caspase 3-positive cells was observed in both DRG and TG (D and H, respectively) from *Sox11*-/-;*Bax*-/- embryos compared to *Sox11*-/- and controls, suggesting that the increased cell death in *Sox11*-/- sensory ganglia can be rescued by the additional loss of *Bax*. N=4 for each genotype at each time point. Student's t-test. Data represents mean +/- SEM. *=p<0.05, **=p<0.01, ***=p<0.005. Scale bars = 100 μm.

Reduced Axonal Growth of Sensory Neurons in *Sox11-/-* Embryos

To examine whether Sox11 also regulates axonal growth of sensory neurons *in vivo*, we performed whole-mount neurofilament staining of E12.5 embryos. As shown in Fig. 2.7, cutaneous projections of the ophthalmic branch of the trigeminal nerve and projections of spinal nerves were shorter and less branched in *Sox11-/-* mice (Fig. 2.7B and 2.7F) compared to wild type (WT) controls (Fig. 2.7A and 2.7E). To test whether the axonal growth defect in *Sox11-/-* embryos is affected by decreased ability to survive, we examined the *Sox11-/-;Bax-/-* embryos in which the cell death of sensory neurons was abolished (Fig. 2.6). As shown in Fig. 2.4N, the number of DRG neurons in E12.5 *Bax*-/- and *Sox11*-/-;*Bax*-/- embryos was not significantly different form control or *Sox11*-/- embryos. However, the axonal growth defects were still present in the *Sox11*-/-;*Bax*-/- embryos (Fig. 2.7D and 2.7H) compared to *Bax*-/- embryos (Fig. 2.7C and 2.7G; and Table 2.2). Taken together, these results indicate that Sox11 is required for *in vivo* axonal growth of sensory neurons in a cell-death-independent manner.

Genotypes		No. of Embryos Examined	No. of Embryos with Phenotype	Percentage of Embryos with Phenotype
Sox11+/+		30	2*	6.67%
Sox11+/-	*Bax+/+* or *+/-*	33	8	24.24%
	Bax-/-	9	2	22.22%
Sox11-/-	*Bax+/+* or *+/-*	15	15	100%
	Bax-/-	4	4	100%

Table 2.2. Summary of whole mount neurofilament staining of E12.5 embryos. Cutaneous projections of the ophthalmic branch of the trigeminal nerve (ONB) and lateral cutaneous branch of spinal nerves (LCB) were compared between E12.5 embryos. Most WT and *Bax*-/- embryos had normal appearance of these nerve branches, with only a small percentage of them having a partial phenotype (*, reduced ONB but normal LCB). Fewer and shorter branches were observed in 100% of *Sox11-/-* (15/15) and *Sox11*-/-;*Bax-/-* (4/4) embryos, as well as about 25% of *Sox11*+/- embryos (8/33).

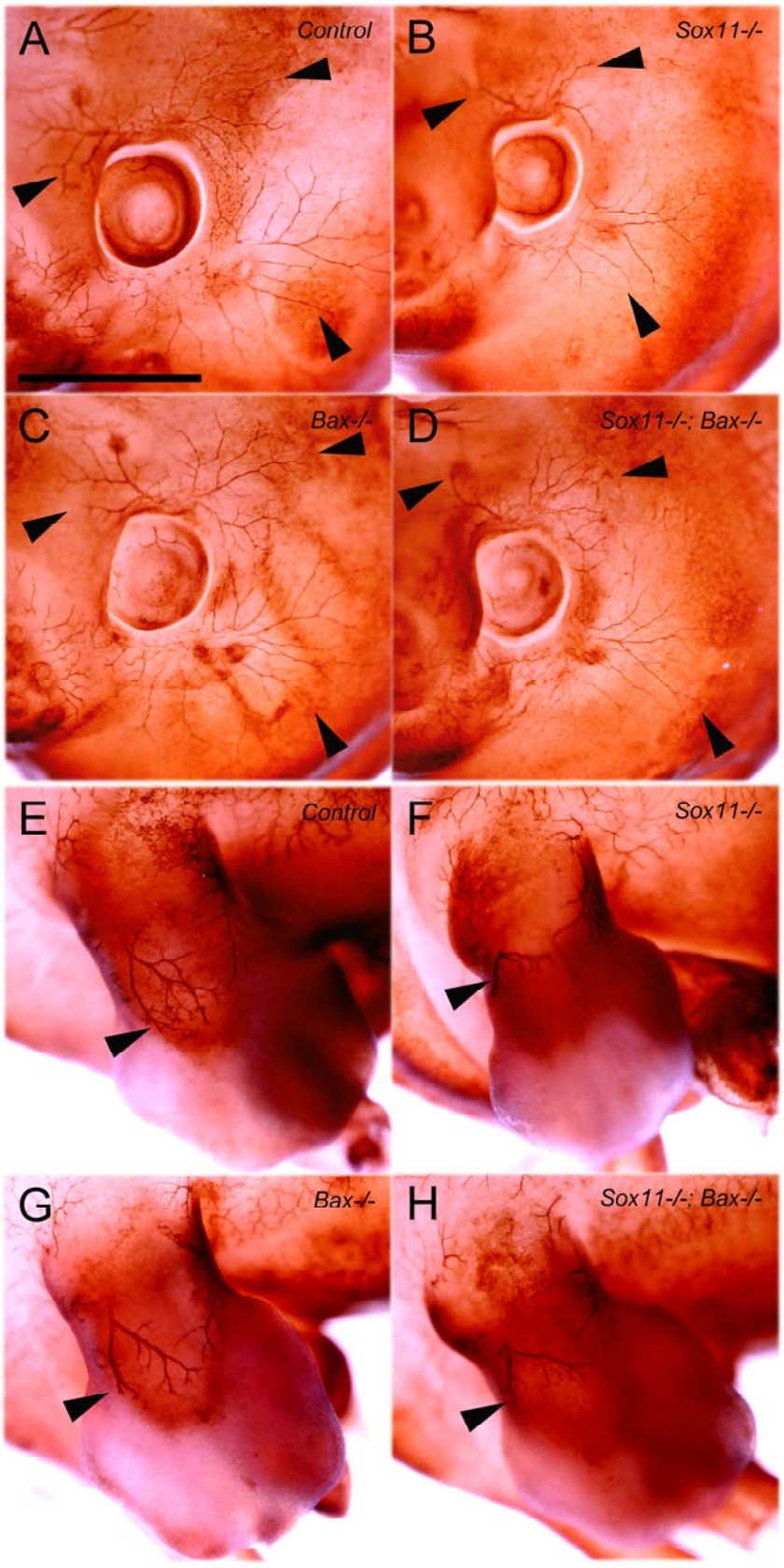
A
Control
B
Sox11-/-
C
Bax-/-
D
Sox11-/-; Bax-/-
E
Control
F
Sox11-/-
G
Bax-/-
H
Sox11-/-; Bax-/-

Fig. 2.7. Cell-death-independent axonal growth defects in *Sox11*-/- embryos. E12.5 control (A, E), *Sox11*-/- (B, F), *Bax*-/- (C, G) and *Sox11*-/-;*Bax*-/- (D, H) embryos were subjected to whole-mount neurofilament staining. Cutaneous projections of ophthalmic branches of the trigeminal nerve (arrowheads in A-D) and projection of spinal nerve branches (arrowheads in E-H) were indicated. Compared to controls (A, E), fewer and shorter nerve branches at these locations were observed in *Sox11*-/- embryos (B, F). The additional loss of *Bax* did not rescue these axonal growth defects (C, G), indicating that the axonal growth defect in *Sox11*-/- embryos is at least partially independent of cell death. Scale bar = 1 mm.

Sox11-/- DRG Neurons Exhibit Decreased NGF-dependent Survival *in vitro*

Because *Sox11*-/- mice are germ-line null mutants, it is unclear whether the sensory neuron defects we observed *in vivo* were caused by the loss of *Sox11* in neurons or in some other cell types. To address the question of whether Sox11 is required in sensory neurons for survival, we cultured DRG neurons in dissociation and examined their survival *in vitro*. In the presence of NGF (10 ng/ml), DRG neurons isolated from E13.5 *Sox11*-/- embryos showed a decreased survival rate at 48 hours after plating when compared to controls, and this difference was more obvious at 72 hours in culture (Fig. 2.8A). This finding supports the idea that the neuronal loss observed *in vivo* reflects, at least in part, a requirement for Sox11 within DRG neurons.

Sox11-/- DRG Neurons Exhibit Decreased Axonal Growth *in vitro*

To examine whether Sox11 is required within DRG for regulating axonal growth, we cultured E13.5 DRG explants in the presence of NGF (10 ng/ml) and examined their axonal growth properties *in vitro*. Consistent with our *in vivo* data, explant cultures revealed a significant decrease of average axonal length in *Sox11*-/- DRG compared to controls (Fig. 2.8B-2.8C). The defect in axonal growth was maintained in *Sox11*-/- DRG explants even in the presence of the apoptosis inhibitor BAF (50 μM) (Fig. 2.8D). Therefore, these data demonstrate that Sox11 is required for axonal growth of sensory neurons *in vitro* in a cell-death-independent manner.

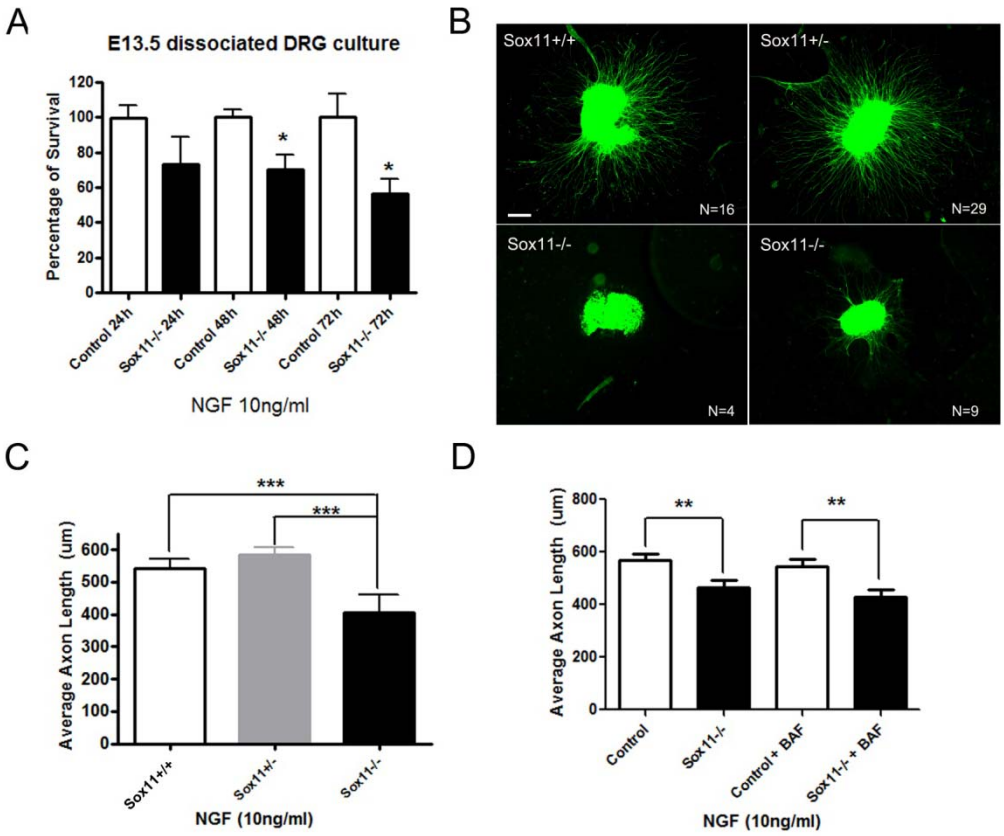

Fig. 2.8. *In vitro* survival and axonal growth defects of *Sox11* -/- DRG neurons. (A) E13.5 dissociated DRG neuronal culture in the presence of NGF (10 ng/ml) revealed a significant decrease of neuronal numbers in *Sox11*-/- cultures compared to controls at 48 hours and 72 hours after plating. All data were normalized to controls for each time point (Duplicate wells each from two embryos for each genotype were used for each time point). (B) DRG explants were taken from E13.5 control and *Sox11*-/- embryos, cultured in NGF containing media for 30 hours and then subjected to 2H3 immunostaining. (C) *Sox11*+/+ (N=16) and *Sox11*+/- (N=29) explants exhibited comparable average axonal length, while significant decrease of average axonal length was observed in *Sox11*-/- DRG explants (N=13). (D) Even in the presence of apoptosis inhibitor BAF, *Sox11*-/- DRG explants still had shorter axons compared to controls (*Sox11*+/+ and *Sox11*+/-), suggesting that the axonal growth defect of *Sox11*-/- DRG neurons *in vitro* is at least partially independent of cell death. Student's t-test. *=$p<0.05$, **=$p<0.01$, ***=$p<0.005$. Data represents mean +/- SEM. Scale bar = 200 μm.

The Loss of *Sox11* Affects the PI3K-Akt Pathway

To investigate the possible molecular mechanisms underlying the increased cell death and decreased axonal growth of *Sox11*-/- sensory neurons, we compared the status of two major signaling pathways downstream of neurotrophins, the MEK-ERK pathway and the PI3K-Akt pathway, between E12.5 control and *Sox11*-/- DRG by Western blots. However, no significant change was observed on the level of either phospho-ERK or phospho-Akt (Fig. 2.9A).

Primary mouse MEF cells have been widely used in studying the signaling cascade related to apoptosis. The cell death of MEFs requires the function of proapoptotic protein Bax or Bak (Zong et al., 2001). By acting on different signaling pathways, specific gene mutations in MEFs render these cells either prone or resistant to apoptosis (Das et al., 2001; Kuang et al., 2000; Liu et al., 2006; Lue et al., 2007; Romano et al., 1999). To further study the possible signaling pathways affected by the loss of *Sox11*, MEFs were generated from control and *Sox11*-/- embryos and subjected to Western blots. Under either normal culture condition or after serum withdrawal, the level of phospho-Akt decreased in *Sox11*-/- MEFs, while phospho-ERK level remained comparable between control and *Sox11*-/- (Fig. 2.9B). Taken together, these data suggest that the loss of *Sox11* may impair the PI3K-Akt pathway without affecting the MEK-ERK pathway.

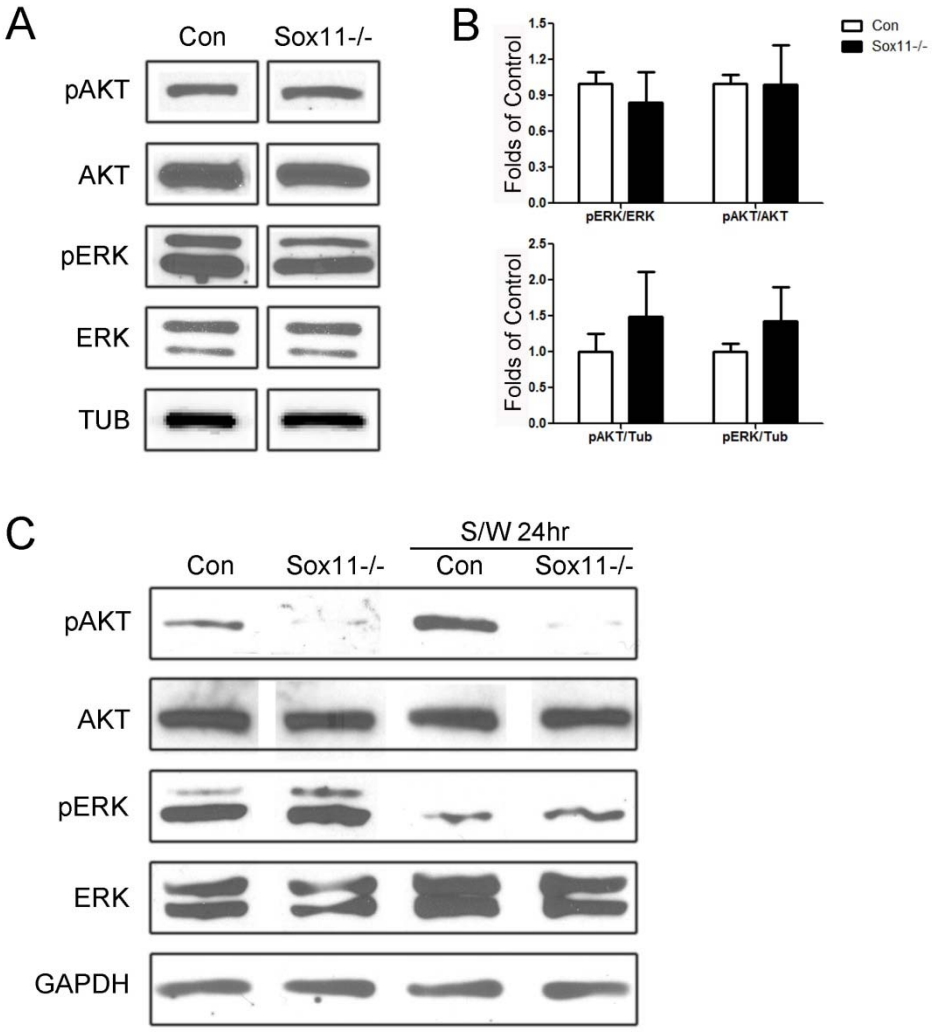

Fig. 2.9. Status of MEK-ERK and PI3K-Akt pathways in *Sox11-/-* DRGs and MEFs. (A) E12.5 control and *Sox11-/-* DRG tissues were subjected to Western blots. No significant difference was found on the relative level of phospho-ERK (pERK)/ERK, phospho-Akt (pAkt)/Akt, pERK/Tubulin (Tub) or pAKT/Tub between control and *Sox11-/-* tissues (B, N=3 for each genotype, data represents mean+/- SEM). (C) The level of pAKT was reduced in *Sox11-/-* MEFs cultured under either normal conditions or serum-free conditions, while the level of pERK was not affected.

Discussion

Sox11 Regulates Multiple Steps in Sensory Neuron Development

Several transcription factors have been shown to regulate sensory neuron development during various stages (Marmigere and Ernfors, 2007). Sox11 is a transcription factor expressed in sensory neurons at a high level during embryonic development but down-regulated in adult DRG. Its expression is up-regulated in adult DRG after peripheral nerve injury (Tanabe et al., 2003). *In vitro* experiments using RNA interference (RNAi) suggested that Sox11 might be required for survival and axonal growth of adult DRG neurons (Jankowski et al., 2006). However, the results of these *in vitro* experiments are greatly affected by the inefficiency of transfection and RNAi knockdown. Genetic ablation leads to complete and homogenous disruption of *Sox11*, thus providing us a better model to study the physiological functions of this gene in sensory neurons. In this study, by using *Sox11*-deficient mice, we demonstrate that Sox11 is not required for NCC migration, sensory ganglia formation, or proliferation of sensory neuron progenitors. Neither is Sox11 required for the specification of the major sensory neuron subtypes as revealed by the normal expression of the neurotrophin receptors in E12.5 *Sox11*-/- TG. However, Sox11 is required for the survival of embryonic sensory neurons and the ablation of this gene leads to the reduction of all subtypes of sensory neurons. Sox11 is also required for normal axonal growth in a cell-death-independent manner both *in vitro* and *in vivo*. We also found that the loss of *Sox11* leads to reduced level of phospho-Akt in MEFs, which may contribute to the defects observed in sensory neuron survival and growth. Therefore, our data establish Sox11 as a novel transcription factor that controls the development of sensory neurons both *in vivo* and *in vitro*.

Sox11 and Proliferation of Progenitors in Embryonic Sensory Ganglia

Multiple members of the Sox family of transcription factors are involved in maintaining neural progenitor identity (Pevny and Placzek, 2005; Wegner and Stolt, 2005). For example, Sox9 is required for initiating NCC development and their subsequent differentiation towards the glia and melanocyte lineage (Cheung and Briscoe, 2003). Sox10 maintains NCC multipotency and inhibits or delays NCC differentiation towards the neuronal lineage (Kim et al., 2003). It was also shown that Sox11 can

promote neuronal maturation in the developing chick neural tube in an *in ovo* electroporation assay (Bergsland et al., 2006). In E11.5 sensory ganglia, the expression of Sox11 was restricted to neurons but not in proliferating cells as revealed by Tuj1/lacZ and BrdU/lacZ double labeling. Furthermore, cell proliferation in both DRG and TG was not affected by the loss of *Sox11*, suggesting that Sox11 may mainly exert its function at later stages of sensory neuron development. It is interesting to note that an increased percentage of lacZ positive cells, thus Sox11-expressing cells, was detected in *Sox11-/-* embryonic sensory ganglia compared to *Sox11+/-* (Table 2.1). This could be explained by the fact that *Sox11-/-* mice carry two copies of lacZ transgenes compared to only one copy in *Sox11+/-* (Sock et al., 2004). The other possibility is that Sox11 can negatively regulate its own expression level, like Brn3a and Mash1 (Meredith and Johnson, 2000; Trieu et al., 2003; Trieu et al., 1999). It is unlikely that the loss of *Sox11* changes the fate of Sox11-expressing cells, since similar percentages of lacZ/Tuj1 double positive cells among lacZ positive cells were found in *Sox11+/-* and *Sox11-/-* sensory ganglia (Table 2.1), suggesting that in either genotype, the majority of Sox11-expressing cells are neurons.

Sox11 and Cell Death within Embryonic Sensory Ganglia

Developmentally regulated apoptosis takes place within sensory ganglia in order to selectively eliminate some neurons generated during early embryonic stages (Vogelbaum et al., 1998). NGF, BDNF, NT3, and their receptors are necessary for survival of specific populations of embryonic sensory neurons (Crowley et al., 1994; Farinas et al., 1994; Jones et al., 1994; Klein et al., 1994; Klein et al., 1993; Liebl et al., 1997; Smeyne et al., 1994; Tessarollo et al., 1994). Increased cell death in DRG of *NGF-/-* and *TrkA-/-* mice starts at E13.5 (White et al., 1996), but cell death is already significant in DRG of *NT3-/-* and *TrkC-/-* mice as early as E11.5, consistent with the notion that some proliferating precursors and early born sensory neurons express TrkC and therefore may require NT3 for survival (White et al., 1996). Significant neuronal loss is also detectable in *BDNF-/-*, *NT3-/-* and *TrkC-/-* DRG as early as E12.5 (Liebl et al., 1997). Our data demonstrated that at E12.5, increased cell death was already apparent in *Sox11-/-* sensory ganglia. However, at this time the expression of TrkA, TrkB, TrkC and Ret did not change in

Sox11-/- TG compared to controls (Figure 2.4), suggesting that the effect of Sox11 on the survival of these neurons may not be through the regulation of neurotrophin receptors. At later time points such as around birth, all subtypes of sensory neurons were lost at a similar proportion in *Sox11*-/- sensory ganglia, supporting a broad role of Sox11 in regulating the survival of sensory neurons.

The proapoptotic gene *Bax* is required for naturally occurring cell death in embryonic sensory ganglia and the additional loss of *Bax* can rescue sensory neuron death in *TrkA*-/-, *NGF*-/-, and *NT3*-/- mice (Patel et al., 2000; Patel et al., 2003; White et al., 1998). The loss of sensory neurons in *CREB*-/-, *Brn3a*-/-, and *Klf7*-/- embryos can be rescued by the loss of *Bax* as well (Lei et al., 2005; Lonze et al., 2002; Ma et al., 2003). Our current study demonstrated that the increased cell death in *Sox11*-/- DRG and TG was also dependent on *Bax*, suggesting a common link between these transcription factors in mediating neurotrophin-dependent neuronal survival. It is interesting to note that the expression of various apoptosis-promoting or apoptosis-inhibiting genes were affected when the level of Sox11 was knocked down by siRNA *in vitro* (Jankowski et al., 2006), suggesting possible regulatory functions of *Sox11* on apoptosis-associated genes. It will be very important in the future to identify the direct target genes of Sox11 that are involved in sensory neuron survival *in vivo*.

Sox11 and Axonal Growth of Embryonic Sensory Ganglia

Although neuron numbers were not affected in E12.5 *Sox11*-/- sensory ganglia, there were significant axonal growth defects in *Sox11*-/- embryos *in vivo* as revealed by whole mount 2H3 staining. To directly examine whether this defect is caused by increased cell death, *Bax*-/- mice were crossed into the *Sox11* null background to block apoptosis. Our data demonstrated that *Sox11*-/-;*Bax*-/- embryos still had axonal growth defects compared to *Bax*-/- embryos, suggesting that Sox11 is required for *in vivo* axonal growth in a cell-death-independent manner. Interestingly, we observed that a small percentage of *Sox11*+/- embryos showed similar axonal growth defects as *Sox11*-/- (Table 2.2), while neuronal numbers were comparable between these two genotypes, suggesting that haplo-insufficiency of *Sox11* may specifically affect *in vivo* axon growth but not survival. The different phenotypes seen in *Sox11*+/- embryos may be caused by the mixed genetic

background. Culture of explants and dissociated neurons from DRG further demonstrated that Sox11 is at least partially required in sensory neurons for survival and axonal growth.

Downstream Targets of Sox11

The molecular mechanisms by which Sox11 regulates sensory neuron survival and axon growth remain to be elucidated. The NGF family of neurotrophic factors and their Trk receptors are crucial for sensory neuronal development, and several transcription factors have been shown to regulate sensory neuron development through regulating the expression of Trk receptors or the components of the neurotrophin-Trk signaling pathways (Chen et al., 2006b; Lei et al., 2005; Levanon et al., 2002; Lonze et al., 2002; Ma et al., 2003). Although Sox11 is not required for the expression of Trk receptors and Ret at E12.5, it remains possible that Sox11 may be required for the maintenance of the expression of these receptors later as multiple putative Sox11 binding sites have been identified within the promoter regions of TrkA, TrkB and TrkC genes (unpublished data). Chromatin immunoprecipitation (ChIP) assays have been widely used to demonstrate *in vivo* protein-DNA interactions. However, it is technically challenging to examine whether Sox11 directly binds these promoters *in vivo* by ChIP due to both the lack of a Sox11 antibody suitable for this assay and the large amount of sensory neurons required to perform the assay. It is equally possible that Sox11 may regulate the expression of other components of the neurotrophin signaling pathways, the dysfunction of which can cause sensory neuron defects as well. The status of two major signaling pathways downstream of neurotrophins, the MEK-ERK pathway and the PI3K-Akt pathway, was examined by Western blots using embryonic DRG tissues and cultured MEF cells. No difference of either phospho-ERK or phospho-Akt level was observed in E12.5 DRG despite the apparent increase of cell death at this time point. This is not surprising because Caspase 3- positive cells only account for a small proportion of total neurons in the ganglia, which may make the possible molecular changes such as phospho-ERK or phospho-Akt difficult to detect. An alternative approach would be to examine phospho-ERK and phospho-Akt by immunohistochemistry on embryo sections; however, we have not succeeded in using these antibodies for immunohistochemistry on sections (data not

shown). Various studies have used MEFs as an effective tool to investigate the apoptosis-related signaling pathways (Das et al., 2001; Kuang et al., 2000; Liu et al., 2006; Lue et al., 2007; Romano et al., 1999). We adopted MEF cultures to search for the possible targets affected by the loss of *Sox11*. The PI3K-Akt pathway has been shown to be important for survival of various types of cells including MEFs and embryonic sensory neurons (Datta et al., 1999). The decreased level of pAkt in *Sox11-/-* MEFs suggested that the increased cell death and/or impaired axonal growth in the absence of *Sox11* may be caused by the down-regulation of the PI3K-Akt pathway. Furthermore, multiple transcription factors can cooperate to affect sensory neuron development (Lei et al., 2006). It has been shown that Sox11 can interact with the POU domain transcription factor Brn2 to regulate expression of the nestin gene in neural primordial cells in the developing spinal cord (Tanaka et al., 2004). It would be interesting to examine whether Sox11 synergizes with Brn3a, a major POU domain transcription factor in sensory neurons, to regulate the development of these neurons.

Caveat and Future Directions

Because mice with a germ-line deletion of *Sox11* were used in this study, we cannot exclude the possibility that the loss of *Sox11* in other cell types may contribute to the sensory neuron defects we observed *in vivo*. Cell type specific and/or temporally controlled *Sox11* conditional knockout mice are required to further dissect the function of this gene in sensory neuron development.

Chapter III

Mice with Neuron-specific *Nf1* Deletion Exhibit Increased Axon Growth and Functional Recovery after Dorsal Root Injury

Abstract

Neurofibromin, the protein encoded by the tumor suppressor gene *Nf1*, is a Ras-GTPase activating protein and functions as a negative regulator of Ras signaling cascade. Two major pathways downstream of Ras: MEK-ERK and PI3K-Akt pathway are involved in multiple cellular processes such as cell survival, differentiation and axonal growth. Previous work in our lab showed that *Nf1*-/- embryonic sensory neurons can survive in the absence of neurotrophin support, which is mainly attributed to enhanced PI3K activity caused by the loss of *Nf1*. In this report, by using mice with *Nf1* specifically deleted in neurons, we demonstrate that *Nf1*-/- adult sensory neurons exhibit enhanced intrinsic capacity for neurite outgrowth *in vitro*. After dorsal root injury, increased axonal sprouting from uninjured sensory neurons is observed in the absence of *Nf1*. Furthermore, *Nf1* deficient mice show spontaneous functional recovery compared to the permanent sensory deficits observed in controls. This phenomenon appears to be mediated both by a cell autonomous capacity of spared *Nf1*-/- DRG neurons for increased collateral branching, and by non-cell autonomous contribution from *Nf1*-/- neurons in the spinal cord, as suggested by co-culture experiments. Hyper-activation of MEK-ERK pathway is detected in tissues from *Nf1* deficient mice.

Introduction

Neurofibromin is a cytoplasmic protein encoded by *Nf1*, the disease gene for neurofibromatosis type 1 (Buchberg et al., 1990; Cawthon et al., 1990; Wallace et al., 1990). Structurally, neurofibromin shares a region of similarity with members of the Ras-GAP family (Gaul et al., 1992; Xu et al., 1990b); functionally, it can also work as a Ras-GAP both *in vitro* and *in vivo* (Martin et al., 1990; Xu et al., 1990a). Two major pathways downstream of Ras are the MEK-ERK and PI3K-Akt pathway. They play different roles in multiple physiological processes of sensory neurons such as proliferation, differentiation, survival and neurite extension (Huang and Reichardt, 2001; Huang and Reichardt, 2003). The loss of *Nf1* can thus activate Ras and its downstream pathways, resulting in abnormality in different types of cells. Different from WT controls, embryonic sensory and sympathetic neurons from *Nf1* knockout (*Nf1-/-*) mice can survive in the absence of neurotrophic factors in culture, which was due to the activation of Ras and PI3K pathway (Klesse and Parada, 1998; Vogel et al., 1995).

Neurons in adult CNS have limited regenerative capability, mostly due to reduced intrinsic growth capacity and a growth inhibitory environment present at the injury site, which primarily consists of myelin-associated inhibitors (MAIs) and chondroitin sulphate proteoglycans (CSPGs)-containing glial scars (Bomze et al., 2001; Spencer et al., 2003; Yiu and He, 2006). Strategies aiming at the modification of the extracellular compartment through cellular grafting (McDonald et al., 1999; Takami et al., 2002; Teng et al., 2002), blockade of inhibitory molecules (Bradbury et al., 2002; GrandPre et al., 2002; Merkler et al., 2001), addition of growth-enticing factors (Ramer et al., 2000; Romero et al., 2001), or combinations thereof (Fouad et al., 2005; Lu et al., 2004; Pearse et al., 2004) have resulted in various degrees of anatomical and functional recovery after CNS injury. On the other hand, PNS neurons can regenerate their axons after injury, probably due to different properties of PNS glia (Schwann cells) as well as different intrinsic abilities of PNS neurons (Goldberg and Barres, 2000). However, the dorsal roots through which DRG neurons send axon projections into the spinal cord are unable to regenerate into the dorsal root entry zone (DREZ) (Carlstedt, 1985). This regenerative failure may be caused by CSPGs and reactive astrogliosis present at the DREZ (Pindzola et al., 1993; Sims and Gilmore, 1994). Modification of the intrinsic growth capacity of

injured neurons, either by exposure to a pre-conditioning injury or neurotrophic factors can promote them to re-grow into the spinal cord after dorsal root injury (Chong et al., 1999; Neumann and Woolf, 1999; Romero et al., 2001).

The purpose of this study is to investigate the role of *Nf1* in adult sensory neurons. We hypothesize that *Nf1* deletion in adult DRG neurons will mimic neurotrophin stimulation, thus giving these neurons growth advantage both *in vitro* and in *vivo*. DRG explant culture and a mouse dorsal root injury model will be used to address these questions.

Materials and Methods

Breeding and Genotyping of *Nf1*$^{flox/flox}$ and Cre Mice

Mice were housed and maintained according to the IACUC guidelines of University of Texas Southwestern Medical Center. *Nf1*$^{flox/flox}$, Synapsin I-Cre and *Nf1*$^{flox/flox}$; Synapsin I-Cre (*Nf1*-SynI-CKO) mice were generated and fully characterized as described previously (Zhu et al., 2001). Peripherin1-Cre (obtained from mutant mouse resource regional centers) and Islet1-Cre mice (generously provided by Dr. Thomas Jessell, Columbia University) were crossed to *Nf1*$^{flox/flox}$ to generate *Nf1*-Prph1-CKO and *Nf1*-Isl1-CKO mice. Due to the small size of *Nf1*-SynI-CKO, *Smad-3* mutants (Zhu et al., 1998) that are also small were included as size controls. Genotyping of the *Nf1*$^{flox/flox}$ and Cre mice was done as previously described (Zhu et al., 2001). *Nf1*$^{flox/flox}$, Synapsin I-Cre and *Nf1*$^{flox/wt}$; Synapsin I-Cre mice were indistinguishable from each other, thus were all pooled as controls.

Adult DRG Explants Culture

Adult DRG were dissected and whole explants were embedded in Matrigel (BD Bioscience) and cultured in Neurobasal-A/B27/L-glutamine media (Gibco). Explants were plated onto Lab-Tek chamber slides (Nalge Nunc) coated with poly-D-ornithine (2 mg/ml; Sigma) with laminin (10 μg/ml; Invitrogen). Cultures were maintained under conditions of no neurotrophin for up to 48-72 hours at 37°C in a humidified atmosphere containing 5% CO2. Mix-match co-culture experiments were done exposing lumbar spinal cords cut into 500 μm slices and DRG obtained from control or *Nf1*-SynI-CKO adult mice, co-embedded in Matrigel, and cultured in Neurobasal-A/B27/L-glutamine media for 48 hours.

Viability of Spinal Cord Slices in Culture

After 48 hours in culture, propidium iodide (PI, Sigma) was added 1 hour prior to imaging. Minimal fluorescence from dead cells was observed in slices of either control or *Nf1*-SynI-CKO spinal cords, compared to that induced after another 48 hours cooling at 4°C. The cell death index was reported as the fluorescent intensity at 1 hour divided by that recorded after 48 hours at 4°C.

Quantification of Neurite Growth

Axon length was determined in phase contrast images acquired using a 20X objective at different focal planes. The axons were traced and measured using the MetaMorph Imaging software (Universal Imaging). About 50 longest axons per explant were counted in each experiment, 4 explants for each genotype were included in 2 separate experiments. Axons were defined as neurites longer than 20 μm. The analyst was blind to the treatments and genotypes. Statistical significance was considered if $p \leq 0.05$ using a two-tailed student's t-test or one way ANOVA.

Immunohistochemistry

Cells and explants were fixed with 4% ice-cold PFA solution for 30-45 minutes. Cells or tissues were incubated with a combination of primary antibodies overnight at 4°C. Antibodies used were: lacZ (rabbit, ICN; 1:500), TrkC (goat, gift from Dr. L. Reichardt, UCSF; 1:200), NF200 (mouse, Sigma; 1:1000), CGRP (mouse, Sigma; 1:2000), CTB (goat, List Biological labs; 1:2000), α-tubulin (mouse, Sigma; 1:200) and GFAP (rabbit, Dako; 1:500). Visualization was achieved by tissue incubation in fluorescent or biotinylated secondary antibodies. Biotin labeled tissue was processed further with the Vectastain Elite ABC reagents (Vector Burlingame) and developed by DAB colorimetric reaction. Immunofluorescence was visualized after 1 hour incubation with appropriate Cy2-, Cy3- and Cy5-conjugated secondary antibodies (Jackson Labs; 1:400) at room temperature. The staining was then evaluated with epifluorescence and confocal (Zeiss 510) microscopy.

X-Gal Staining/DAB Immunocytochemistry

β-gal activity was detected by incubation of the tissues or sections in X-Gal/ Ferricyanide/Ferrocyanide solution which produces a blue precipitate. Sections were subsequently processed for immunocytochemical detection of CGRP or NF200 with DAB colorimetric reaction which produces a brown colored product.

DRG Cell Size Distribution Analysis

Serial frozen sections (15 μm) of DRG from adult *Rosa26;Synapsin I-Cre* reporter mice were processed for lacZ immunostaining (rabbit, Chemicon; 1:500). In cross section, sensory neurons containing a clearly visible nucleus and nucleolus were digitalized and their soma diameter evaluated using the AxioVision imaging software.

Animal Surgery

Dorsal root injury was performed on mice as previously described with modifications (Romero et al., 2001). Six experimental groups were tested in nine independent experiments: control sham (n = 4), control crushed (n = 17), control cut (n=2), *Nf1*-SynI-CKO crushed (n = 13), *Nf1*-SynI-CKO cut (n = 7), *Smad3-/-* crushed (n = 2).

After anesthesia (Ketamine 70 mg/kg and Dormitor 0.33 mg/kg, i.p), adult mice underwent unilateral hemilaminectomy to expose the L3-6 lumbar dorsal roots, which relay sensory information from the hind limb into the spinal cord, and collateralize in the dorsal spinal cord anterior-posterior for several segments. L4 and L5 roots were either crushed or cut/ligated in different groups of animals. L6 root was transected in all animals to allow us to distinguish between L4-5 regeneration and collateral sprouting from L3. Sensory information from the hind limb was transduced from sciatic nerve to lumber DRG. To visualize the proprioceptive sensory afferents, 1% cholera toxin β-subunit (CTB, List Biological labs) solution was injected into the sciatic nerve of a cohort of animals after injury. Four days after CTB injection, mice were perfused transcardially with PBS and 4% PFA. Spinal cords and DRG were removed, post-fixed, and cryoprotected overnight in 30% sucrose at 4°C. Frozen sections were cut at 20-30 μm for subsequent staining.

Behavioral Analysis

Behavior analysis was performed as previously described (Romero et al., 2001). Briefly, for the grid walking test, the accuracy of paw placement on a grid runway was measured to assess regeneration of proprioceptive axons. The animals were videotaped making two complete crossings per trial. Analysts blinded to the treatment scored foot

placement accuracy by analyzing the video in slow motion. Accurate placement of the hind paw on the pegs was scored as a correct. The percentage of correct foot placements per trial was calculated and averaged for the two trials. For toe spread index, footprints of mice were recorded in a 90-cm-long and 8-cm-wide runway on plain paper after the hind paws had been painted with ink. Before the actual experiment, the animals were trained to walk through the runway several times. The traces left by the mice were measured in 8-day intervals from day 8 to day 40 after surgery. The toe spread was estimated as the distance between the first and the fifth toes and the toe-spread index was calculated as a function of the contra-lateral non-injured paw. Raw data were analyzed by ANOVA followed by Fisher's PLSD post hoc test (StatView 4.5; Abacus Concepts).

Tissue Extraction and Western Blotting

Cortex, cerebellum, spinal cord and DRG were dissected from 8-week-old control or *Nf1*-SynI-CKO mice (n=4 each) and frozen in liquid nitrogen. Whole cell proteins were extracted and subjected to Western blot as described before (Zhu et al., 2001). Briefly, tissues were homogenized in RIPA buffer (50ml Tris-HCL, PH 7.4, 1%NP-40, 0.25% Na-deoxycholate, 150mm NaCL, 1mm EDTA, 1mm Na3VO4, 1mm NaF, Complete Mini, Roche; 1 tablet/10ml) at 0.1g tissue weight/ml, incubated on ice for 30 minutes and centrifuged at 14000 rpm for 20 minutes at 4°C. Supernatant was collected and protein concentration was determined by the BCA Protein Assay Kit (Pierce). Primary antibodies used for blotting including phospho-Erk1/2 (rabbit, 1:1000), Erk1/2 (rabbit, 1:1000), phospho-Akt (rabbit, 1:1000), Akt (rabbit, 1:1000), phospho-Gsk3β (rabbit, 1:1000) and Gsk3β (rabbit, 1:1000) were all from Cell Signaling Technology. Secondary antibodies used were HRP anti-rabbit (Santa Cruz Biotechnology; 1: 5000). Immunoreactivity was detected with ChemiGlow (Alpha Innotech), and densitometry analysis was performed with the KODAK 1D Image Analysis Software.

Results

Synapsin I – Cre is Expressed in Proprioceptive DRG Neurons

Mice with *Nf1* germ line mutation are embryonic lethal, likely due to severe heart malformation (Brannan et al., 1994). To study the role of this gene in adult sensory neurons, we used the Cre-loxP system to generate *Nf1* conditional knockout mice.

Synapsin I-Cre was neuron-specific and expressed in the majority of CNS neurons (Zhu et al., 2001). To investigate whether it is also expressed in sensory neurons, *Rosa26*-stop-lacZ Cre reporter mice were crossed with Cre-carrying animals (Soriano, 1999), and β-galactosidase activity was carefully examined inside adult DRG. X-gal staining revealed that in DRG, only a subset of neurons stained positive for β-gal, thus containing Cre activity (Fig. 3.1G). Inside DRG, different sub-types of neurons express specific Trk receptors for neurotrophins: nociceptive neurons are positive for TrkA, mechanoreceptive neurons are positive for TrkB, and proprioceptive neurons mainly express TrkC (Huang and Reichardt, 2001). To further confirm the sub-type of DRG neurons in which Synapsin I-Cre is expressed, we performed double immunofluorescent staining for lacZ (Fig. 3.1B) and TrkC (Fig. 3.1A). 71% of TrkC positive neurons were also positive for lacZ (Fig. 3.1C and 3.1D), indicating in *Nf1*-SynI-CKO mice, and the majority of proprioceptive neurons have Cre activity and are expected to undergo *Nf1* deletion. We also performed size distribution analysis of perikaryal diameter of lacZ-expressing cells. In DRG, proprioceptive sensory neurons represent the majority of histologically distinguishable large-diameter neurons, while small-diameter neurons are nociceptive (Averill et al., 1995; Molliver et al., 1995). A majority (73.97%) of lacZ positive neurons exhibited large diameter (>22 μm; Fig. 3.1E and 3.1F) and co-localized with the proprioceptive marker NF200 (Fig. 3.1H) (Goldstein et al., 1991; Lawson et al., 1993). Consistent with this, lacZ staining did not co-localize with the nociceptive marker calcitonin gene-related peptide (CGRP; Fig. 3.1G) (Traub et al., 1990).

Taken together, our data indicate that DRG neurons undergoing Synapsin I-Cre mediated *Nf1* deletion primarily express TrkC and are proprioceptive neurons.

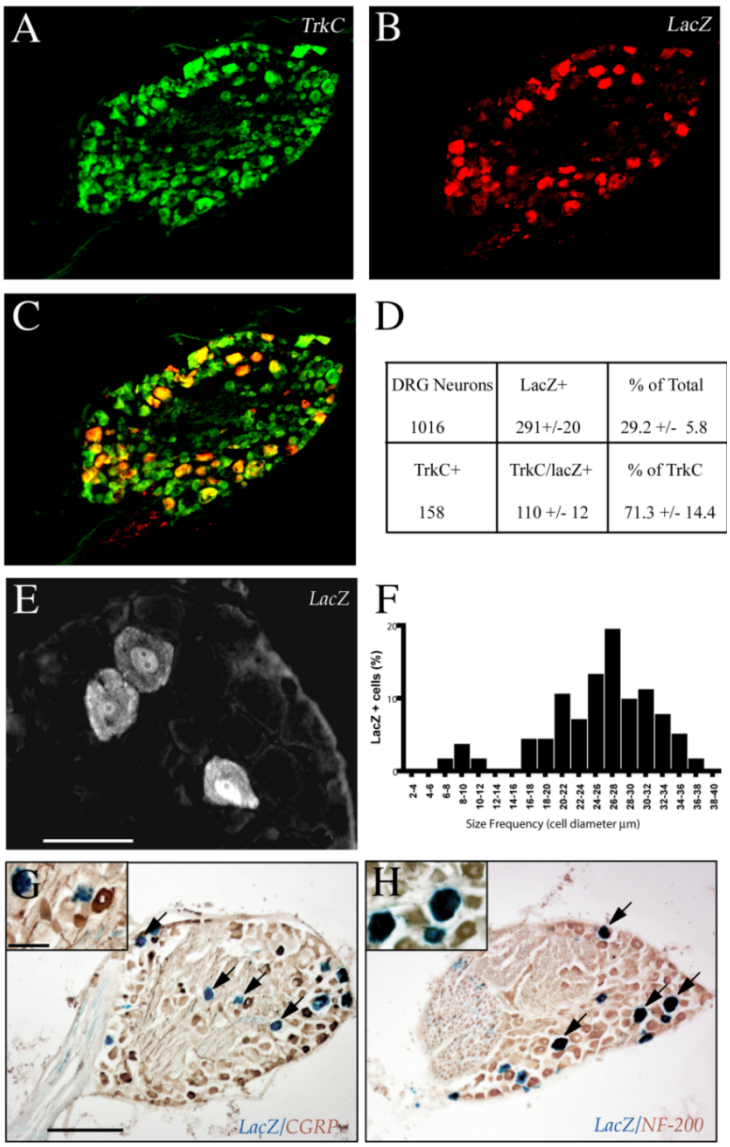

DRG Neurons	LacZ+	% of Total
1016	291+/-20	29.2 +/- 5.8
TrkC+	TrkC/lacZ+	% of TrkC
158	110 +/- 12	71.3 +/- 14.4

Fig. 3.1. Synapsin I-Cre is expressed in proprioceptive DRG neurons. Double labeling of TrkC (A) and lacZ (B) in thoracic and lumbar DRG neurons in adult *Rosa26;Synapsin I-Cre* mice revealed that the majority of lacZ positive cells were TrkC positive, thus proprioceptive in nature (C; merged image). Quantification of 1016 DRG neurons from 3 different ganglia showed that 29.2 ± 5.8% of them were lacZ positive, thus undergo Cre-mediated recombination (D). Size distribution analysis of lacZ positive cells indicated that the majority of the recombined cells were the size of proprioceptive neurons (>22 µm in diameter: E, F). Co-localization of lacZ with NF-200 (Ia proprioceptive cells; H, arrows), but not with CGRP (C-type nocioceptive neurons; G, arrows) further confirmed the proprioceptive nature of most Cre-recombined DRG neurons. Scale bars = 50 µm for A-C and E; 200 µm for G and H; 50 µm for insets.

Adult *Nf1-/-* DRG Neurons Exhibit Increased Axon Growth in vitro

Previous studies in our lab have shown that *Nf1-/-* embryonic sensory neurons can survive in the absence of neurotrophic support (Vogel et al., 1995). Although the survival of adult sensory neurons in culture is not dependent on neurotrophins, these trophic factors can stimulate neurite outgrowth and sprouting of these neurons (Hu-Tsai et al., 1994). The loss of *Nf1* should mimic neurotrophic stimulation, thus enhancing the intrinsic growth capacity of adult DRG neurons *in vitro*. To test this hypothesis, adult DRG explants from control and *Nf1*-SynI-CKO mice were cultured in the absence of neurotrophins and their axonal growth was evaluated. Compared to controls (Fig. 3.2A, and 3.2B), explants from *Nf1*-SynI-CKO mice showed increased axonal length (Fig. 3.2C and 3.2D). Despite the fact that only a small percentage of DRG neurons were *Nf1* deficient, quantitative analysis showed a significant increase in axonal growth of adult *Nf1*-SynI-CKO DRG neurons (Fig. 3.2E). These results demonstrate that adult sensory neurons lacking *Nf1* have increased capacity for neurite outgrowth in *vitro*.

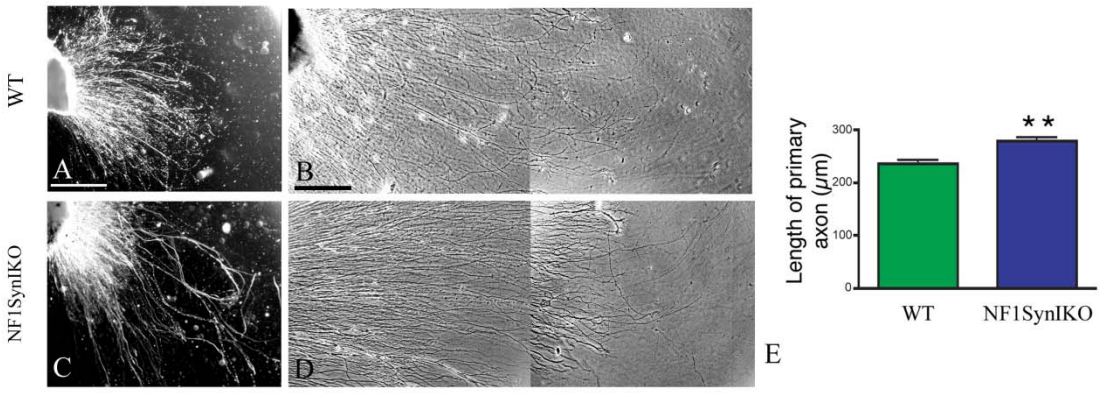

Fig. 3.2. *Nf1-/-* adult DRG neurons exhibit enhanced axonal growth. Compared to control (A, B), a subset of neurons in the adult *Nf1*-SynI-CKO DRG explants growed longer axons (C, D). (E) Quantitative analysis confirmed that longer axons were present in the *Nf1*-SynI-CKO DRG (278.5 ± 6.8μm vs. 235.6 ± 6.6μm). Scale bars = 250 μm for A and C; 100 μm for B and D. Two-tailed student's t-test. Data represents mean ± SEM.

_Nf1_-SynI-CKO Mice Spontaneously Recovered Proprioceptive Functions after Dorsal Rhizotomy

To examine whether the increased axonal growth properties of *Nf1-/-* adult DRG neurons in culture might have effects on regenerative response of these neurons *in vivo*, we tested the ability of *Nf1*-SynI-CKO mice to recover from unilateral dorsal rhizotomy. Pain and proprioceptive information is relayed into the spinal cord through central dorsal root axonal projections from DRG neurons. After crush injury, these axons undergo spontaneous regeneration through the PNS compartment but abort their growth at the DREZ (PNS-CNS interface), causing denervation of the dorsal spinal cord and consequent permanent sensory-motor deficits (Carlstedt et al., 1987; Golding et al., 1999). Cut and ligated roots are prevented from any regeneration (Romero et al., 2001).

Crush or transection injuries were performed on L4-5 dorsal roots, which carry the majority of the primary hind limb sensory afferents. L6 root was also cut in all animals, so that lumbar spinal cord in L4-5 crushed injured animals were expected to bear axons from L3 collateral branches into the denervated area, as well as L4-5 axons that might have regenerated though the DREZ into the spinal cord. In sharp contrast, animals with cut and ligated L4-5 were expected to have only L3 afferents into the lumbar spinal cord at the L4-5 entry levels.

We first used the L4-5 crush paradigm (Fig. 3.3A). All mice exhibited immediate loss of limb function after injury as assessed by behavioral analysis for nociception (plantar pinch test) and proprioception (Fig. 3.3B-3.3F; abductor reflex, grid walking, and paw print tests). However, in contrast to the permanent sensory loss observed in control animals, *Nf1*-SynI-CKO mice showed gradual recovery of proprioceptive function as early as three weeks post surgery as indicated by grid walking (Fig. 3.3C) and abductor reflex analysis (Fig. 3.3E). Quantification of accurate paw placement during grid walking by slow motion video analysis demonstrated significant functional deficits in all injured animals after dorsal rhizotomy during the first two weeks post-injury (Fig. 3.3F; supplemental data No. 2 (Romero et al., 2007)). Thereafter, *Nf1*-SynI-CKO mice began to show recovery (Fig. 3.3F). To examine whether functional recovery could be due to an overcoming of CNS impediments at the DREZ (glial scar formation and myelin mediated inhibition), a cohort of mice were subjected to L4-5 sensory afferent transection and

ligation (Fig. 3.3A). Surprisingly, the L4-5 "cut and ligated" *Nf1*-SynI-CKO mice also recovered limb function (Fig. 3.3F; supplemental data No. 3, (Romero et al., 2007)). In contrast, all control mice exhibited permanent functional deficits (Fig. 3.3F; supplemental data No. 4, (Romero et al., 2007)).

Walking patterns assessed by paw print analysis (Fig. 3.4A) also showed permanent unilateral deficits in paw placement (claw foot) in all control injured animals, including *Smad-3*-/- mice (see below). In contrast, conditional *Nf1* mutants regained normal foot placement after the third week post injury. Further analysis of paw prints demonstrated significant reduction in toe spread index (Fig. 3.4B). This reduction was permanent in injured control animals. Conversely, *Nf1* conditional mutants showed significant improvement in toe spreading, evident in the third week post injury. To additionally control for possible non-specific effects due to animal size, as well as to "blind" the surgeon to the genotype of the animals, we included *Smad-3*-/- animals in our study. Like *Nf1*-SynI-CKO mice, *Smad-3*-/- mice are small (Zhu et al., 1998; Zhu et al., 2001) and therefore visually indistinguishable. After dorsal rhizotomy, injured *Smad-3*-/- animals showed permanent functional deficits similar to injured control mice (Fig. 3.3F and 3.4, supplemental data No. 5, (Romero et al., 2007)).

Despite the apparent recovery of proprioceptive function by the *Nf1* deficient mutants, all injured animals showed permanent nociceptive sensory loss, failing to respond to plantar pinch stimulation.

Taken together, our data indicated that Synapsin I-Cre mediated *Nf1* deletion in neurons renders mice capable of functionally overcoming loss of L4-5 afferent innervation but not through regeneration of injured axons.

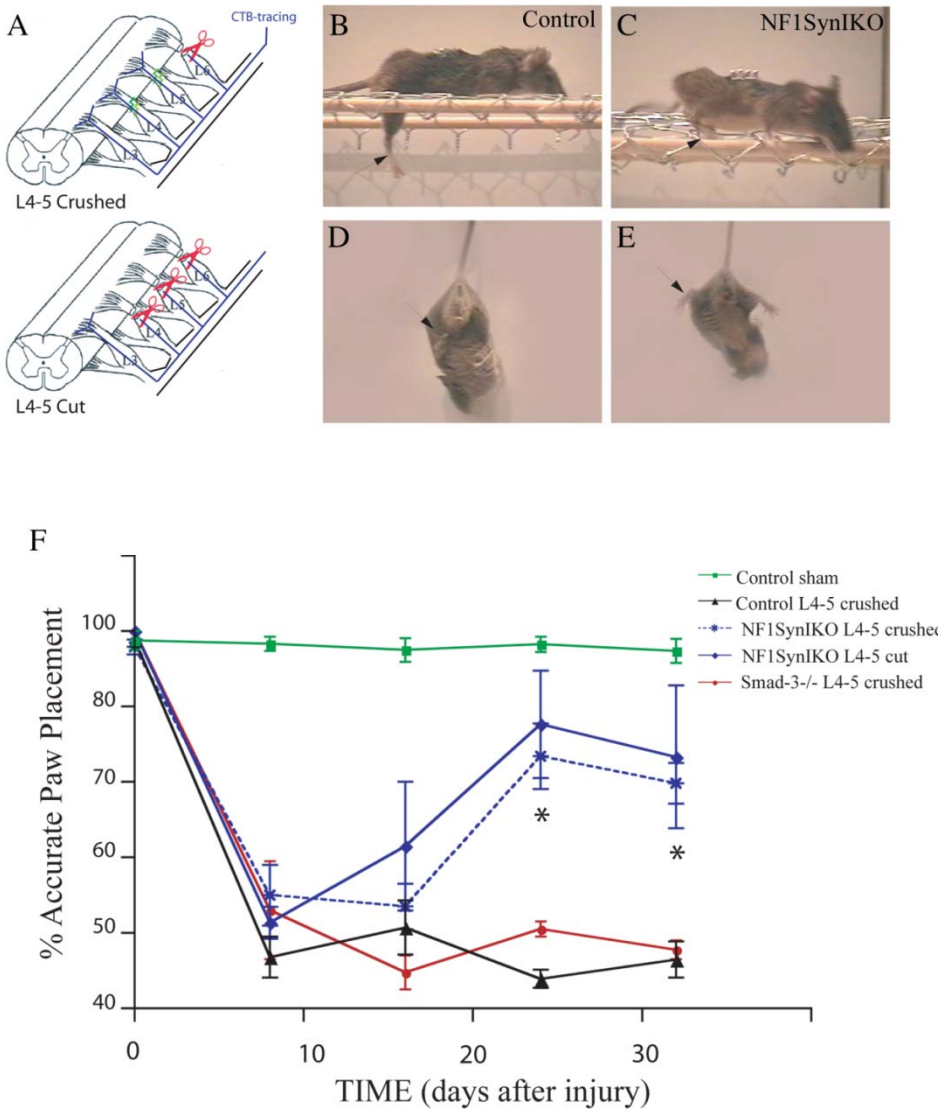

Fig. 3.3. *Nf1*-SynI-CKO mice spontaneously recover proprioceptive function after sensory denervation (in collaboration with Dr. Mario Romero). (A) Diagrammatic representation of the injury paradigm. L4-5 dorsal roots were either crushed or cut. Distinction between L4-5 regeneration and collateral sprouting from L3 was achieved by transecting L6 in all animals. Labeling of proprioceptive axons was achieved by injection of the cholera toxin β-subunit tracer (CTB) into the sciatic nerve. Compared to control mice (B, D), *Nf1*-SynI-CKO mice spontaneously recovered proprioceptive functions (C, E), as indicated by regaining accurate locomotion in the grid assay, as well as deploying normal abductor responses. (F) Compared to normal sham controls (n=4), paw placement accuracy was dramatically and permanently reduced after L4-5 crush injury in control animals (n=7). In contrast, *Nf1*-SynI-CKO mice recovered capacity for precise paw placement after either crush (59.60 ± 5.42%, n=5) or cut (66.66 ±

18.94%, n=3) L4-5 injuries compared to permanent functional deficits in control mice (12.96 ± 4.77%) and *Smad-3-/-* mice (9.50 ± 4.50%) after crush injuries. * = P < 0.001. ANOVA with Fisher's test. Data represents mean ± SEM.

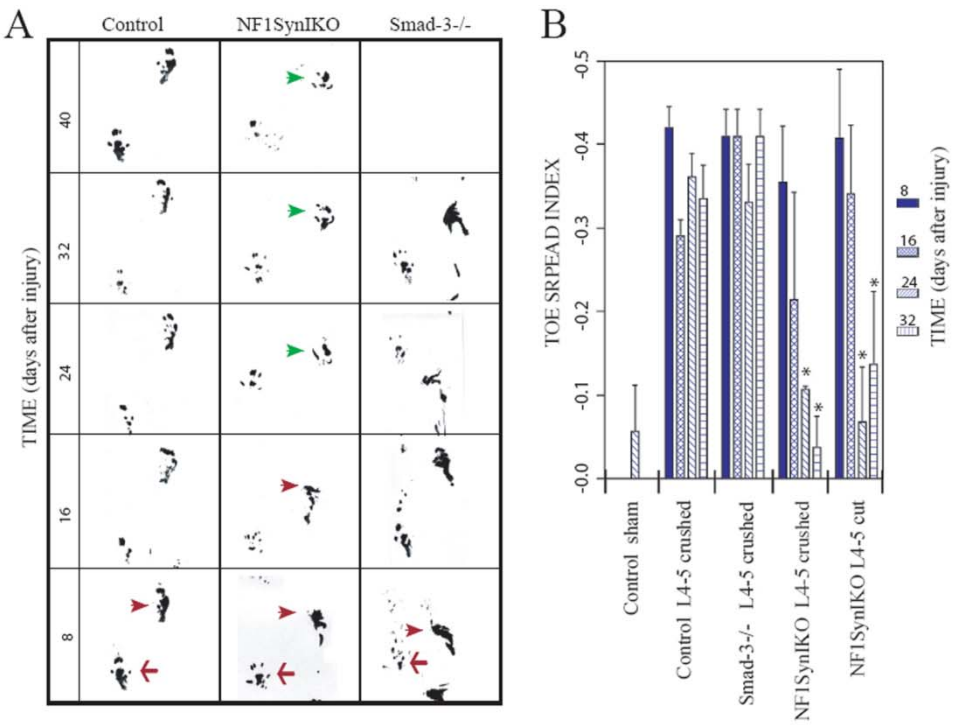

Fig. 3.4. Paw print analysis (in collaboration with Dr. Mario Romero). (A) Abnormal "claw foot" prints of the affected hind limb (red arrowhead) were observed in all animal genotypes at 8 days after unilateral dorsal rhizotomy, compared to the non-injured side (red arrow). This functional deficit was permanent in control and *Smad3*-/- mice (>32 days post injury). Conversely, mice bearing a conditional *Nf1* mutation showed spontaneous recovery of their hind limb use, evident at the third week post lesion (green arrowhead). (B) Quantitative analysis of the toe spread index, corroborates the ability of *Nf1*-SynI-CKO conditional mutants (n=6; -0.10 ± 0.05) to spontaneously regain proper use of their affected hind limb, as compared to injured control (n=6; -0.34 ± 0.04) and *Smad3*-/- (n=2; -0.41 ± 0.03) mice. * = P < 0.001. ANOVA with Fisher's test. Data represents mean ± SEM.

Proprioceptive Primary Afferents from Uninjured *Nf1-/-* Neurons Sprout into the Denervated Spinal Cord

Previous studies suggested that DRG axons cannot regenerate into DREZ after dorsal root injury unless certain pre-conditional injuries were performed or neurotrophic factors were added (Chong et al., 1999) (Neumann and Woolf, 1999) (Romero et al., 2001). We first examined whether the functional recovery of *Nf1*-SynI-CKO mice we observed was due to increased re-growth of injured axons into the spinal cord. By using NF-200 staining to visualize DREZ at the lumbar level, we found that all mutant and control surgically injured mice (crushed, or cut and ligated) exhibited a typical glial scar that correlates with the absence of NF-200 positive fibers penetrating through DREZ (supplemental data 6, (Romero et al., 2007)). Thus, permanent denervation occurs in all animals after dorsal rhizotomy and injured *Nf1-/-* neurons showed no significant regenerative advantage after this type of injury.

Since *Nf1*-SynI-CKO mice recovered proprioceptive functions even after cut and ligation injury, we hypothesized that spared DRG collaterals are sprouting into the injured area and providing partial functional compensation. To examine whether *Nf1* deletion induces spontaneous abnormal sprouting, double immunofluorescence staining was performed at different spinal cord levels of uninjured control and *Nf1*-SynI-CKO mice. We combined tract-tracing of proprioceptive primary afferents via transganglionic transport of CTB label from the ipsilateral sciatic nerve, with visualization of nociceptive afferents by CGRP signals (Rivero-Melian et al., 1992). Compared to controls (Fig. 3.5A-3.5C, 3.5G-3.5I), mice lacking neuronal *Nf1* showed no visible difference in the labeling of pain fibers by CGRP (Fig. 3.5D-3.5F) or proprioceptive fibers by CTB (Fig. 3.5J-3.5L) in the lumbar-sacral spinal cord. Both the staining intensity and afferent distribution were indistinguishable from the aged-matched controls. We concluded that the loss of *Nf1* does not affect the normal development of sensory primary afferents from DRG neurons into the spinal cord.

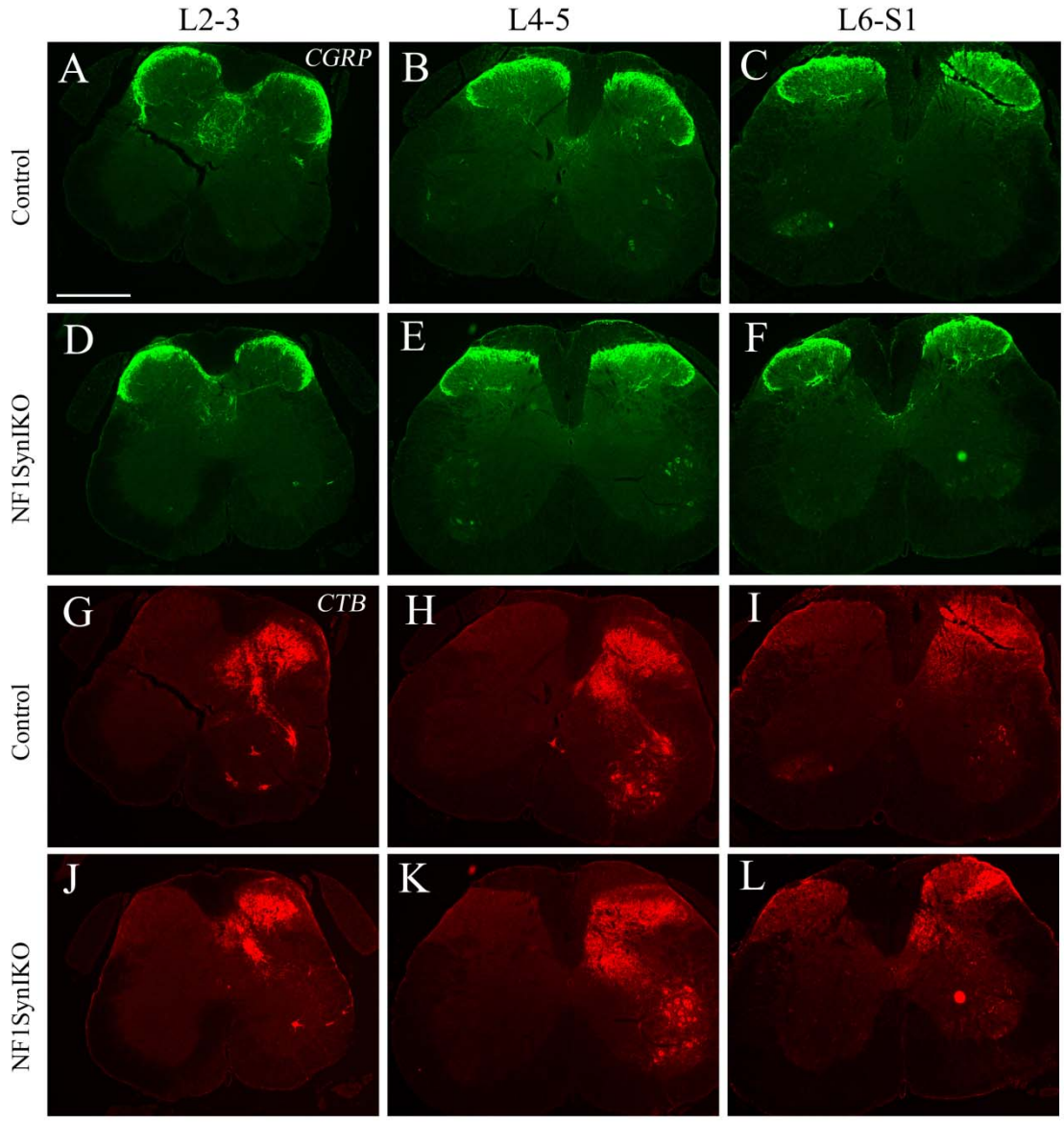

Fig. 3.5. Uninjured *Nf1*-SynI-CKO mice possess normal nociceptive and proprioceptive afferents. Staining of proprioceptive (CTB; red) and nociceptive (CGRP; green) fibers in the lumbar-sacral spinal cord showed that compared to controls (A-C, G-I), CGRP innervation in lamina II, and CTB innervation in laminae III-V did not increase in uninjured *Nf1*-SynI-CKO mice (D-F, J-L, respectively). Coronal sections were shown at different anterior-to-posterior lumbar-sacral spinal cord levels: Lumbar 2-3 (A, D, G, J), Lumbar 4-5 (B, E, H, K), and Lumbar 6-Sacral 1(C, F, I, L). CTB-labeling of ventral motor neurons (Lumbar 4-5) served as positive control for tracing. Scale bar = 250 μm.

We then evaluated pain and proprioceptive sensory innervation to the spinal cord in injured animals. Analysis of sagittal sections of the spinal cord at the L4-5 DREZ of control mice with either cut or crushed dorsal rhizotomies demonstrated that CTB-positive fibers were mostly absent from dorsal horn laminae III-V (Fig. 3.6A and 3.6B). In contrast, *Nf1*-SynI-CKO mice with either type of injury demonstrated robust labeling of proprioceptive axons in deep dorsal horn laminae (Fig. 3.6C and 3.6D). These results were confirmed by simultaneous visualization of CTB-labeled and CGRP-positive fibers in coronal sections of the spinal cord at the L4-5 level (Fig. 3.6E-3.6P). CTB-labeled proprioceptive fibers and CGRP-labeled nociceptive afferents occupied non-overlapping target areas in laminae III-X, and lamina II, respectively (Fig. 3.6E, 3.6I and 3.6M). Compared to sham controls, both CTB and CGRP labeling of primary afferents were lost after crush injury in control animals (Fig. 3.6F, 3.6J and 3.6N). Conversely, *Nf1*-SynI-CKO mice with either crushed (Fig. 3.6G, 3.6K and 3.6O) or cut (Fig. 3.6H, 3.6L and 3.6P) dorsal roots, showed robust labeling of CTB-positive axons, and to a lesser extent of CGRP nociceptive fibers, throughout the lumbar spinal cord. The amount of CTB-positive fibers in the injured *Nf1*-SynI-CKO mice was somewhat variable. However, compared with the absolute absence of Ia afferents in the injured control mice (0 of 4), these fibers were unequivocally present in most of the *Nf1-/-* animals with crushed (4 of 5) and cut lesions (4 of 4), respectively. This difference is unlikely to be due to variable tract-tracing of these fibers, since positive CTB labeling of motor neurons in the ventral spinal cord was demonstrated for all animals (Fig. 3.6A-3.6D left inset; 3.6E-3.6H asterisks). The visualization of proprioceptive fibers in animals in which regeneration of the dorsal roots was prevented by the transection/ligation protocol ruled out any possibility of functional recovery being mediated via L4-5 DRG. These data therefore indicate a greatly enhanced sprouting potential of uninjured (L3 sensory) neurons that lack *Nf1 in vivo.*

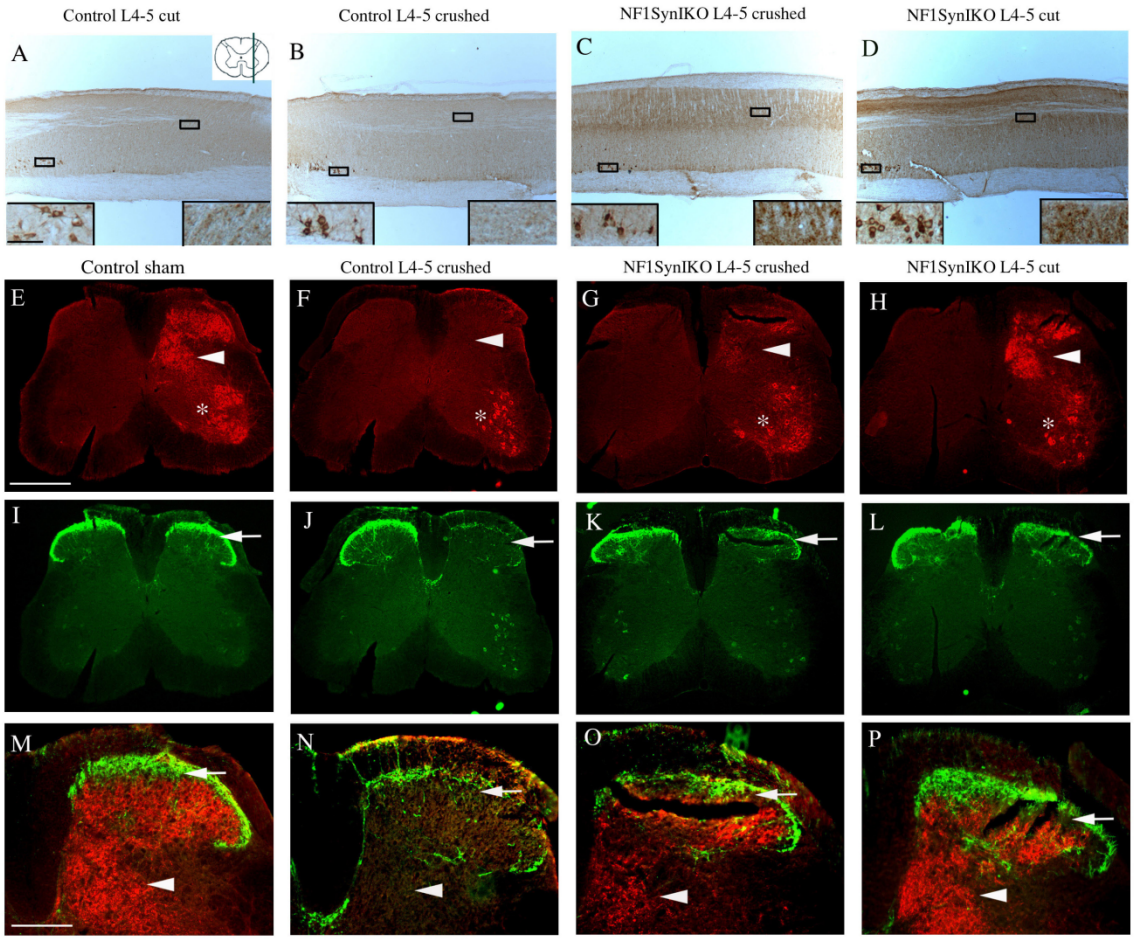

Fig. 3.6. *Nf1* deletion enhances axonal sprouting of uninjured proprioceptive afferents (in collaboration with Dr. Mario Romero). (A-D) Visualization of Ia fibers by CTB-tracing in parasagittal sections of the lumbar spinal cord, taken at approximately similar levels from the midline (see upper corner inset in A). Control animals showed a dramatic reduction of proprioceptive afferents in deep dorsal horn laminae after L4-5 cut or crush rhizotomy (A, B, right insets), despite efficient tracing of the ventral motor neurons (left insets). In contrast, robust CTB-labeling was observed in *Nf1*-SynI-CKO mice with either crushed (C), or cut-ligated (D) L4-5 injuries. (E-P) Double immunofluorescence of proprioceptive (CTB; red) and nociceptive (CGRP; green) fibers in the dorsal spinal cord at L4-5 DREZ level, showed that compared to sham controls (E, I, M), CGRP innervation in lamina II (arrows), was reduced in all injured animals (J, K, L). However, CTB innervation in laminae III-V (arrowheads), lost after crush injury in control animals (F, N), was evident in the dorsal horn of *Nf1*-SynI-CKO mice with either crush (G, O), or cut injuries (H, P), indicating the sprouting of L3 afferents into L4-5 ventral motor neurons. Scale bars = (A; inset) 60µm, (E) 250 µm and (M) 100 µm.

Spinal Cord from *Nf1*-SynI-CKO Mice Contribute to the Sprouting Activity of *Nf1*-/- DRG

The increase in axonal branching we observed after dorsal rhizotomy in *Nf1*-SynI-CKO mice could be explained by the cell-autonomous capacity of *Nf1*-/- DRG neurons for collateral branching and neurite growth, as suggested by the increased axonal growth of DRG neurons *in vitro* (Fig. 3.2). However, because Synapsin I-Cre is also active in some neurons of the spinal cord (Zhu et al., 2001), it remains possible that the absence of *Nf1* in the denervated region could contribute in a paracrine manner to the compensatory sprouting by spared L3 afferents.

To address this possibility, we co-cultured control or *Nf1*-SynI-CKO DRGs together with control or *Nf1*-SynI-CKO spinal cord (SC) explants, and evaluated their growth response. Consistent with previous experiments (Fig. 3.2), *Nf1*-deficient sensory neurons exhibited enhanced intrinsic capacity for outgrowth (Fig. 3.7A and 3.7B). To specifically trace the growth of proprioceptive neurons in the DRG explants, we injected a separate cohort of adult animals with CTB in the sciatic nerve, 4 days before harvesting L4–L5 DRGs. The pre-labeled ganglia were then co-cultured with either control or *Nf1*-SynI-CKO SC and processed for the co-visualization of CTB, CGRP, and the general axonal marker β-tubulin. Non-overlapping labeling of proprioceptive and nociceptive neurons was seen in all DRGs (Fig. 3.7C), demonstrating the equal viability and efficient tract-tracing of the proprioceptive neurons. Axonal labeling by β-tubulin showed a qualitative increase in neurite growth from the *Nf1*-SynI-CKO DRG compared to control ganglia, whether co-cultured with control or *Nf1*-/- SC slices (Fig. 3.7C). Quantitative analysis performed on CTB-positive neurites showed almost threefold increase in axonal length of *Nf1*-SynI-CKO DRG compared with those from control animals, when co-cultured with control SC (Fig. 3.7D). Moreover, when cultured with SC from *Nf1*-SynI-CKO mice, the *Nf1*-deficient ganglia showed up to twofold enhancement in axonal length over that observed with the control SC. No significant effect of the *Nf1*-SynI-CKO SC was observed on control DRG (Fig. 3.7C and 3.7D). This effect cannot be explained by differential neuron survival in the cultured *Nf1*-/- spinal cord slices, because labeling of dead cells using PI dye was comparable with control slices (Fig. 3.8).

These results demonstrate the increased capacity for axonal elongation in proprioceptive neurons from *Nf1*-SynI-CKO mice, and indicate that *Nf1* loss in the spinal cord may also contribute to the enhancement of *in vivo* spared nerve sprouting and thus to the spontaneous functional recovery of *Nf1*-SynI-CKO mice after dorsal rhizotomy.

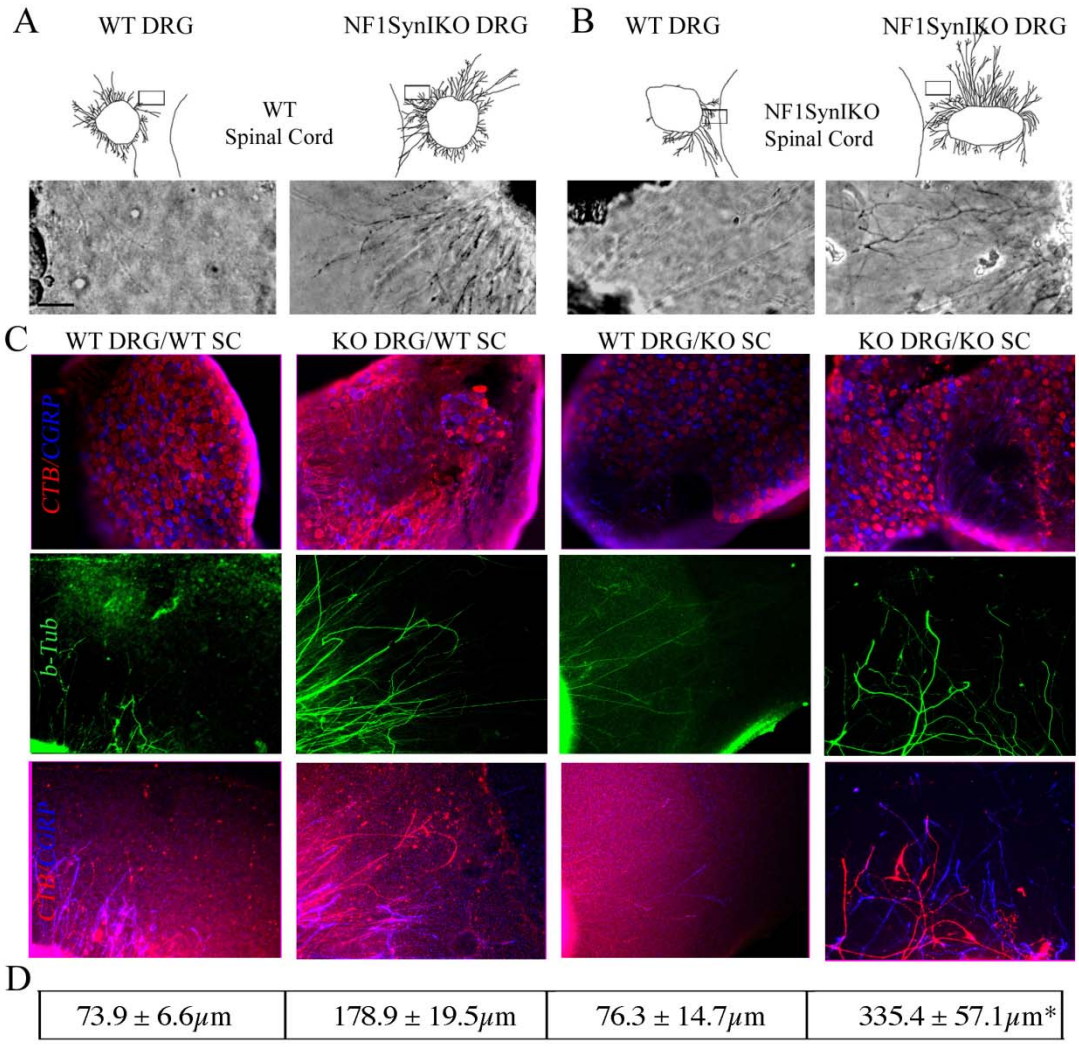

Fig. 3.7. *Nf1*-SynI-CKO spinal cord (SC) enhances axon growth of *Nf1*-SynI-CKO DRG. Co-culture of control and *Nf1*-SynI-CKO DRG explants with control (A) or *Nf1*-SynI-CKO SC (B) showed increased neurite growth of the *Nf1*-SynI-CKO explants compared to control DRG in either condition. (C) Triple immunofluorescence analysis demonstrated the non-overlapping labeling of proprioceptive and nociceptive neurons (CTB: red, CGRP: blue, β-Tubulin: green), and a qualitative increase in axonal growth of *Nf1*-/- ganglia. (D) Quantitative analysis of CTB-

positive neurites showed a two-fold increase in axonal length of *Nf1*-SynI-CKO DRG when co-cultured with control SC. Moreover, when cultured with SC from conditional mutants, the *Nf1*-SynI-CKO ganglia showed a four-fold increase in axonal length over that of WT DRG/WT SC cultures, demonstrating the synergistic effect of the *Nf1*-/- SC on the *Nf1*-/- DRG. Tracings of whole DRG explants and micrographs of axons in each explant were shown according to their actual placing in relation to the SC slices. Squares indicate the photographed area. Scale bar = 50 μm. * = $P<0.01$, KO DRG/WT SC vs. KO DRG/KO SC. ANOVA Newman/Keuls multiple comparisons. Data represents mean ± SEM. of 6-38 axons per treatment group.

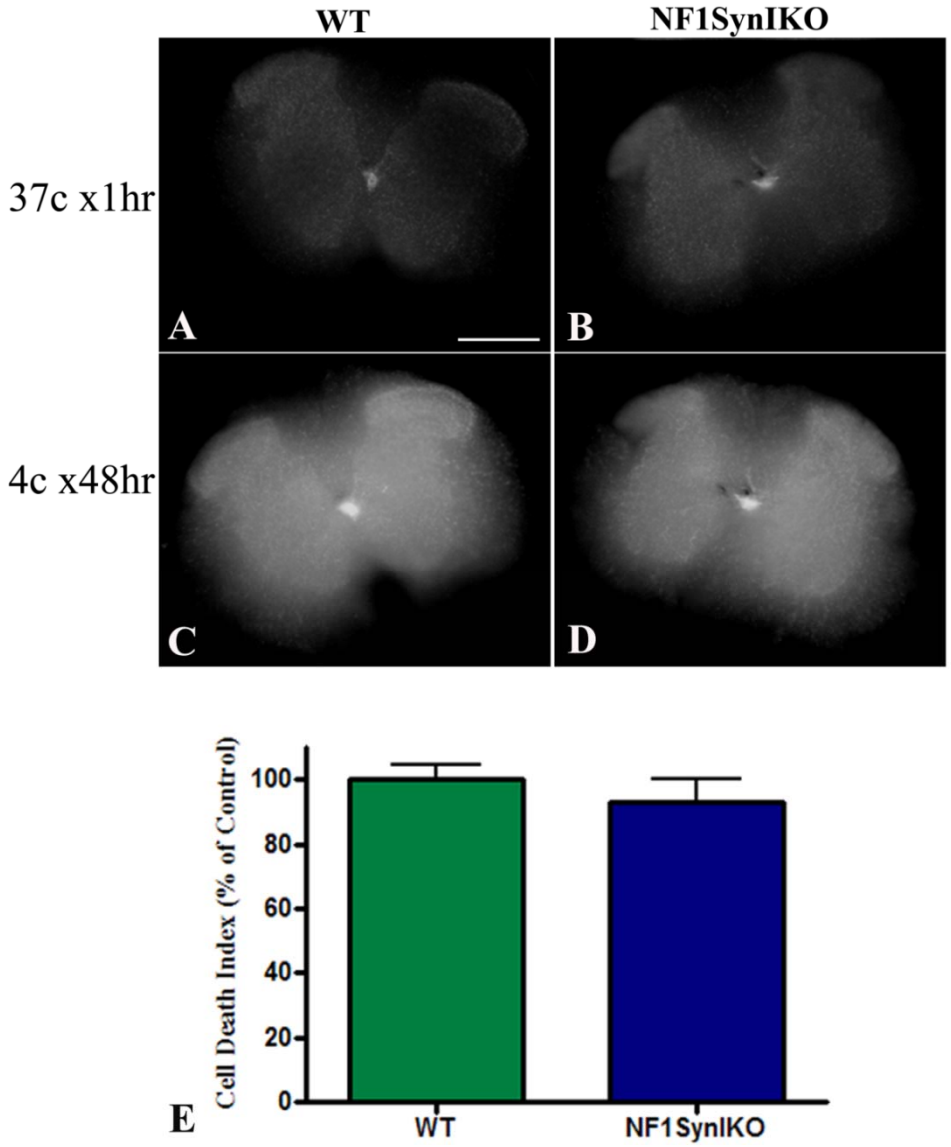

Fig. 3.8. *Nf1*-/- spinal cord slices have no survival advantage. After 48 hours in culture, Propidium iodide (PI) was added 1 hour prior to imaging. Minimal fluorescence from dead cells was observed in slices of either WT (A) or *Nf1*-SynI-CKO (B) spinal cords, compared to that induced after another 48 hour cooling at 4°C (C, D). The cell death index was reported as the fluorescent intensity at 1 hour divided by that recorded after 48 hour at 4°C. No statistical difference in cell death index was observed between WT and *Nf1*-SynI-CKO slices (E). Scale bar = 250 μm. Student's t-test. Numerical values were expressed in the figures as percentage of control. At least 10 slices from 2 different animals of each genotype were included.

The Loss of *Nf1* Results in Hyper-activation of MEK-ERK Pathways

To investigate the molecular mechanism underlying the enhanced intrinsic growth capacity of the *Nf1*-/- DRG neurons, we sought to evaluate the status of Ras-dependent pathways. In agreement with our previous report (Zhu et al., 2001), we found elevated levels of activated MEK-ERK pathway (phospho-ERK1/2, pERK) in the *Nf1*-SynI-CKO cerebral cortex, cerebellum, and spinal cord. In addition, we observed a 2-fold increase of pERK levels in *Nf1*-/- DRG compared to control littermates (Fig. 3.9). These data corroborate our previous observations in the *Nf1*-SynI-CKO CNS, and extend that to DRG, demonstrating the constitutive activation of the Raf-MEK-ERK signaling pathway in the *Nf1*-SynI-CKO PNS.

The PI3K-Akt-glycogen synthase kinase 3β (GSK3β) cascade has also been associated with neurotrophin-induced survival and neurite outgrowth (Zhou et al., 2004). In contrast to the changes observed with pERK in CNS, the phosphorylation and activated state of Akt (phospho-Akt, pAkt) and inactive state of GSK3β (phospho-GSK3β, pGSK3β) in different *Nf1*-SynI-CKO CNS regions were comparable to those of controls (Fig. 3.9). In adult *Nf1*-/- DRG, however, pAkt levels appeared to increase and pGSK3β levels appeared to decrease compared to controls (Fig. 3.9), although these values do not reach statistical significance. Together, these data demonstrate a differential activation of Ras-effector cascades in response to *Nf1* deletion in CNS and PNS neurons, and reveal a possible co-activation of both the Raf-MEK-MAPK and the PI3K-Akt-GSK3β cascades in Ras-deregulated *Nf1*-/- adult DRG neurons.

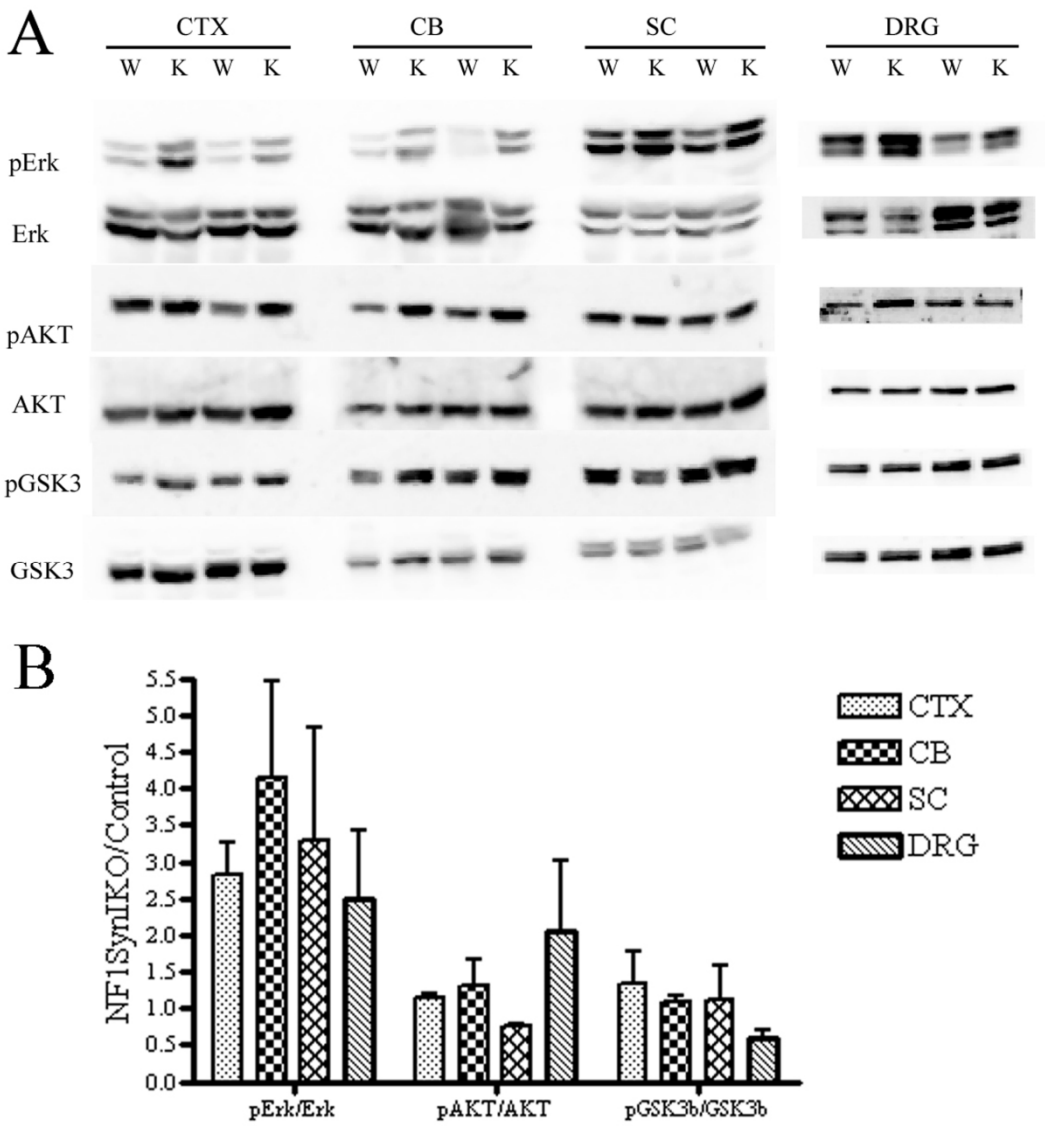

Fig. 3.9. MEK-ERK pathway is activated in the CNS and DRG of *Nf1*-SynI-CKO mice. (A) Western blot visualization of phospho-Erk1/2, Erk1/2, phospho-Akt, Akt, phospho-Gsk3β, and Gsk3β in the cerebral cortex (CTX), cerebellum (CB), spinal cord (SC) and dorsal root ganglia (DRG) from control (W) and *Nf1*-SynI-CKO (K) animals. (B) Densitometry quantification of phospho/non-phospho protein ratio (n=4 for each genotype) shows increased relative amounts in phospho-Erk1/2 in all tissues of *Nf1*-SynI-CKO. Although phospho-Akt level appears to increase in DRG of some *Nf1*-SynI-CKO mice, the average difference is not significant from controls. Data represents mean ± SEM.

Comparison of Different Cre-carrying Mouse Lines

To further investigate whether the *in vivo* phenotype of *Nf1*-SynI-CKO mice after injury is attributed to SC or DRG neurons or both, we obtained two different Cre lines with more specific and broader expression in DRG: Peripherin1-Cre and Islet1-Cre. Peripherin1-Cre is expressed in all types of sensory neurons (TrkA, B and C) from E14 (Zhou et al., 2002). Islet1-Cre is expressed in almost all sensory neurons as well as in spinal cord motor neurons (Srinivas et al., 2001). *Rosa26*-stop-lacZ reporter mice were used to examine their expression pattern. β-gal activity was detected in about 50% of DRG neurons in *Rosa26;Peripherin1-Cre (R26;Prph1)* mice with no neuronal-subtype preference (Fig. 3.10 E and 3.10G). No obvious Cre activity was seen outside the DRG (Fig. 3.10A and 3.10C). In *Rosa26;Islet1-Cre (R26;Isl1)* mice, almost 100% of DRG neurons were β-gal positive (Fig. 3.10F and 3.10H). However, Islet1-Cre was also expressed in hind limb (Fig. 3.10B), brain (Fig. 3.10D) and other organs (see Chapter IV). These data suggest Peripherin1-Cre and Islet1-Cre may be better tools for us to study the role of *Nf1* in adult DRG neurons *in vivo*.

We then crossed $Nf1^{floxflox}$ mice with these two Cre lines to generate *Nf1*-Prph1-CKO and *Nf1*-Isl1-CKO mice. *Nf1*-Prph1-KO mice showed normal life span and normal appearance. DRG explants from these mice were subjected to neurite growth assay and Western blot. To our surprise, no significant growth advantage or hyper-activation of MEK-ERK pathway was observed in mutant DRG compared to controls (Fig. 3.11). *Nf1*-Isl1-CKO mice exhibited decreased body weight and shorter life span compared to controls. Detail characterization of these mice will be included in Chapter IV. The comparison of three different *Nf1*-CKO mice was summarized in Table 3.1.

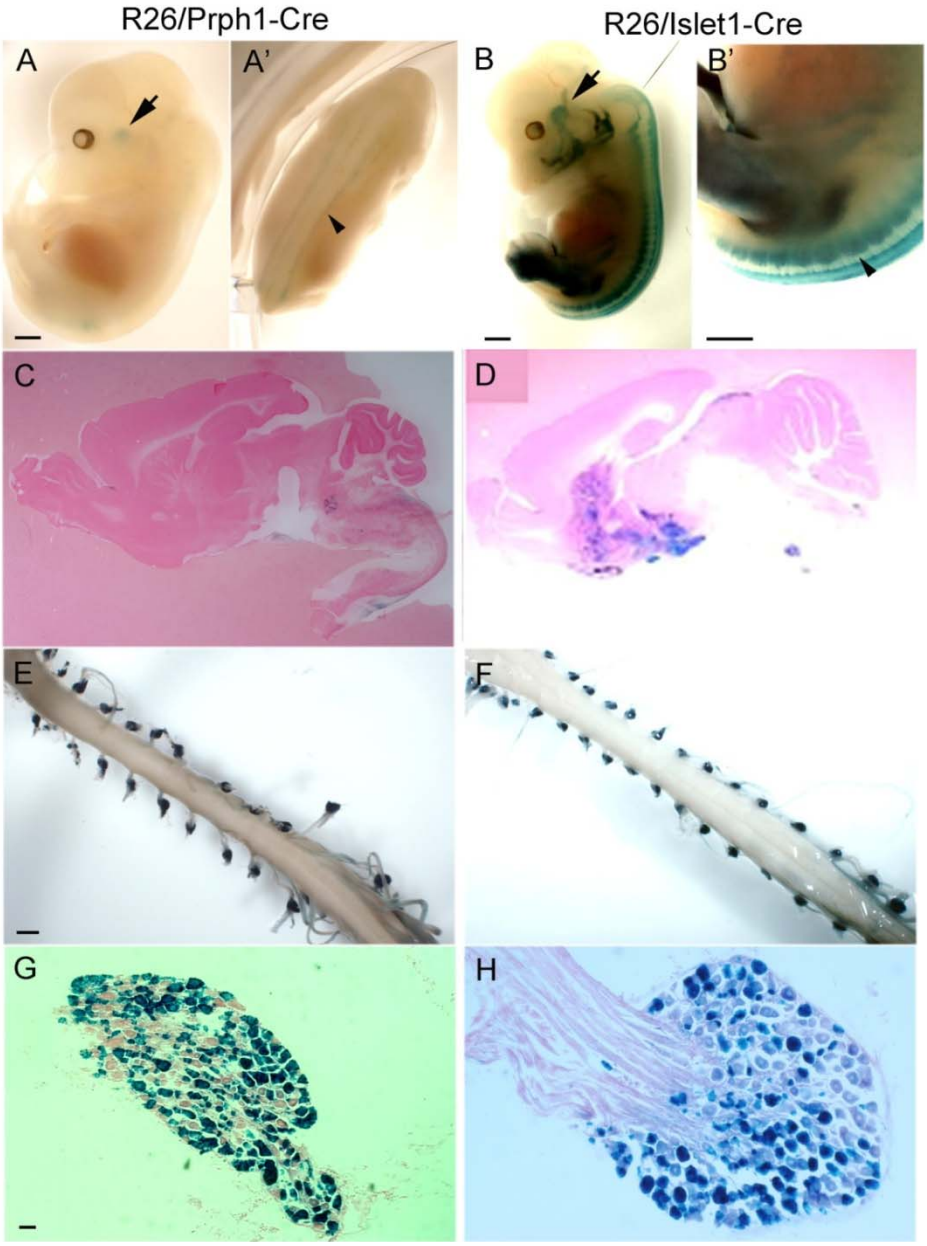

Fig. 3.10. Comparison of expression pattern of Peripherin I-Cre and Islet1-Cre in adult nervous system. *R26;Prph1* and *R26;Isl1* mice were subjected to X-gal staining at different stages. Prph1-Cre was expressed in TG (arrow in A) and DRG (arrowhead in A') at E14.5; in adulthood, Cre expression was restricted to DRG (C, E, G), with about 50% of DRG neurons were lacZ positive (G). Isl1-Cre was expressed in TG (arrow in B), DRG (arrowhead in B'), hind limb (B) and other tissues (not shown) at E12.5. In adult mice, Cre was expressed in part of the brain (D) and almost 100% of DRG neurons (F, H). Scale bars = 1mm in A-F; 100 μm in G and H.

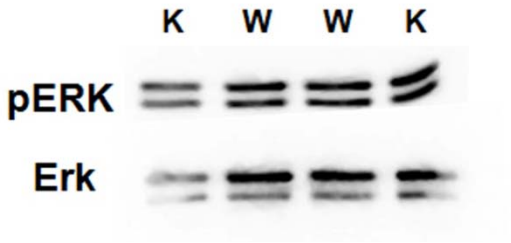

Fig. 3.11. MEK-ERK pathway is not activated in *Nf1*-Prph1-CKO DRGs. DRG from adult *Nf1*-Prph1-CKO mice were subjected to Western blot analysis. No significant difference in the level of pERK was observed between control (W) and mutant (K).

	Synapsin I-Cre	**Peripherin1-Cre**	**Islet1-Cre**
Expression onset	E11	E14	E9.5
Expression pattern	DRG; cortex, cerebellum SC neurons,	DRG; trigeminal ganglia; olfactory epithelium	DRG; SC motor neurons; brain; outside NS
***Nf1*-CKO**	Runty	Indistinguishable from littermates	Runty
Advantage		1. Specific expression in the DRG 2. Expression in most DRG neurons	
Phenotype	pERK level increased in DRG increased axonal growth of DRG explants functional recovery after injury	No pERK increase in DRG; No increased axon growth of DRG explants	CKO smaller than littermates, survival time < 3 months

Table 3.1 Comparison of three different *Nf1*-KO mice.

Discussion

Nf1-/- Adult Sensory Neurons Exhibit Enhanced Axonal Growth

Neurotrophins and their receptors (Trks) are important in regulating survival, differentiation and axonal growth of sensory neurons mainly through the activation of their downstream effectors including Ras, PI3K-Akt, MEK-ERK, and phospholipase C-gamma (Atwal et al., 2000; Huang and Reichardt, 2001; Markus et al., 2002b). Neurofibromin, the protein encoded by *Nf1*, is a negative regulator of Ras, thus serves as a checkpoint for Ras-mediated signaling downstream of neurotrophins (Klesse et al., 1999; Klesse and Parada, 1998). The loss of *Nf1* renders embryonic sensory neurons able to survive without neurotrophic support *in vitro* (Vogel et al., 1995). In this report, we demonstrate that ablation of *Nf1* in adult proprioceptive DRG neurons endows these cells with enhanced capacity for axonal growth in culture.

Functional Recovery

To study the *in vivo* role of *Nf1* in adult DRG neurons, we turned to a classic model for nerve injury and repulsion by CNS, the dorsal rhizotomy (Carlstedt et al., 1987; Goldstein et al., 1991). In contrast to the permanent sensory deficits described in the literature and observed in control mice after dorsal rhizotomy, over the course of several weeks *Nf1*-SynI-CKO mice progressively recovered proprioceptive function. This remarkable spontaneous recovery was observed in the *Nf1* conditional mutant mice despite surgical resection and ligation. Therefore, such robust recovery cannot be due to an inadequate or inconsistent injury technique, and is likely achieved through compensatory collateral sprouting of spared adjacent sensory afferents. Consistent with this view, the mutant mice showed no significant changes in astrocytic scar formation at the DREZ and no evidence of regeneration from the damaged DRG afferents (supplemental data No. 6, (Romero et al., 2007)), suggesting that the environment remains unfavorable for regeneration in the mutant cord.

The ability of DRG neurons to sprout after injury is well documented for pain and mechanoceptor fibers (LaMotte and Kapadia, 1993; McMahon and Kett-White, 1991), whereas non-pepdidergic (IB-4-positive) and muscle proprioceptive afferents have limited capacity for collateral branching (Belyantseva and Lewin, 1999). This limited

sprouting capacity is insufficient to mediate functional recovery after dorsal rhizotomy in normal animals. In the context of *Nf1* loss, the capacity of neighboring spared proprioceptive sensory neurons to invade the damaged area by sprouting is enhanced to sufficient degree that in all cases partial functional recovery could be monitored. Functional collateralization of the *Nf1*-SynI-CKO L3 DRG into the L4-5 denervated motor neurons for proprioceptive control seems feasible since these neurons are known to project through the sciatic nerve in mice (Forsberg et al., 1996). Although the precise mechanism by which L3 DRG *Nf1*-/- neurons control muscle targets in the hind limb is unknown, it is not unlikely that these neurons also sprout peripherally (Sanapanich et al., 2002).

Paracrine Effects

Interestingly, normal axonal sprouting was seen in spinal cords of uninjured *Nf1*-SynI-CKO mice, suggesting that after experimental injury *Nf1*-/- neurons have an enhanced capacity to sense and respond to spinal cord denervation and the environment may play a role. Because neurons in the spinal cord of *Nf1*-SynI-CKO mice also lack *Nf1*, we considered whether paracrine effects from these *Nf1* deficient neurons might also contribute to the *in vivo* functional recovery we observed. To test this possibility we co-cultured spinal cord explants with pre-labeled DRG and found enhanced sprouting activity in mutant spinal cord co-cultures. Therefore, the increased neurite growth observed in *Nf1*-/- neurons reflects not only improved intrinsic growth but also an enhanced response of these neurons to local growth cues. This is in agreement with the "growth factor hypersensitivity" that *Nf1*-/- and *Nf1*+/- cells exhibit to certain paracrine factors such as neurotrophins, CSF-1, and Kit ligand in other cellular contexts that relate to *Nf1* associated pathology (Largaespada et al., 1996; Le et al., 2004; Vogel et al., 1995; Yang et al., 2003). Identification of the factor(s) responsible for this activity may have utility in future development of nerve regeneration therapies.

Molecular Mechanism

Sensory neurons respond to neurotrophins for cell survival and axonal growth primarily through the activation of the PI3K-Akt-GSK3β and Raf-MEK-ERK (Atwal et

al., 2000; Vogel et al., 2000; Zhou et al., 2004). Whereas most evidence points to the critical role for the PI3K-Akt effectors as mediators of cell survival in both WT and *Nf1*-/- DRG neurons (Klesse and Parada, 1998), the molecular mechanism underlying cytoskeletal reorganization during neurotrophin-induced axonal growth and collateral branching is less clearly defined. In embryonic DRG neurons, NGF elicits axonal growth through PI3K phosphorylation and GSK-3β inactivation, and proceeds despite ERK signaling blockade, suggesting a necessary and sufficient role for the PI3K-Akt-GSK3β cascade in neurite growth (Jones et al., 2003; Zhou et al., 2004). However, when neurotrophin-induced axonal growth is studied independently from cell survival in embryonic sensory neurons, neurite extension is blocked by either MEK or PI3K inhibitors (Atwal et al., 2000), and specific activation of either the Raf-MEK-ERK or the PI3K-Akt-GSK3β cascade in *Bax-/-* embryonic DRG neurons, selectively induces axonal elongation and distal branching, respectively (Markus et al., 2002b). Our results indicate that both the Raf-MEK-ERK and the PI3K-Akt-GSK3β pathways are likely constitutively activated in adult *Nf1*-SynI-CKO DRG neurons, suggesting that both Ras-effector cascades may underlie the increased capacity of *Nf1*-/- neurons for collateral sprouting.

The precise mechanisms by which activation of the Raf and the PI3K pathways might coordinate the assembly of microtubules for axonal sprouting in response to injury, remain to be fully elucidated. Transcription factors elicited by injury such as cJun, ATF3, CREB, and STATs, are likely candidates downstream of ERK activation (Pearson et al., 2003; Sheu et al., 2000). Alternatively, molecules downstream of neurofibromin might also be involved, since activation of Ras signaling either by expression of a constitutively activated form (Genot et al., 1996) or by *Nf1* deletion (Gitler et al., 2003), is known to activate the transcription factor NFATc1 in endothelial cells. Interestingly, calcineurin/NFAT activation is critically involved in elongation and arborizing growth of sensory neurons (Graef et al., 2003).

Our data are most consistent with a scenario in which the elevated ERK/PI3K activity in *Nf1*-/- neurons endows these cells with increased intrinsic capacity for growth, and renders them hypersensitive to stimulation by extracellular signals, such as those likely to emanate from the denervated spinal cord.

Significance for Neural Trauma and Regeneration

Current studies on nerve regeneration after injury focus most attention on understanding and neutralizing the unfavorable environment created by inhibitory myelin components, extracellular matrix and glial scar (Fouad et al., 2005; Fournier et al., 2003). However, since mature neurons have reduced intrinsic capacity for growth and sprouting compared to embryonic neurons, identifying cell autonomous mechanisms that enhance adult neuron collateral branching could also be an important area of research (Homma et al., 2003; Rico et al., 2004).

We selected DRG neurons as a physiologically relevant model to study nerve injury since cultured DRG neurons are routinely used in the nerve regeneration field to examine the inhibitory qualities of myelin components such as NOGO (Chen et al., 2000; GrandPre et al., 2000), myelin-associated glycoprotein (MAG) (McKerracher et al., 1994), and oligodendrocyte-myelin glycoprotein (OMgp) (Wang et al., 2002). The present study indicates that *Nf1* deletion in sensory neurons provides these cells with an enhanced capacity for functional collateral sprouting in response to spinal cord denervation injury. These results underline neurofibromin as a useful therapeutic target to increase the sprouting capacity of spared neurons after neural trauma.

Dual roles of Tumor Suppressor Genes

By using different Cre lines, we planned to delete *Nf1* in a temporal and tissue-specific manner, allowing us to further study the role of this gene in sensory neuron plasticity. However, interpretation of the phenotypes we observed in the *Nf1* conditional mutant mice was complicated by the variable onset time and expression pattern of the Cre transgene. The lack of pERK activation and axonal growth advantage in DRG from *Nf1*-Prph1-CKO mice may be due to the fact that this Cre starts to express at much later stages compared to Synapsin I-Cre. On the other hand, in *Nf1*-Isl1-CKO mice, although *Nf1* was effectively deleted in most DRG neurons, the ectopic expression of Islet1-Cre made this Cre line unsuitable for our *in vivo* experiment.

Tumor suppressor genes (TSG) are negative regulators of various signaling pathways that are important for cell survival, proliferation, and differentiation. Deletion

or inhibition of these genes may provide cells more activity, thus making them possible targets for improving recovery after nerve injury. However, dysfunction of TSGs can also result in cellular abnormalities and even tumor formation. Therefore, the application of disrupting these genes must be done in a very cautious way.

Possible alternative methods for future studies include either local delivery of Cre-expressing virus, or directly targeting downstream effectors of *Nf1*.

Chapter IV

Mice with *Nf1* deficiency Develop Gastric Hyperplasia

Abstract

Gastric cancer is the second most prevalent tumor in the world. GI neoplasms are also among many manifestations of NF1 patients. However, the physiological and pathological functions of the *Nf1* gene in GI system have not been clearly investigated due to lack of mouse models. In this report, we generate conditional knockout mice with *Nf1* deficiency in the GI tract. These mice develop gastric epithelium hyperplasia and inflammation, which are precancerous lesions of gastric cancer. Increased proliferation and apoptosis are also observed in the gastric epithelium of *Nf1* mutant mice. The hyperplasia of gastric epithelium seems to be contributed mainly by the loss of *Nf1* in the gastric fibroblasts. Hyper-activation of ERK and STAT3 pathways are detected in mutant gastric epithelium. These mice can be useful animal models to study the pathogenesis of GI lesions in NF1 patients as well as to investigate the role of the *Nf1* gene in the development of GI neoplasms.

Introduction

NF1 is an autosomal dominantly inherited disorder which appears in about 1/3500 births worldwide (Riccardi, 1999). Major clinical features of this disorder are cafe-au-lait spots and benign tumors of peripheral and optic nerves. Less penetrant manifestations include pathologies involving the skin, bones, endocrine organs, blood vessels, etc (Le and Parada, 2007). In addition, gastric tumors were reported in about 2 to 25 percent of NF1 patients with various tumor locations and tumor types, including those of epithelial origin (adenoma and adenocarcinoma), stromal origin (gastrointestinal stromal tumor) and others (Petersen and Ferguson, 1984; Riccardi, 1981; Rutgeerts et al., 1981; Uflacker et al., 1985), some of which can even cause gastric outlet obstruction in NF1 patients (Bakker et al., 2005). Non-neoplastic lesions such as IFPs were also seen in GI tract of patients with NF1 (Ng et al., 2004). However, the etiological mechanisms of GI lesions in NF1 patients have not been studied yet.

NF1 is caused by mutation in the *Nf1* gene, which spans about 335 kb on human chromosome 17 (Wallace et al., 1990). Neurofibromin, the protein encoded by *Nf1*, functions as a Ras-GAP, thus acting as a negative regulator of Ras-mediated signaling pathways (Bourne et al., 1990). Signaling pathways downstream of Ras such as MEK/ERK and PI3K/Akt pathway can therefore be regulated or modified by neurofibromin (Zhu and Parada, 2001a). In addition, *Nf1* has both cell-autonomous and non-cell autonomous effects in various cell types (Bajenaru et al., 2001; Courtois-Cox et al., 2006; Daginakatte and Gutmann, 2007; Romero et al., 2007; Vogel et al., 1995; Yang et al., 2006; Yang et al., 2003).

Gastric cancer is the second most prevalent tumor in the world and the second most common cause of global cancer death (Hatakeyama, 2004; Ushijima and Sasako, 2004). Different rodent models have been developed to study the pathogenic mechanisms of GI tumors, which can be classified into three categories: mice infected with Helicobacter pylori (Goldenring and Nomura, 2006); mice with disturbed levels of gastrin (Wang et al., 2000; Zavros et al., 2005); and mice with genetic modification (Gut et al., 2002; Ishikawa et al., 1997; Kaestner et al., 1997; Lee et al., 2000; Lefebvre et al., 1996; Li et al., 2002; Li et al., 2000; Ramalho-Santos et al., 2000; Saitou et al., 2000; Scarff et al., 1999; Schultheis et al., 1998; Sharp et al., 1995; Xu et al., 2000). In one model, the SHP2

binding site on IL-6 cytokine co-receptor *gp130* was mutated resulting in impairment of IL-6 dependent SHP2-Ras-ERK activation; whereas the STAT3 activation remains normal, these mice develop gastric hyperplasia and ultimately gastric adenoma (Tebbutt et al., 2002). On the other hand, activation of Ras-ERK pathway is also involved in the pathological mechanisms of Helicobacter pylori infections (Macarthur et al., 2004). All these data suggest that Ras-ERK pathway plays important roles in the gastric epithelial cells, although the direct effect of activating this pathway inside the GI tract has not been studied yet.

Nf1 traditional knockout mice are embryonic lethal due to defects in multiple organs (Jacks et al., 1994), which results in difficulties of studying the physiological and pathological role of *Nf1* in the GI system. Using mice carrying $Nf1^{flox/flox}$ alleles and a Cre transgene specifically expressed in GI tract, we are able to demonstrate that region-specific deletion of *Nf1* in GI tract leads to gastric hyperplasia and inflammation, which are precancerous lesions of gastric cancer. Increased cell proliferation and apoptosis are observed in *Nf1* mutant gastric epithelium. These phenotypes are possibly mediated by non-cell autonomous contribution from *Nf1* deficient fibroblasts. Hyperactiviation of ERK and STAT3 pathways are detected in the mutant gastric epithelium. These mice can thus be useful animal models to study the pathogenesis of GI lesions in NF1 patients, as well as to investigate the molecular mechanisms of *Nf1* in gastric tumor initiation and/or progression.

Materials and Methods

Breeding and Genotyping of *Nf1*$^{flox/flox}$ and Islet1-Cre Mice

Nf1$^{flox/flox}$ mice were crossed with mice carrying Islet1-Cre (provided by Dr. Thomas Jessell at Columbia University) to generate *Nf1*$^{flox/flox}$*;Islet1-Cre* conditional knockout mice (*Nf1*-Isl1-CKO). *Rosa26*^{lacZ}*;Islet1-Cre* mice (*R26-Isl1*) were generated by crossing Islet1-Cre mice with *Rosa26*-Stop-lacZ reporter mice (Jackson Laboratories, Bar Harbor, ME). All mice were kept on a mixed genetic background. Age-matched littermates with the genotypes of *Nf1*$^{flox/flox}$, *Nf1*$^{flox/wt}$ and *Nf1*$^{flox/wt}$*;Islet1-Cre* were phenotypically indistinguishable, thus were all pooled as controls. Genotyping for *Nf1*^{flox} allele and Cre transgene was done by PCR as previously described (Zhu et al., 2001). All mouse protocols were approved by the Institutional Animal Care and Research Advisory Committee guidelines of the University of Texas Southwestern Medical Center.

X-gal Staining

B-gal activity was examined in *R26;Isl1* mice at different ages. Embryos were collected in PBS and then fixed in 2% PFA for 1 hour at 4°C. Postnatal mice were transcardially perfused with PBS and 2% PFA, organs were then carefully dissected out, washed with PBS, and post-fixed in 2% PFA for 1 hour at 4°C. For sections, after fixation embryos or organs were protected in 30% sucrose until sunk and cryostat sections were cut at 14 μm. X-gal staining for whole mount tissues or sections was performed as previously described (Romero et al., 2007).

Detection of recombined *Nf1* allele

Genomic DNA was extracted from tissue. Recombination of the *Nf1* allele was examined as previously described (Kwon et al., 2008). The PCR primers were: 5'-AATGTGAAATTGGTGTCGAGTAAGGTAACCAC-3'; 5'-TTAAGAGCAT CTGCTG CTCTTAGAGGGAA-3' and 5'-TCAGACTGATTGTTGTACCTGATGG TTGTACC-3'. The size of PCR products were *Nf1*^{wt} allele: 493bp; *Nf1*^{flox} allele: about 600bp and recombined *Nf1* allele: about 300bp.

Histology

Mice were transcardially perfused with PBS and 4% PFA. Stomachs were removed and cut along the greater curvature, pinned out, and photographed. After processing, tissues were cut in 5 μm paraffin sections and stained with H&E, periodic acid-Schiff staining (PAS, Sigma, St Louis, MO) or Alcian blue staining (Sigma, St Louis, MO) according to manufacturer's instruction.

Morphometric and Statistical Analysis

At least three mice each for control and *Nf1*-Isl1-CKO were included at each time point of every measurement. Image J software was used to analyze the data. For area measurement of the gastric mucosa, the software was used to manually outline the object and the program was used to generate values. For gland length measurement, the average value of at least 10 longitudinally glands were shown.

Immunohistochemistry

Paraffin sections were deparaffinized and rehydrated. After microwave antigen retrieval, sections were incubated with one of the following primary antibodies: proliferating cell nuclear antigen (PCNA) (mouse, 1:10000; Santa Cruz Biotechnology, Santa Cruz, CA), smooth muscle actin (SMA, mouse, 1:500, Dako, Denmark), vimentin (mouse, 1:500, Invitrogen, Carlsbad, CA), phospho-p44/42 MAP Kinase (pERK, rabbit, 1:200; Cell Signaling Technology, Danvers, MA), phospho-AKT (rabbit, 1:50; Cell Signaling Technology), phospho-STAT3 (rabbit, 1:200; Cell Signaling Technology). The visualization of primary antibodies was performed with a horseradish peroxidase system (Vectastain ABC kit, Vector Laboratories, Burlingame, CA). Digital images were captured with a CCD camera under a light microscope (Olympus).

Immunofluorescent staining on cryostat sections was carried out by incubating with primary antibodies in 5% normal donkey serum overnight at 4 °C. Primary antibodies included lacZ (rabbit, 1:2000; ICN, Costa Mesa, CA), Tuj1 (mouse, 1:500, Covance, Berkeley CA), SMA (mouse, 1:50, Dako) and vimentin (mouse, 1:50, Invitrogen). Immunofluorescence was visualized after 1 hour incubation with appropriate Cy2- or Cy3-conjugated secondary antibodies (1:200, Jackson Labs) at room temperature. DAPI

(1 μg/ml, Fluka, Switzerland) was added together with the secondary antibodies to stain nuclei. The immunostaining was visualized using a Nikon Eclipse TE2000-U fluorescence microscope. Digital images were analyzed using the Metamorph software (Universal Imaging).

Cell Proliferation

Mice were injected IP with 100 μg/g of body weight BrdU (Sigma) 2 hours before sacrifice. Anti-BrdU staining was performed as described above using an antibody against BrdU (mouse, 1:100, DAKO). The average number of BrdU positive cells in at least ten longitudinal glands was reported. All cell counts were performed in a genotype-blind manner.

Apoptosis

Detection of apoptotic cells was performed as described above using an antibody against cleaved Caspase-3 (rabbit, 1:400, Cell Signaling Technology). Epithelial cells positively stained for cleaved Caspase-3 were counted in at least 10 random selected fields per section. All cell counts were performed in a genotype-blind manner.

Statistics

Statistical analysis was done using Student's *t*-test with P values ≤ 0.05 as being statistically significant. *, $P \leq 0.05$; **, $P \leq 0.01$; ***, $P \leq 0.001$. Error bar, SEM.

Results

Islet1-Cre is Expressed in Gastrointestinal Tract

Islet1 is a transcriptional factor widely expressed in neural crest derivatives such as sensory ganglia, cardiovascular progenitors and foregut endoderm (Sun et al., 2007). To examine whether Islet1-Cre is expressed in the GI tract, we crossed Islet1-Cre mice with the *R26*-stop-lacZ reporter mice and performed X-gal staining. Consistent with previous reports, at embryonic day 12.5 (E12.5), β-gal activities were detected in the TG, DRG and hind limb of *R26-Isl1* embryos (Fig. 4.2B) (Srinivas et al., 2001). At E14.5, whole-mount X-gal staining of GI tract revealed β-gal signals in the stomach and proximal duodenum of *R26-Isl1* embryos (Fig. 4.1A). Histological analysis showed that β-gal activities were mainly restricted to the muscular layer of GI tract (Fig. 4.1B). Double immunofluorescent staining was then performed to confirm the identity of β-gal positive, thus Cre-expressing cells. LacZ signals were found to be co-localized with a mesenchymal marker, SMA (Fig. 4.1D); but not with Tuj1, a marker for neurons (Fig. 4.1E), suggesting that Islet1-Cre is not expressed in enteric neurons, which are also derivatives of neural crest cells (Heanue and Pachnis, 2007). At postnatal day 14 (P14), β-gal activities were observed within gastric mucosal and muscular layer (Fig. 4.1G-4.1I). Within pyloric region, β-gal signals were detected mainly in muscular layer and periglandular fibroblasts (Fig. 4.1I), the identity of which was confirmed by positive staining of SMA and Vimentin, markers for smooth muscle cells and fibroblasts (Fig. 4.1J and 4.1K) (Leedham et al., 2006). Within regions distant from pylorus, β-gal signals were also observed in both the muscular layer and some mucosal cells (Fig. 4.1H). Outside the GI tract, β-gal activity was detected in ventral spinal cord (Fig. 4.2D) and DRG from adult animals (Fig. 4.2F).

Taken together, these data suggest that Islet1-Cre is expressed in the gastric fibroblasts and gastric smooth muscles within pylorus, as well as some epithelial cells in the non-pyloric region.

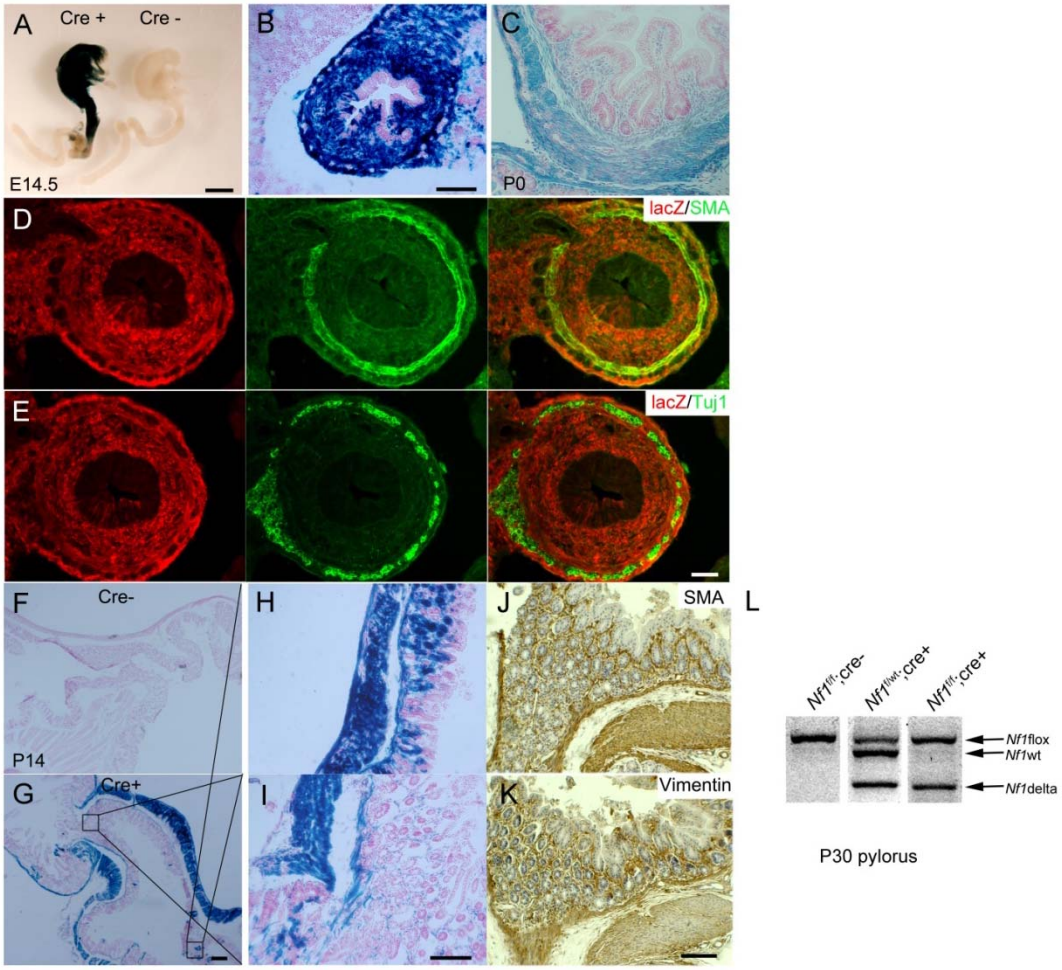

Fig. 4.1. Islet1-Cre is expressed in GI tract. (A) Whole mount X-gal staining of E14.5 GI tract revealed β-gal activity in stomach and proximal duodenum of *R26;Isl1* embryos. (B) X-gal staining of E14.5 sections counterstained with nuclear fast red showed β-gal signals mainly restricted to muscular layer of GI tract. (C) At P0, β-gal signals were detected in muscular layer and periglandular cells, but not in epithelial cells within pyloric region. (D) Double immunofluorescent staining of E14.5 sections showed co-localization of lacZ (red) and SMA (green), suggesting Islet1-Cre is expressed in smooth muscles. (E) LacZ (red) signals did not co-localize with Tuj1 (green), suggesting the Cre is not expressed in the enteric neurons. (F-K) At P14, β-gal activities were detected in the stomach of *R26;Isl1* mice (G), but not in controls (F). B-gal signals were observed in gastric fibroblasts and muscular layer of pyloric regions (I), and epithelial cells in non-pyloric region (H). Immunostaining of SMA and vimentin further confirmed the identity of periglandular fibroblasts (J and K, respectively). (L) PCR showed the presence of recombined *Nf1* alleles in pyloric tissues from P30 *Nf1*-Isl1-CKO ($Nf1^{f/f;Cre+}$) mice. Arrows indicate three different bands: WT *Nf1* allele (*Nf1WT*), *Nf1* allele with loxP sites (*Nf1flox*)

and recombined *Nf1* allele (*Nf1 delta*). Scale bars= 1 mm in A, 100 µm in B-E, H and I; 200 µm in F and G; 50 µm in J and K.

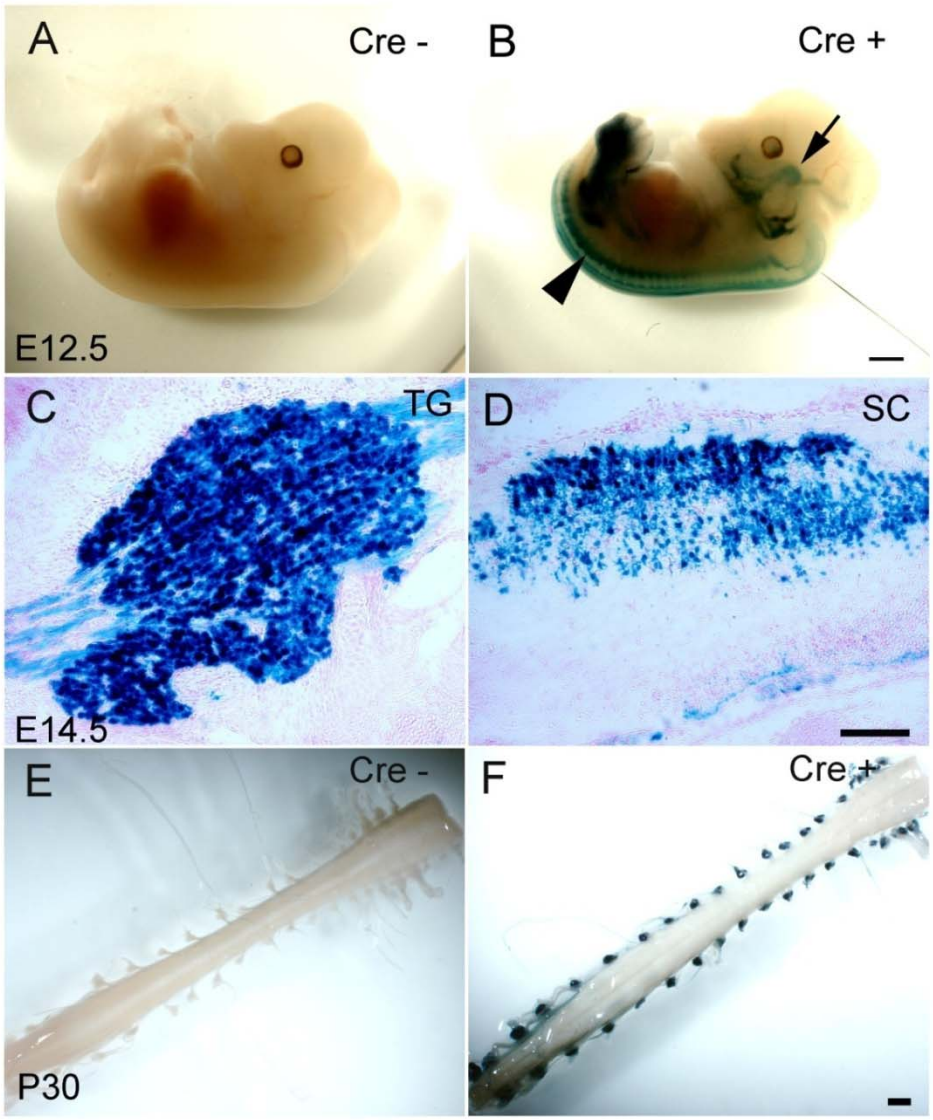

Fig. 4.2. **Expression pattern of Islet1-Cre in tissues other than the GI tract.** Whole-mount X-gal staining of E12.5 embryos showed β-gal activity in TG (arrow), DRG (arrowhead) and hind limbs of *R26;Isl1* mice (B), compared to no signals in control (A). X-gal staining of E14.5 sections showed β-gal activities in TG and spinal cord (SC). At P30, β-gal activity was also detected in DRG as revealed by whole-mount X-gal staining of spinal cord from control (E) and *R26;Isl1* mice (F). Scare bar = 100 µm in C and D; 1 mm in A-B and E-F.

Nf1-Isl1-CKO Mice Exhibit Progressive Body Weight Loss and Decreased Survival Rate

To study the role of *Nf1* in GI system, we then crossed $Nf1^{flox/flox}$ mice to Islet1-Cre mice to generate *Nf1* conditional knockout animals (*Nf1*-Isl1-CKO). We first examined the efficiency of Islet1-Cre in the GI tract. DNA was extracted from pyloric tissue of P30 control and *Nf1*-Isl1-CKO mice and subjected to PCR. Recombined *Nf1* allele was detected in CKO tissues (Fig. 4.1L), suggesting Islet1-Cre was effective.

Nf1-Isl1-CKO mice were born in Mendelian ratio with no obvious abnormalities at birth. However, they began to exhibit significant loss of body weight compared to their littermate controls starting as early as one week after birth. The body weight loss became more severe as the mice aged (Fig. 4.3B). The majority of *Nf1*-Isl1-CKO mice died between the age of 2 to 3 months (mean survival time = 70 days), possibly due to malnutrition; the mice had almost no fat deposits under the skin, and few survived for longer than four months (Fig. 4.3A). The premature death and age dependent weight loss in these mice cannot be attributed to the Islet1-Cre transgene, because no significant difference was observed between $Nf1^{flox/wt}$*;Islet1-Cre*, $Nf1^{wt/wt}$*;Islet1-Cre* and non-Cre animals in their survival rate and body weight (Fig. 4.3B). Neither were these phenotypes gender-specific, since both female and male *Nf1*-Isl1-CKO mice exhibited similar survival rates and progressive body weight loss (Fig. 4.4A and 4.4B).

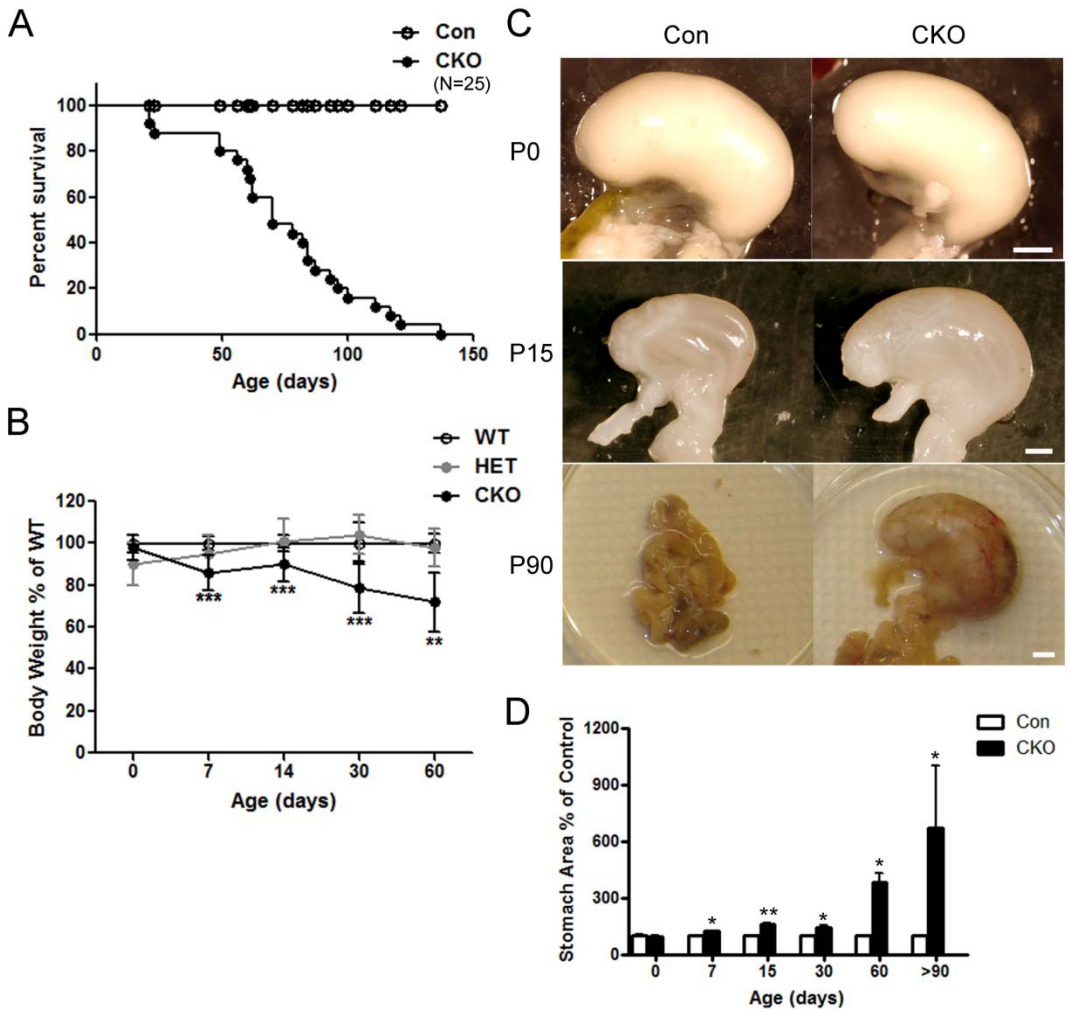

Fig. 4.3. *Nf1*-Isl1-CKO mice exhibit decreased survival rate, age dependent body weight loss and stomach enlargement. (A) *Nf1*-Isl-CKO mice (CKO) usually died between 2 to 3 months of age, with the mean survival time 70 days (N=25 for each genotype). (B) *Nf1*-Isl-CKO mice exhibited significant decrease of body weight as early as one week after birth compared to their littermate controls (HET: $Nf1^{flox/wt}$;*Islet1-Cre* mice, WT: $Nf1^{wt/wt}$;*Islet1-Cre* and non-Cre mice). This weight loss became more severe as the mice aged. No difference was observed between WT and HET in their body weight or survival rate. (C) Mice were sacrificed at specified ages and stomachs were removed for macroscopic examinations. Stomach from P0, P15 and P90 control and *Nf1*-Isl-CKO mice were shown. (D) Stomach area of *Nf1*-Isl-CKO mice was measured and represented as percentage of age and gender-matched littermate controls. Enlargement of stomach was observed in *Nf1*-Isl-CKO mice as early as one week after birth and became more obvious as the mice aged (N=3 for each genotype at each time point). Data represents Mean +/- SEM. *=P<0.05; **=p<0.01, ***=p<0.005. Student's t-test. Scale bars = 1 mm.

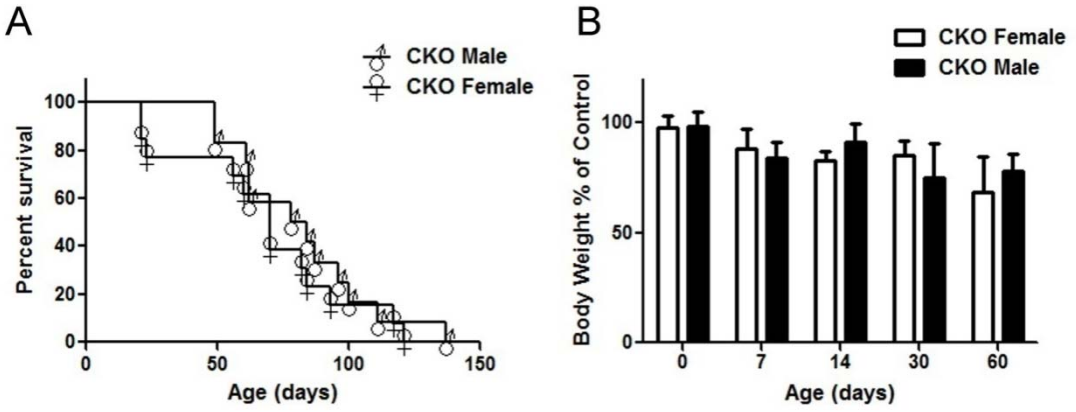

Fig. 4.4. Decreased survival rate and progressive body weight loss in *Nf1*-Isl1-CKO mice are not gender-specific. Female (N=13) and male (N=12) *Nf1*-Isl1-CKO (CKO) mice exhibited similar survival rate (A) and body weight change (B). Data represents Mean+/- SEM.

Nf1-Isl1-CKO Mice Develop Age-dependent Gastric Hyperplasia

To understand the cause of premature mortality in *Nf1*-Isl1-CKO mice, we performed detailed histological examination of mice at different ages. We observed age-dependent enlargement of the stomach in the mutant mice with an early onset at 1 week after birth (Fig. 4.3C and 4.3D) compared to their littermate controls, which was coincident with the beginning of weight loss in these mice (Fig. 4.3B). As the animals aged, the stomach enlargement became more severe (Fig. 4.3C and 4.3D). In mice older than 3 months, a huge abdomen mass could be observed due to the gigantic stomach. Macroscopic examinations revealed presence of antro-pyloric lesions in *Nf1*-Isl1-CKO mice with 100% penetrance. These lesions were macroscopically evident by 1 month of age (Fig. 4.5E), and in mice older than 3 months, often resulted in gastric outlet obstruction (Fig. 4.5F), which may be one of the reasons for the weight loss and premature death in these mice.

H&E staining revealed hyperplastic response of gastric mucosa in the pyloric region of *Nf1*-Isl1-CKO mice, which started as early as 2 weeks after birth (Fig. 4.5I) and became more pronounced in older animals (Fig. 4.5J). Signs of inflammation were also observed in the mutant gastric epithelium. At postnatal 2 weeks, inflammation was already present in the sub-mucosal layer of gastric epithelium in *Nf1*-Isl1-CKO mice

(Fig. 4.6D), when no obvious difference in the length of pyloric glands was observed yet compared to control (Fig. 4.6A and 4.5I). In older mutant mice, the gastric glands were enlarged and the pits were elongated (Fig. 4.6B and 4.6C). Signs of inflammation such as a huge amount of infiltrating lymphocytes and increased number of small blood vessels can be observed (Fig. 4.6B and 4.6E). In severe cases, ulceration can be seen (Fig. 4.6B and 4.6F). No metaplastic or dysplastic cells were observed at this time or in the few surviving older animals.

To further study the properties of these hyperplastic mucosal cells, we performed PAS staining to detect mucin-secreting cells and Alcian-blue staining to detect intestinal metaplasia, a precancerous pathological change for gastric tumor. PAS staining showed that the majority of hyperplastic cells were PAS positive, thus were mucin-secreting pit cells (Fig. 4.6J). Alcian-blue staining positive cells were also detected within pyloric glands of *Nf1*-Isl1-CKO mice (Fig. 4.6K and 4.6L), suggesting that they might undergo intestinal metaplasia.

Taken together, these data suggest that *Nf1*-Isl1-CKO mice develop progressive gastric hyperplasia, inflammation and even intestinal metaplasia of pyloric glands in some cases.

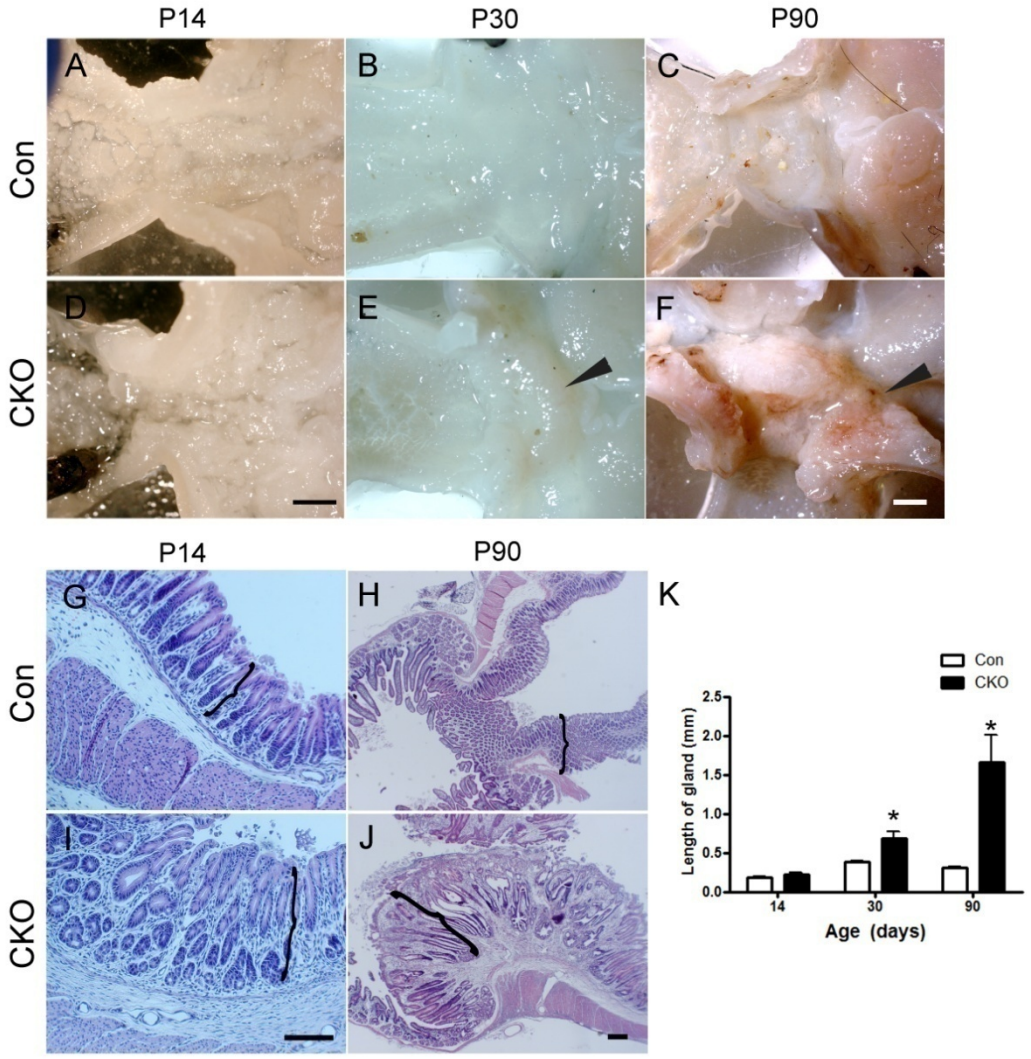

Fig. 4.5. *Nf1*-Isl1-CKO mice develop gastric hyperplasia. Stomachs from control (A-C) and *Nf1*-Isl-CKO mice (D-F) at different ages (P14: A and D, P30: B and E; P60: C and F) were subjected to macroscopic examination. Antro-pyloric lesions were visible in *Nf1*-Isl-CKO mice by 1 month of age (E, arrowhead), which became more obvious and severe at 3 months of age (F, arrowhead). (G-J) H&E staining of sections from pyloric region of 2 weeks (G and I) and 3 months (H and J) old control (G and H) and *Nf1*-Isl-CKO mice (I and J) were shown. Right brackets indicate the epithelium. (K) Quantification of average gland length at different time points indicated that in aged *Nf1*-Isl-CKO mice the gland length significantly increased compared to controls. (N=3 for each genotype at each time point). Data represents Mean+/- SEM. *=$p<0.05$, Student's t-test. Scale bars = 1mm in A - F; 100 µm in G and I; 200 µm in H and J.

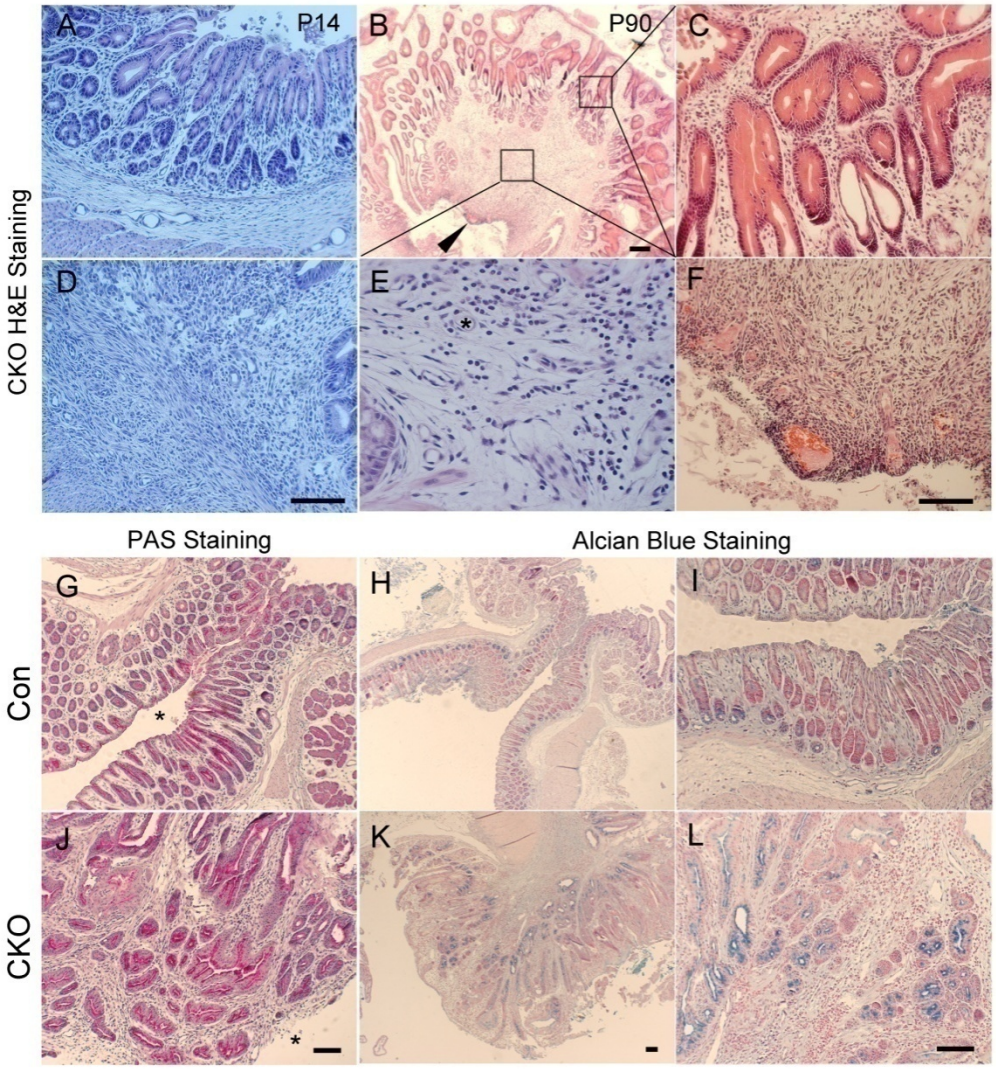

Fig. 4.6. Histology of *Nf1*-Isl1-CKO gastric epithelium. H&E staining of P14 (A and D) and P90 (B-C and E-F) pyloric tissues from *Nf1*-Isl1-CKO mice revealed hyperplastic and inflammatory changes within the gastric epithelium. Hyperplastic changes were shown as elongated and branching glands (B and C). Inflammatory signs were shown as the infiltrating lymphocytes and the increased number of small blood vessels (B and asterisk in E). Ulceration could be observed in aged mice (arrowhead in B and F). Sections of pyloric region from P90 *Nf1*-Isl1-CKO (J, K and L) and control (G, H and I) mice were subjected to PAS (G and J) and Alcian blue staining (H, I, K and L). PAS and Alcian blue positive cells were detected in *Nf1*-Isl1-CKO pyloric glands. Scale bars = 200 μm in B; 100 μm in A and D, C, E and F, G and J, H and K, I and L.

Increased Cell Proliferation and Cell Death in *Nf1*-Isl1-CKO Gastric Epithelium

The gastric hyperplasia we observed in *Nf1*-Isl1-CKO mice could be due to increased cell proliferation or decreased cell apoptosis in the gastric epithelium.

To examine the status of cell proliferation in gastric epithelium, control and *Nf1*-Isl1-CKO mice at difference ages were IP injected with BrdU, a thymidine analog which is incorporated into the DNA of dividing cells during S phase of the cell cycle, and thus used as an indicator of cell proliferation. At P14 and P30, the majority of BrdU positive cells were found to be localized to the isthmus region of pyloric glands in both control (Fig. 4.7A and 4.7B) and *Nf1*-Isl1-CKO mice (Fig. 4.7D and 4.7E), which are reported locations of gastric progenitor cells (Goldenring and Nomura, 2006). No significant difference in the number of BrdU positive cells was observed in gastric epithelium between CKO and controls at these time points. However, in gastric epithelium of P60 *Nf1*-Isl1-CKO mice (Fig. 4.7F), the number of BrdU positive cells significantly increased compared to controls (Fig. 4.7C), and BrdU positive cells were found throughout the pyloric glands in *Nf1*-Isl1-CKO mice. Similar results were seen in immunostaining for PCNA, another maker for proliferative cells (data not shown).

To examine the status of cell death, we performed immunostaining using an antibody against cleaved Caspase-3, which specifically labels apoptotic cells. At P14, no difference in the number of cleaved Caspase-3 positive cells was detected in the gastric epithelium of control and *Nf1*-Isl1-CKO mice (Fig. 4.7G and 4.7I, respectively). However, the number of apoptotic cells increased dramatically in the gastric epithelium of mutant mice older than 3 months compared to controls (Fig. 4.7H, 4.7J, respectively, and 4.7K).

Taken together, these results suggest that both cell proliferation and cell death are affected in gastric epithelium of *Nf1*-Isl1-CKO mice.

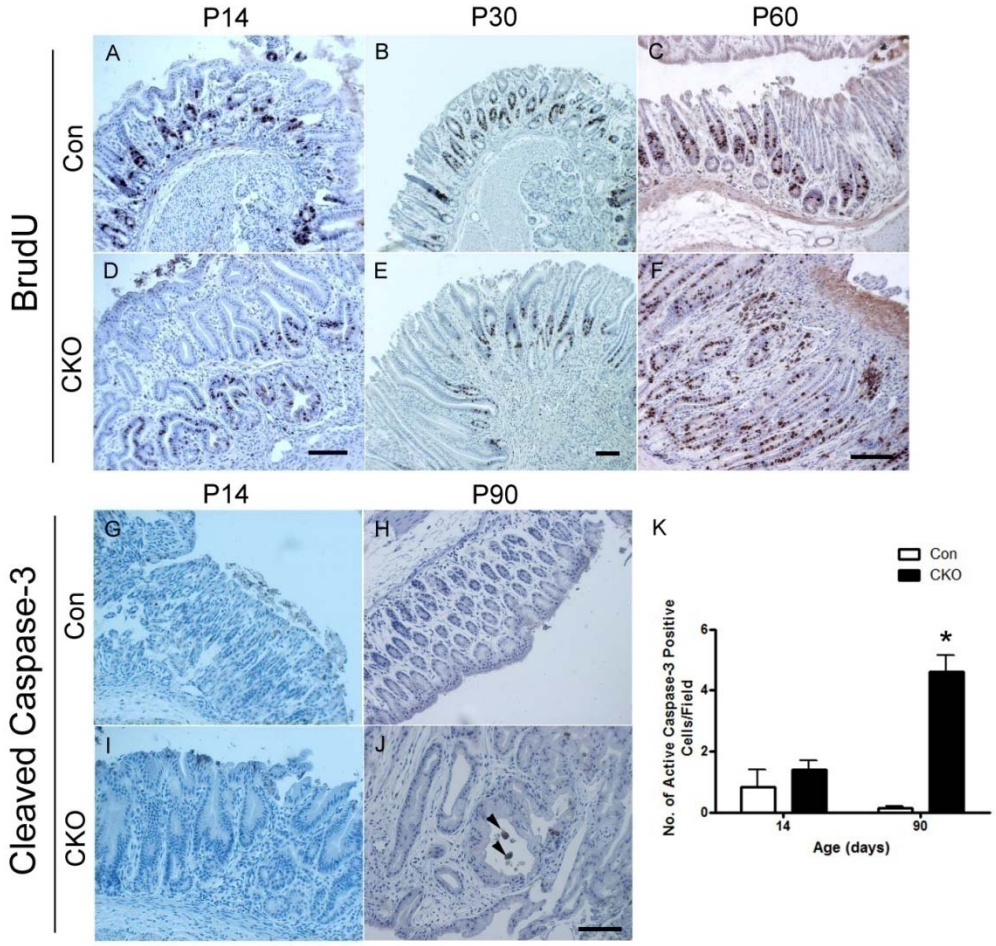

Fig. 4.7. Increased proliferation and apoptosis in *Nf1*-Isl1-CKO gastric epithelium. (A-F) BrdU staining of control (A-C) and *Nf1*-Isl1-CKO (D-F) gastric epithelium at different stages (P14: A and D, P30: B and E, P60: C and F) showed increased proliferation in *Nf1*-Isl1-CKO mice at older age compared to controls. (G-K) Apoptotic cells were visualized by staining with antibody against cleaved Caspase-3. Pictures from 2 week (G and I) and 3 month (H and J) old control (G and H) and *Nf1*-Isl1-CKO (I and J) mice are shown. Arrowheads indicate the apoptotic cells. Quantification of cleaved Caspase-3 positive cells showed increased apoptosis in gastric epithelium of aged *Nf1*-Isl1-CKO mice compared to controls (K). Data represents Mean+/- SEM. *=$p<0.05$, Student's t-test. Scale bars = 100 µm.

Non-cell autonomous Role of *Nf1* in Gastric Hyperplasia

Because Islet1-Cre was mainly expressed in smooth muscle cells and fibroblasts within the pylorus (Fig. 4.1I), it is very likely that the hyper-proliferation of gastric

mucosal cells in *Nf1*-Isl1-CKO mice was due to a non-cell-autonomous role of *Nf1* in non-epithelial cells.

To explore this possibility, we took advantage of the *R26*-stop-lacZ alleles present in a subset of *Nf1*-Isl1-CKO mice and performed X-gal staining. Cells with β-gal activity were thus deficient for *Nf1*. At different ages (P7, P14 and P60), β-gal activity was mainly detected in the muscular layer and the periglandular fibroblasts, while as majority of mucosal cells in the pyloric region were not positive for β-gal (Fig. 4.8A-4.8E). Immunofluorescent staining of lacZ with SMA or vimentin (Fig. 4.8F and 4.8G) showed that lacZ positive cells also expressed SMA or vimentin, thus were fibroblasts and smooth muscles.

Taken together, these results suggest that the loss of *Nf1* in gastric fibroblasts or smooth muscle cells may play roles in the proliferative response of gastric epithelial cells in our mouse model.

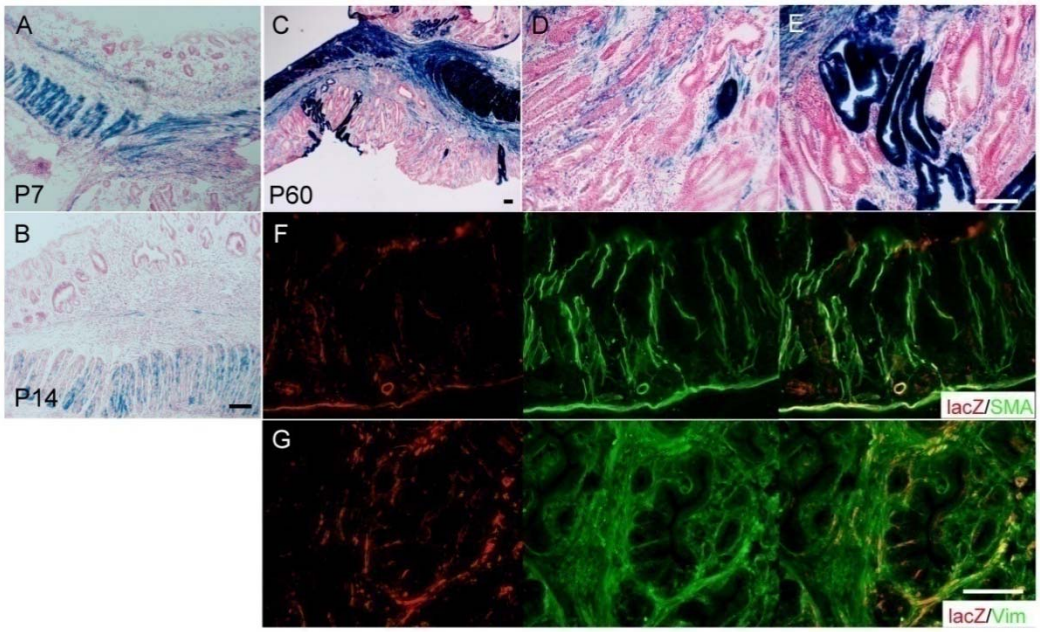

Fig. 4.8. LacZ staining of pyloric lesions in *Nf1*-Isl1-CKO mice. Sections from P7 (A), P14 (B) and P60 (C-E) *Nf1*$^{flox/flox}$*; R26;Islet1-Cre* mice were subjected to X-gal staining. B-gal activities were detected mainly in muscular layer and fibroblasts within the pyloric region. Immunofluorescent staining of lacZ (red, F and G) with SMA (F, green) or vimentin (G, green) revealed the co-localization of lacZ with SMA and vimentin, markers for smooth muscles and fibroblasts. Scale bars = 100 μm.

Hyper-activation of ERK and STAT3 Pathways in *Nf1*-Isl1-CKO Gastric Epithelium

To study the possible molecular mechanisms of these phenotypes, we examined the status of two major signaling cascades involved in gastric hyperplasia and tumor: ERK pathway and STAT3 pathway. The level of phospho-ERK and phospho-STAT3 dramatically increased in gastric mucosal cells of P90 *Nf1*-Isl1-CKO mice compared to controls (Fig. 4.9B and 4.9F). Despite the limited number of *Nf1*-deficient mucosal cells in the pyloric region as revealed by X-gal staining (Fig. 4.8), hyper-activation of ERK and STAT3 were observed throughout the pyloric glands, suggesting this may be due to cytokine or growth factor stimulation on the gastric epithelium, rather than the loss of *Nf1* in specific cells. In contrast, the level of phospho-AKT, another downstream effecter of Ras, did not change in the mutant gastric epithelium compared to controls (Fig. 4.9D).

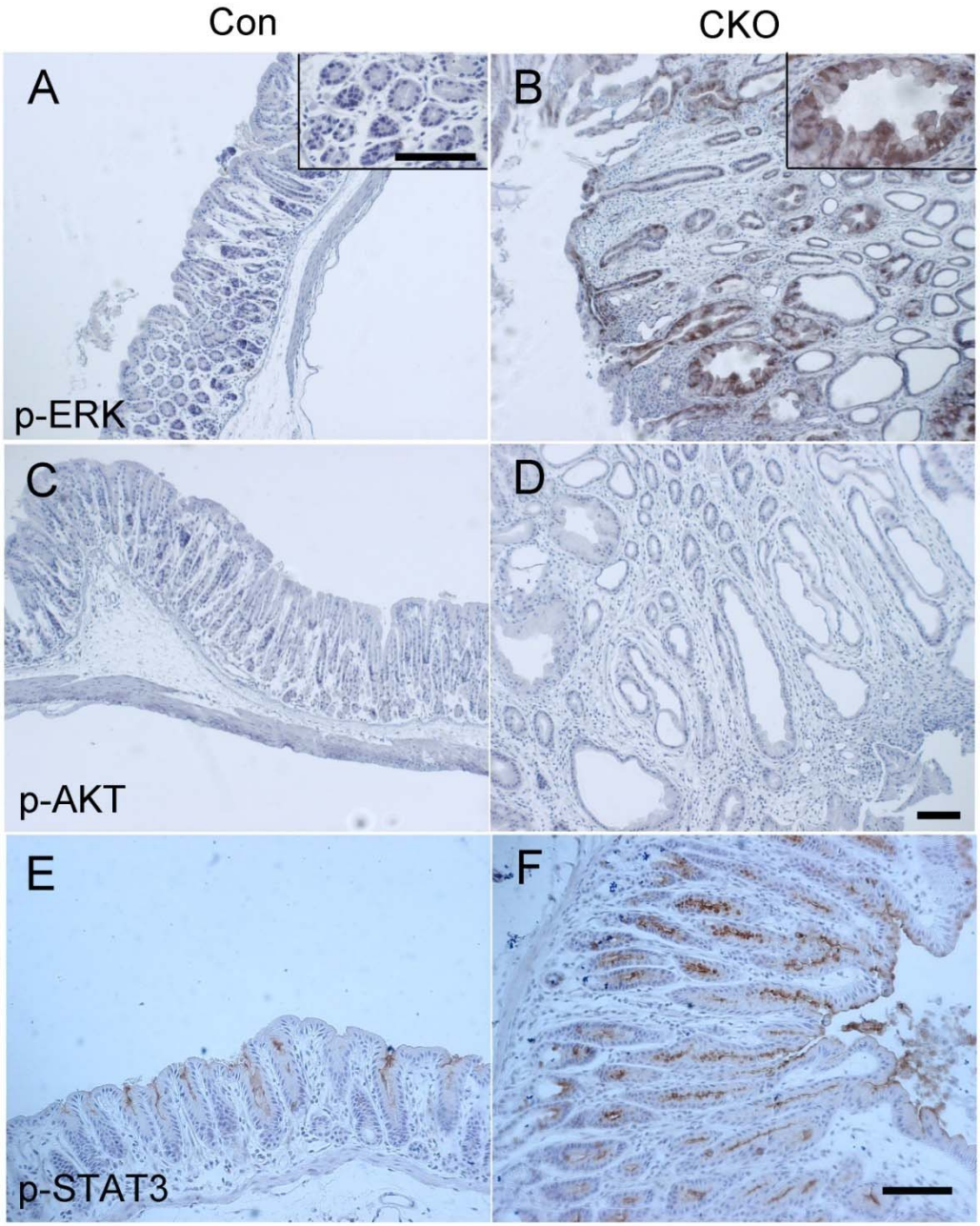

Fig. 4.9. ERK and STAT3 pathways are activated in gastric epithelium of *Nf1*-Isl1-CKO mice. Immunohistochemical staining of sections from P90 control (A, C and E) and *Nf1*-Isl1-CKO (B, D and F) mice revealed increased level of phospho-ERK (p-ERK, A and B) and phospho-STAT3 (p-STAT3, E and F) in the gastric epithelium of *Nf1*-Isl1-CKO mice compared to controls. No difference in phospho-Akt (p-Akt, C and D) level was detected between control and *Nf1*-Isl1-CKO mice. Scale bars = 100 μm in A-D and E-F; 50 μm in insets.

Discussion

GI lesions have been reported in several NF1 patients. However, the specific features and mechanism underlying these lesions have not been clearly elucidated, possibly due to the lack of animal models. In this report, we generated a conditional knockout mouse with *Nf1* deleted in GI tract. These mice exhibited progressive body weight loss and decreased survival rate. They developed age-dependent stomach enlargement and gastric outlet obstruction. Histological examination showed gastric hyperplasia and inflammation in these *Nf1* mutant mice. Increased cell proliferation and cell death were also observed in gastric epithelium of these mice. Both ERK and STAT3 pathways were hyper-activated in mutant gastric epithelium. More interestingly, the loss of *Nf1* in non-epithelial cells may play cell-non-autonomous roles in these processes.

Mouse Models for Gastric Hyperplasia and Gastric Tumor

Several rodent models have been developed to study the physiology and pathology of GI system. The functions of the *Nf1* gene in GI tract have not been clearly studied because the traditional knockout mice are embryonic lethal (Jacks et al., 1994).

Using Islet1-Cre, we generated a conditional knockout mouse model (*Nf1*-Isl1-CKO), in which *Nf1* was deleted in gastric smooth muscle cells, gastric fibroblasts and some gastric mucosal cells. These mice developed gastric hyperplasia, inflammation and intestinal metaplasia, which are all precancerous lesions for gastric tumor and closely associated with tumor formation (Goldenring and Nomura, 2006). We did not detect any signs of dysplasia or malignancy, which is probably due to the short life-span of these mice. In other mouse models of gastric cancer, it usually takes several months to one year for the mice to develop the tumor phenotype, although gastric hyperplasia can be observed much earlier. For example, hyperplastic tumors with inflammation were detected in $gp130^{735F/735F}$ mice as early as 4 weeks after birth, while dysplasia was only seen when the mice were older than 30 weeks (Judd et al., 2004; Tebbutt et al., 2002). *Nf1*-Isl1-CKO mice usually die before three months of age possibly owing to gastric outlet obstruction and malnutrition, which may be the reason for lack of dysplasia in their gastric epithelium.

Non-cell autonomous Role of *Nf1* in Gastric Hyperplasia

The origin of gastric epithelial tumor has been controversial. Gastric epithelial cells themselves obviously play prominent roles in tumor initiation and progression. It is also reported that genetic modification in lymphocytes is sufficient for gastric tumor development in some mouse models (Smad4, Runx3) (Brenner et al., 2004; Kim et al., 2006). Bone marrow stem cells are able to incorporate into the epithelial tumors (Houghton et al., 2004). Stromal cells also play important roles in the initiation and progression of epithelial tumors. These cells can secrete various types of factors and affect the proliferation, apoptosis and transformation of epithelial cells (Bhowmick et al., 2004b). Mice with TGF-β deleted specifically in fibroblasts developed squamous cell carcinoma of the forestomach, possibly through paracrine activation of HGF pathway (Bhowmick et al., 2004a).

In our mouse model, Islet1-Cre was mainly expressed in the muscular layer and gastric fibroblasts in the pyloric region, where the lesion developed. The hyperplasia of mucosal cells, where Cre was not active, was thus not likely due to autonomous effect of *Nf1* loss in these cells. It is possible that other types of cells, after losing *Nf1*, secrete factors to stimulate the growth of mucosal cells. The source of these paracrine factors remains to be further investigated. It is highly unlikely that the loss of *Nf1* in mucosal cells distant from pyloric region affects the growth of pyloric glands. The loss of *Nf1* in gastric smooth muscles does not result in gastric hyperplasia, since conditional *Nf1* mutant mice carrying a widely-expressed smooth-muscle-specific Cre (SM22α) develop normally without any gastric phenotypes reported (Lepore et al., 2005; Xu et al., 2007). Moreover, other mouse lines with *Nf1* deleted in blood cells developed lymphoma instead of the phenotypes we observed (Gitler et al., 2004), suggesting *Nf1* deletion in lymphocytes alone is not sufficient for the mice to grow gastric tumors. The most likely candidates are thus the gastric fibroblasts, which were already shown to be able to affect epithelium growth (Bhowmick et al., 2004b). The fibroblast-specific Cre line, FSP-Cre, could be used to further address this question (Bhowmick et al., 2004a).

It is also our interest to explore the possible factors (trophic factors and cytokines) involved in these processes. Since it has been reported that the loss of *Nf1* in several other

cell types can result in secretion of factors such as TGFα, KitL, IGF and HGF et al (Daginakatte and Gutmann, 2007; Yang et al., 2006; Yang et al., 2003).

Molecular Changes in *Nf1*-Isl1-CKO Gastric Epithelium

Cytokines and their related signaling pathways are important in gastric tumor development. Study of point mutations in IL-6 receptor-gp130 revealed two reciprocally regulated downstream pathways associated with different pathogenesis. Through inactivation of the SHP2 binding site on gp130, STAT3 pathway can be activated while ERK pathway is inhibited. Mice with this mutation ($gp130^{757F/757F}$) develop gastric tumors, while mice with SHP2/Ras/ERK pathway activated do not (Tebbutt et al., 2002). STAT3 is also necessary for the tumor genesis since further crossing of heterozygous *STAT3* mutant mice (*STAT3*+/-) to $gp130^{757F/757F}$ mice partially reverses the gastric phenotype (Jenkins et al., 2005). However, studies in Helicobacter pylori infection and gastric tumor suggest that Ras/ERK pathway is also important for gastric tumor development. Helicobacter bacteria inject CagA proteins into the epithelial cells upon binding to these cells. Binding of CagA with SHP2 leads to ERK activation, which may be the reason for the pathogenesis of Helicobacter infection (Hatakeyama, 2004). Although it is possible that the SHP2 pool is reduced due to CagA binding, thus relieving the inhibition of SHP2 on STAT3, it is hard to explain the lack of inhibition on STAT3 pathways by the activated ERK pathway in this model.

In *Nf1*-Isl1-CKO gastric epithelium, we found hyper-activation of both ERK and STAT3 pathways throughout the pyloric glands, suggesting the activation of these two pathways may not be the direct effect of the loss of *Nf1* in these cells, but due to the stimulative effects of secretive factors present in the gastric epithelium. It would be interesting to examine whether *Nf1* has cell autonomous effects on gastric epithelial cells as well.

In summary, *Nf1*-Isl1-CKO mice can be a useful mouse model to study the features of GI neoplasms present in a subpopulation of NF1 patients, as well as to study the role of *Nf1* in gastric tumor development. Investigating possible secreted factors and downstream pathways may aid in understanding the developmental process of gastric tumors and future therapy.

Bibliography

Atwal, J. K., Massie, B., Miller, F. D. and Kaplan, D. R. (2000). The TrkB-Shc site signals neuronal survival and local axon growth via MEK and P13-kinase. *Neuron* **27**, 265-77.

Averill, S., McMahon, S. B., Clary, D. O., Reichardt, L. F. and Priestley, J. V. (1995). Immunocytochemical localization of trkA receptors in chemically identified subgroups of adult rat sensory neurons. *Eur J Neurosci* **7**, 1484-94.

Bajenaru, M. L., Donahoe, J., Corral, T., Reilly, K. M., Brophy, S., Pellicer, A. and Gutmann, D. H. (2001). Neurofibromatosis 1 (NF1) heterozygosity results in a cell-autonomous growth advantage for astrocytes. *Glia* **33**, 314-23.

Bakker, J. R., Haber, M. M. and Garcia, F. U. (2005). Gastrointestinal neurofibromatosis: an unusual cause of gastric outlet obstruction. *Am Surg* **71**, 100-5.

Bannerman, P. G. and Pleasure, D. (1993). Protein growth factor requirements of rat neural crest cells. *J Neurosci Res* **36**, 46-57.

Baudet, C., Mikaels, A., Westphal, H., Johansen, J., Johansen, T. E. and Ernfors, P. (2000). Positive and negative interactions of GDNF, NTN and ART in developing sensory neuron subpopulations, and their collaboration with neurotrophins. *Development* **127**, 4335-44.

Belyantseva, I. A. and Lewin, G. R. (1999). Stability and plasticity of primary afferent projections following nerve regeneration and central degeneration. *Eur J Neurosci* **11**, 457-68.

Bergsland, M., Werme, M., Malewicz, M., Perlmann, T. and Muhr, J. (2006). The establishment of neuronal properties is controlled by Sox4 and Sox11. *Genes Dev* **20**, 3475-86.

Bhowmick, N. A., Chytil, A., Plieth, D., Gorska, A. E., Dumont, N., Shappell, S., Washington, M. K., Neilson, E. G. and Moses, H. L. (2004a). TGF-beta signaling in fibroblasts modulates the oncogenic potential of adjacent epithelia. *Science* **303**, 848-51.

Bhowmick, N. A., Neilson, E. G. and Moses, H. L. (2004b). Stromal fibroblasts in cancer initiation and progression. *Nature* **432**, 332-7.

Bibel, M. and Barde, Y. A. (2000). Neurotrophins: key regulators of cell fate and cell shape in the vertebrate nervous system. *Genes Dev* **14**, 2919-37.

Bomze, H. M., Bulsara, K. R., Iskandar, B. J., Caroni, P. and Skene, J. H. (2001). Spinal axon regeneration evoked by replacing two growth cone proteins in adult neurons. *Nat Neurosci* **4**, 38-43.

Bourne, H. R., Sanders, D. A. and McCormick, F. (1990). The GTPase superfamily: a conserved switch for diverse cell functions. *Nature* **348**, 125-32.

Bowles, J., Schepers, G. and Koopman, P. (2000). Phylogeny of the SOX family of developmental transcription factors based on sequence and structural indicators. *Dev Biol* **227**, 239-55.

Bradbury, E. J., Moon, L. D., Popat, R. J., King, V. R., Bennett, G. S., Patel, P. N., Fawcett, J. W. and McMahon, S. B. (2002). Chondroitinase ABC promotes functional recovery after spinal cord injury. *Nature* **416**, 636-40.

Brannan, C. I., Perkins, A. S., Vogel, K. S., Ratner, N., Nordlund, M. L., Reid, S. W., Buchberg, A. M., Jenkins, N. A., Parada, L. F. and Copeland, N. G. (1994). Targeted disruption of the neurofibromatosis type-1 gene leads to developmental abnormalities in heart and various neural crest-derived tissues. *Genes Dev* **8**, 1019-29.

Brenner, O., Levanon, D., Negreanu, V., Golubkov, O., Fainaru, O., Woolf, E. and Groner, Y. (2004). Loss of Runx3 function in leukocytes is associated with spontaneously developed colitis and gastric mucosal hyperplasia. *Proc Natl Acad Sci U S A* **101**, 16016-21.

Buchberg, A. M., Cleveland, L. S., Jenkins, N. A. and Copeland, N. G. (1990). Sequence homology shared by neurofibromatosis type-1 gene and IRA-1 and IRA-2 negative regulators of the RAS cyclic AMP pathway. *Nature* **347**, 291-4.

Carlstedt, T. (1985). Regenerating axons form nerve terminals at astrocytes. *Brain Res* **347**, 188-91.

Carlstedt, T., Dalsgaard, C. J. and Molander, C. (1987). Regrowth of lesioned dorsal root nerve fibers into the spinal cord of neonatal rats. *Neurosci Lett* **74**, 14-8.

Cawthon, R. M., Weiss, R., Xu, G. F., Viskochil, D., Culver, M., Stevens, J., Robertson, M., Dunn, D., Gesteland, R., O'Connell, P. et al. (1990). A major segment

of the neurofibromatosis type 1 gene: cDNA sequence, genomic structure, and point mutations. *Cell* **62**, 193-201.

Chen, A. I., de Nooij, J. C. and Jessell, T. M. (2006a). Graded activity of transcription factor Runx3 specifies the laminar termination pattern of sensory axons in the developing spinal cord. *Neuron* **49**, 395-408.

Chen, C. L., Broom, D. C., Liu, Y., de Nooij, J. C., Li, Z., Cen, C., Samad, O. A., Jessell, T. M., Woolf, C. J. and Ma, Q. (2006b). Runx1 determines nociceptive sensory neuron phenotype and is required for thermal and neuropathic pain. *Neuron* **49**, 365-77.

Chen, M. S., Huber, A. B., van der Haar, M. E., Frank, M., Schnell, L., Spillmann, A. A., Christ, F. and Schwab, M. E. (2000). Nogo-A is a myelin-associated neurite outgrowth inhibitor and an antigen for monoclonal antibody IN-1. *Nature* **403**, 434-9.

Chen, Z. F., Rebelo, S., White, F., Malmberg, A. B., Baba, H., Lima, D., Woolf, C. J., Basbaum, A. I. and Anderson, D. J. (2001). The paired homeodomain protein DRG11 is required for the projection of cutaneous sensory afferent fibers to the dorsal spinal cord. *Neuron* **31**, 59-73.

Cheung, M. and Briscoe, J. (2003). Neural crest development is regulated by the transcription factor Sox9. *Development* **130**, 5681-93.

Chong, M. S., Woolf, C. J., Haque, N. S. and Anderson, P. N. (1999). Axonal regeneration from injured dorsal roots into the spinal cord of adult rats. *J Comp Neurol* **410**, 42-54.

Cichowski, K. and Jacks, T. (2001). NF1 tumor suppressor gene function: narrowing the GAP. *Cell* **104**, 593-604.

Courtois-Cox, S., Genther Williams, S. M., Reczek, E. E., Johnson, B. W., McGillicuddy, L. T., Johannessen, C. M., Hollstein, P. E., MacCollin, M. and Cichowski, K. (2006). A negative feedback signaling network underlies oncogene-induced senescence. *Cancer Cell* **10**, 459-72.

Crowley, C., Spencer, S. D., Nishimura, M. C., Chen, K. S., Pitts-Meek, S., Armanini, M. P., Ling, L. H., McMahon, S. B., Shelton, D. L., Levinson, A. D. et al. (1994). Mice lacking nerve growth factor display perinatal loss of sensory and sympathetic neurons yet develop basal forebrain cholinergic neurons. *Cell* **76**, 1001-11.

Daginakatte, G. C. and Gutmann, D. H. (2007). Neurofibromatosis-1 (Nf1) heterozygous brain microglia elaborate paracrine factors that promote Nf1-deficient astrocyte and glioma growth. *Hum Mol Genet* **16**, 1098-112.

Das, A., Chendil, D., Dey, S., Mohiuddin, M., Milbrandt, J., Rangnekar, V. M. and Ahmed, M. M. (2001). Ionizing radiation down-regulates p53 protein in primary Egr-1-/- mouse embryonic fibroblast cells causing enhanced resistance to apoptosis. *J Biol Chem* **276**, 3279-86.

Datta, S. R., Brunet, A. and Greenberg, M. E. (1999). Cellular survival: a play in three Akts. *Genes Dev* **13**, 2905-27.

Donovan, S., Shannon, K. M. and Bollag, G. (2002). GTPase activating proteins: critical regulators of intracellular signaling. *Biochim Biophys Acta* **1602**, 23-45.

Eng, S. R., Gratwick, K., Rhee, J. M., Fedtsova, N., Gan, L. and Turner, E. E. (2001). Defects in sensory axon growth precede neuronal death in Brn3a-deficient mice. *J Neurosci* **21**, 541-9.

Farinas, I., Jones, K. R., Backus, C., Wang, X. Y. and Reichardt, L. F. (1994). Severe sensory and sympathetic deficits in mice lacking neurotrophin-3. *Nature* **369**, 658-61.

Farinas, I., Yoshida, C. K., Backus, C. and Reichardt, L. F. (1996). Lack of neurotrophin-3 results in death of spinal sensory neurons and premature differentiation of their precursors. *Neuron* **17**, 1065-78.

Fitzli, D., Stoeckli, E. T., Kunz, S., Siribour, K., Rader, C., Kunz, B., Kozlov, S. V., Buchstaller, A., Lane, R. P., Suter, D. M. et al. (2000). A direct interaction of axonin-1 with NgCAM-related cell adhesion molecule (NrCAM) results in guidance, but not growth of commissural axons. *J Cell Biol* **149**, 951-68.

Fode, C., Gradwohl, G., Morin, X., Dierich, A., LeMeur, M., Goridis, C. and Guillemot, F. (1998). The bHLH protein NEUROGENIN 2 is a determination factor for epibranchial placode-derived sensory neurons. *Neuron* **20**, 483-94.

Forsberg, E., Hirsch, E., Frohlich, L., Meyer, M., Ekblom, P., Aszodi, A., Werner, S. and Fassler, R. (1996). Skin wounds and severed nerves heal normally in mice lacking tenascin-C. *Proc Natl Acad Sci U S A* **93**, 6594-9.

Fouad, K., Schnell, L., Bunge, M. B., Schwab, M. E., Liebscher, T. and Pearse, D. D. (2005). Combining Schwann cell bridges and olfactory-ensheathing glia grafts with

chondroitinase promotes locomotor recovery after complete transection of the spinal cord. *J Neurosci* **25**, 1169-78.

Fournier, A. E., Takizawa, B. T. and Strittmatter, S. M. (2003). Rho kinase inhibition enhances axonal regeneration in the injured CNS. *J Neurosci* **23**, 1416-23.

Frank, E. and Sanes, J. R. (1991). Lineage of neurons and glia in chick dorsal root ganglia: analysis in vivo with a recombinant retrovirus. *Development* **111**, 895-908.

Gaul, U., Mardon, G. and Rubin, G. M. (1992). A putative Ras GTPase activating protein acts as a negative regulator of signaling by the Sevenless receptor tyrosine kinase. *Cell* **68**, 1007-19.

Genot, E., Cleverley, S., Henning, S. and Cantrell, D. (1996). Multiple p21ras effector pathways regulate nuclear factor of activated T cells. *Embo J* **15**, 3923-33.

Giraud, A. S., Jackson, C., Menheniott, T. R. and Judd, L. M. (2007). Differentiation of the Gastric Mucosa IV. Role of trefoil peptides and IL-6 cytokine family signaling in gastric homeostasis. *Am J Physiol Gastrointest Liver Physiol* **292**, G1-5.

Gitler, A. D., Kong, Y., Choi, J. K., Zhu, Y., Pear, W. S. and Epstein, J. A. (2004). Tie2-Cre-induced inactivation of a conditional mutant Nf1 allele in mouse results in a myeloproliferative disorder that models juvenile myelomonocytic leukemia. *Pediatr Res* **55**, 581-4.

Gitler, A. D., Zhu, Y., Ismat, F. A., Lu, M. M., Yamauchi, Y., Parada, L. F. and Epstein, J. A. (2003). Nf1 has an essential role in endothelial cells. *Nat Genet* **33**, 75-9.

Goldberg, J. L. and Barres, B. A. (2000). The relationship between neuronal survival and regeneration. *Annu Rev Neurosci* **23**, 579-612.

Goldenring, J. R. and Nomura, S. (2006). Differentiation of the gastric mucosa III. Animal models of oxyntic atrophy and metaplasia. *Am J Physiol Gastrointest Liver Physiol* **291**, G999-1004.

Golding, J. P., Bird, C., McMahon, S. and Cohen, J. (1999). Behaviour of DRG sensory neurites at the intact and injured adult rat dorsal root entry zone: postnatal neurites become paralysed, whilst injury improves the growth of embryonic neurites. *Glia* **26**, 309-23.

Goldstein, M. E., House, S. B. and Gainer, H. (1991). NF-L and peripherin immunoreactivities define distinct classes of rat sensory ganglion cells. *J Neurosci Res* **30**, 92-104.

Graef, I. A., Wang, F., Charron, F., Chen, L., Neilson, J., Tessier-Lavigne, M. and Crabtree, G. R. (2003). Neurotrophins and netrins require calcineurin/NFAT signaling to stimulate outgrowth of embryonic axons. *Cell* **113**, 657-70.

GrandPre, T., Li, S. and Strittmatter, S. M. (2002). Nogo-66 receptor antagonist peptide promotes axonal regeneration. *Nature* **417**, 547-51.

GrandPre, T., Nakamura, F., Vartanian, T. and Strittmatter, S. M. (2000). Identification of the Nogo inhibitor of axon regeneration as a Reticulon protein. *Nature* **403**, 439-44.

Guo, H. F., The, I., Hannan, F., Bernards, A. and Zhong, Y. (1997). Requirement of Drosophila NF1 for activation of adenylyl cyclase by PACAP38-like neuropeptides. *Science* **276**, 795-8.

Gut, M. O., Parkkila, S., Vernerova, Z., Rohde, E., Zavada, J., Hocker, M., Pastorek, J., Karttunen, T., Gibadulinova, A., Zavadova, Z. et al. (2002). Gastric hyperplasia in mice with targeted disruption of the carbonic anhydrase gene Car9. *Gastroenterology* **123**, 1889-903.

Hargrave, M., Wright, E., Kun, J., Emery, J., Cooper, L. and Koopman, P. (1997). Expression of the Sox11 gene in mouse embryos suggests roles in neuronal maturation and epithelio-mesenchymal induction. *Dev Dyn* **210**, 79-86.

Hatakeyama, M. (2004). Oncogenic mechanisms of the Helicobacter pylori CagA protein. *Nat Rev Cancer* **4**, 688-94.

Heanue, T. A. and Pachnis, V. (2007). Enteric nervous system development and Hirschsprung's disease: advances in genetic and stem cell studies. *Nat Rev Neurosci* **8**, 466-79.

Homma, N., Takei, Y., Tanaka, Y., Nakata, T., Terada, S., Kikkawa, M., Noda, Y. and Hirokawa, N. (2003). Kinesin superfamily protein 2A (KIF2A) functions in suppression of collateral branch extension. *Cell* **114**, 229-39.

Houghton, J., Stoicov, C., Nomura, S., Rogers, A. B., Carlson, J., Li, H., Cai, X., Fox, J. G., Goldenring, J. R. and Wang, T. C. (2004). Gastric cancer originating from bone marrow-derived cells. *Science* **306**, 1568-71.

Hu-Tsai, M., Winter, J., Emson, P. C. and Woolf, C. J. (1994). Neurite outgrowth and GAP-43 mRNA expression in cultured adult rat dorsal root ganglion neurons: effects of NGF or prior peripheral axotomy. *J Neurosci Res* **39**, 634-45.

Huang, E. J. and Reichardt, L. F. (2001). Neurotrophins: roles in neuronal development and function. *Annu Rev Neurosci* **24**, 677-736.

Huang, E. J. and Reichardt, L. F. (2003). Trk receptors: roles in neuronal signal transduction. *Annu Rev Biochem* **72**, 609-42.

Huang, E. J., Zang, K., Schmidt, A., Saulys, A., Xiang, M. and Reichardt, L. F. (1999). POU domain factor Brn-3a controls the differentiation and survival of trigeminal neurons by regulating Trk receptor expression. *Development* **126**, 2869-82.

Ishikawa, H., Carrasco, D., Claudio, E., Ryseck, R. P. and Bravo, R. (1997). Gastric hyperplasia and increased proliferative responses of lymphocytes in mice lacking the COOH-terminal ankyrin domain of NF-kappaB2. *J Exp Med* **186**, 999-1014.

Jacks, T., Shih, T. S., Schmitt, E. M., Bronson, R. T., Bernards, A. and Weinberg, R. A. (1994). Tumour predisposition in mice heterozygous for a targeted mutation in Nf1. *Nat Genet* **7**, 353-61.

Jankowski, M. P., Cornuet, P. K., McIlwrath, S., Koerber, H. R. and Albers, K. M. (2006). SRY-box containing gene 11 (Sox11) transcription factor is required for neuron survival and neurite growth. *Neuroscience* **143**, 501-14.

Jenkins, B. J., Grail, D., Nheu, T., Najdovska, M., Wang, B., Waring, P., Inglese, M., McLoughlin, R. M., Jones, S. A., Topley, N. et al. (2005). Hyperactivation of Stat3 in gp130 mutant mice promotes gastric hyperproliferation and desensitizes TGF-beta signaling. *Nat Med* **11**, 845-52.

Jones, D. M., Tucker, B. A., Rahimtula, M. and Mearow, K. M. (2003). The synergistic effects of NGF and IGF-1 on neurite growth in adult sensory neurons: convergence on the PI 3-kinase signaling pathway. *J Neurochem* **86**, 1116-28.

Jones, K. R., Farinas, I., Backus, C. and Reichardt, L. F. (1994). Targeted disruption of the BDNF gene perturbs brain and sensory neuron development but not motor neuron development. *Cell* **76**, 989-99.

Judd, L. M., Alderman, B. M., Howlett, M., Shulkes, A., Dow, C., Moverley, J., Grail, D., Jenkins, B. J., Ernst, M. and Giraud, A. S. (2004). Gastric cancer development in mice lacking the SHP2 binding site on the IL-6 family co-receptor gp130. *Gastroenterology* **126**, 196-207.

Kaestner, K. H., Silberg, D. G., Traber, P. G. and Schutz, G. (1997). The mesenchymal winged helix transcription factor Fkh6 is required for the control of gastrointestinal proliferation and differentiation. *Genes Dev* **11**, 1583-95.

Kamachi, Y., Uchikawa, M. and Kondoh, H. (2000). Pairing SOX off: with partners in the regulation of embryonic development. *Trends Genet* **16**, 182-7.

Kim, B. G., Li, C., Qiao, W., Mamura, M., Kasprzak, B., Anver, M., Wolfraim, L., Hong, S., Mushinski, E., Potter, M. et al. (2006). Smad4 signalling in T cells is required for suppression of gastrointestinal cancer. *Nature* **441**, 1015-9.

Kim, J., Lo, L., Dormand, E. and Anderson, D. J. (2003). SOX10 maintains multipotency and inhibits neuronal differentiation of neural crest stem cells. *Neuron* **38**, 17-31.

Klein, R., Silos-Santiago, I., Smeyne, R. J., Lira, S. A., Brambilla, R., Bryant, S., Zhang, L., Snider, W. D. and Barbacid, M. (1994). Disruption of the neurotrophin-3 receptor gene trkC eliminates la muscle afferents and results in abnormal movements. *Nature* **368**, 249-51.

Klein, R., Smeyne, R. J., Wurst, W., Long, L. K., Auerbach, B. A., Joyner, A. L. and Barbacid, M. (1993). Targeted disruption of the trkB neurotrophin receptor gene results in nervous system lesions and neonatal death. *Cell* **75**, 113-22.

Klesse, L. J., Meyers, K. A., Marshall, C. J. and Parada, L. F. (1999). Nerve growth factor induces survival and differentiation through two distinct signaling cascades in PC12 cells. *Oncogene* **18**, 2055-68.

Klesse, L. J. and Parada, L. F. (1998). p21 ras and phosphatidylinositol-3 kinase are required for survival of wild-type and NF1 mutant sensory neurons. *J Neurosci* **18**, 10420-8.

Kramer, I., Sigrist, M., de Nooij, J. C., Taniuchi, I., Jessell, T. M. and Arber, S. (2006). A role for Runx transcription factor signaling in dorsal root ganglion sensory neuron diversification. *Neuron* **49**, 379-93.

Kuang, A. A., Diehl, G. E., Zhang, J. and Winoto, A. (2000). FADD is required for DR4- and DR5-mediated apoptosis: lack of trail-induced apoptosis in FADD-deficient mouse embryonic fibroblasts. *J Biol Chem* **275**, 25065-8.

Kuhlbrodt, K., Herbarth, B., Sock, E., Enderich, J., Hermans-Borgmeyer, I. and Wegner, M. (1998). Cooperative function of POU proteins and SOX proteins in glial cells. *J Biol Chem* **273**, 16050-7.

Kwon, C. H., Zhao, D., Chen, J., Alcantara, S., Li, Y., Burns, D. K., Mason, R. P., Lee, E. Y., Wu, H. and Parada, L. F. (2008). Pten haploinsufficiency accelerates formation of high-grade astrocytomas. *Cancer Res* **68**, 3286-94.

LaMotte, C. C. and Kapadia, S. E. (1993). Deafferentation-induced terminal field expansion of myelinated saphenous afferents in the adult rat dorsal horn and the nucleus gracilis following pronase injection of the sciatic nerve. *J Comp Neurol* **330**, 83-94.

Largaespada, D. A., Brannan, C. I., Jenkins, N. A. and Copeland, N. G. (1996). Nf1 deficiency causes Ras-mediated granulocyte/macrophage colony stimulating factor hypersensitivity and chronic myeloid leukaemia. *Nat Genet* **12**, 137-43.

Lawson, S. N., Perry, M. J., Prabhakar, E. and McCarthy, P. W. (1993). Primary sensory neurones: neurofilament, neuropeptides, and conduction velocity. *Brain Res Bull* **30**, 239-43.

Le, D. T., Kong, N., Zhu, Y., Lauchle, J. O., Aiyigari, A., Braun, B. S., Wang, E., Kogan, S. C., Le Beau, M. M., Parada, L. et al. (2004). Somatic inactivation of Nf1 in hematopoietic cells results in a progressive myeloproliferative disorder. *Blood* **103**, 4243-50.

Le, L. Q. and Parada, L. F. (2007). Tumor microenvironment and neurofibromatosis type I: connecting the GAPs. *Oncogene* **26**, 4609-16.

Lee, M. P., Ravenel, J. D., Hu, R. J., Lustig, L. R., Tomaselli, G., Berger, R. D., Brandenburg, S. A., Litzi, T. J., Bunton, T. E., Limb, C. et al. (2000). Targeted disruption of the Kvlqt1 gene causes deafness and gastric hyperplasia in mice. *J Clin Invest* **106**, 1447-55.

Leedham, S. J., Brittan, M., Preston, S. L., McDonald, S. A. and Wright, N. A. (2006). The stomach periglandular fibroblast sheath: all present and correct. *Gut* **55**, 295-6.

Lefebvre, O., Chenard, M. P., Masson, R., Linares, J., Dierich, A., LeMeur, M., Wendling, C., Tomasetto, C., Chambon, P. and Rio, M. C. (1996). Gastric mucosa abnormalities and tumorigenesis in mice lacking the pS2 trefoil protein. *Science* **274**, 259-62.

Lei, L., Laub, F., Lush, M., Romero, M., Zhou, J., Luikart, B., Klesse, L., Ramirez, F. and Parada, L. F. (2005). The zinc finger transcription factor Klf7 is required for TrkA gene expression and development of nociceptive sensory neurons. *Genes Dev* **19**, 1354-64.

Lei, L., Zhou, J., Lin, L. and Parada, L. F. (2006). Brn3a and Klf7 cooperate to control TrkA expression in sensory neurons. *Dev Biol* **300**, 758-69.

Lepore, J. J., Cheng, L., Min Lu, M., Mericko, P. A., Morrisey, E. E. and Parmacek, M. S. (2005). High-efficiency somatic mutagenesis in smooth muscle cells and cardiac myocytes in SM22alpha-Cre transgenic mice. *Genesis* **41**, 179-84.

Levanon, D., Bettoun, D., Harris-Cerruti, C., Woolf, E., Negreanu, V., Eilam, R., Bernstein, Y., Goldenberg, D., Xiao, C., Fliegauf, M. et al. (2002). The Runx3 transcription factor regulates development and survival of TrkC dorsal root ganglia neurons. *EMBO J* **21**, 3454-63.

Li, Q. L., Ito, K., Sakakura, C., Fukamachi, H., Inoue, K., Chi, X. Z., Lee, K. Y., Nomura, S., Lee, C. W., Han, S. B. et al. (2002). Causal relationship between the loss of RUNX3 expression and gastric cancer. *Cell* **109**, 113-24.

Li, S., Wang, Q., Chakladar, A., Bronson, R. T. and Bernards, A. (2000). Gastric hyperplasia in mice lacking the putative Cdc42 effector IQGAP1. *Mol Cell Biol* **20**, 697-701.

Li, Y., O'Connell, P., Breidenbach, H. H., Cawthon, R., Stevens, J., Xu, G., Neil, S., Robertson, M., White, R. and Viskochil, D. (1995). Genomic organization of the neurofibromatosis 1 gene (NF1). *Genomics* **25**, 9-18.

Liebl, D. J., Tessarollo, L., Palko, M. E. and Parada, L. F. (1997). Absence of sensory neurons before target innervation in brain-derived neurotrophic factor-, neurotrophin 3-, and TrkC-deficient embryonic mice. *J Neurosci* **17**, 9113-21.

Lin, J. H., Saito, T., Anderson, D. J., Lance-Jones, C., Jessell, T. M. and Arber, S. (1998). Functionally related motor neuron pool and muscle sensory afferent subtypes defined by coordinate ETS gene expression. *Cell* **95**, 393-407.

Liu, X., Shi, Y., Birnbaum, M. J., Ye, K., De Jong, R., Oltersdorf, T., Giranda, V. L. and Luo, Y. (2006). Quantitative analysis of anti-apoptotic function of Akt in Akt1 and Akt2 double knock-out mouse embryonic fibroblast cells under normal and stressed conditions. *J Biol Chem* **281**, 31380-8.

Lonze, B. E., Riccio, A., Cohen, S. and Ginty, D. D. (2002). Apoptosis, axonal growth defects, and degeneration of peripheral neurons in mice lacking CREB. *Neuron* **34**, 371-85.

Lu, P., Yang, H., Jones, L. L., Filbin, M. T. and Tuszynski, M. H. (2004). Combinatorial therapy with neurotrophins and cAMP promotes axonal regeneration beyond sites of spinal cord injury. *J Neurosci* **24**, 6402-9.

Lu, X., Kambe, F., Cao, X., Yoshida, T., Ohmori, S., Murakami, K., Kaji, T., Ishii, T., Zadworny, D. and Seo, H. (2006). DHCR24-knockout embryonic fibroblasts are susceptible to serum withdrawal-induced apoptosis because of dysfunction of caveolae and insulin-Akt-Bad signaling. *Endocrinology* **147**, 3123-32.

Lue, H., Thiele, M., Franz, J., Dahl, E., Speckgens, S., Leng, L., Fingerle-Rowson, G., Bucala, R., Luscher, B. and Bernhagen, J. (2007). Macrophage migration inhibitory factor (MIF) promotes cell survival by activation of the Akt pathway and role for CSN5/JAB1 in the control of autocrine MIF activity. *Oncogene* **26**, 5046-59.

Ma, L., Lei, L., Eng, S. R., Turner, E. and Parada, L. F. (2003). Brn3a regulation of TrkA/NGF receptor expression in developing sensory neurons. *Development* **130**, 3525-34.

Ma, Q., Chen, Z., del Barco Barrantes, I., de la Pompa, J. L. and Anderson, D. J. (1998). neurogenin1 is essential for the determination of neuronal precursors for proximal cranial sensory ganglia. *Neuron* **20**, 469-82.

Ma, Q., Fode, C., Guillemot, F. and Anderson, D. J. (1999). Neurogenin1 and neurogenin2 control two distinct waves of neurogenesis in developing dorsal root ganglia. *Genes Dev* **13**, 1717-28.

Macarthur, M., Hold, G. L. and El-Omar, E. M. (2004). Inflammation and Cancer II. Role of chronic inflammation and cytokine gene polymorphisms in the pathogenesis of gastrointestinal malignancy. *Am J Physiol Gastrointest Liver Physiol* **286**, G515-20.

Markus, A., Patel, T. D. and Snider, W. D. (2002a). Neurotrophic factors and axonal growth. *Curr Opin Neurobiol* **12**, 523-31.

Markus, A., Zhong, J. and Snider, W. D. (2002b). Raf and akt mediate distinct aspects of sensory axon growth. *Neuron* **35**, 65-76.

Marmigere, F. and Ernfors, P. (2007). Specification and connectivity of neuronal subtypes in the sensory lineage. *Nat Rev Neurosci* **8**, 114-27.

Maro, G. S., Vermeren, M., Voiculescu, O., Melton, L., Cohen, J., Charnay, P. and Topilko, P. (2004). Neural crest boundary cap cells constitute a source of neuronal and glial cells of the PNS. *Nat Neurosci* **7**, 930-8.

Martin, G. A., Viskochil, D., Bollag, G., McCabe, P. C., Crosier, W. J., Haubruck, H., Conroy, L., Clark, R., O'Connell, P., Cawthon, R. M. et al. (1990). The GAP-related domain of the neurofibromatosis type 1 gene product interacts with ras p21. *Cell* **63**, 843-9.

McDonald, J. W., Liu, X. Z., Qu, Y., Liu, S., Mickey, S. K., Turetsky, D., Gottlieb, D. I. and Choi, D. W. (1999). Transplanted embryonic stem cells survive, differentiate and promote recovery in injured rat spinal cord. *Nat Med* **5**, 1410-2.

McKerracher, L., David, S., Jackson, D. L., Kottis, V., Dunn, R. J. and Braun, P. E. (1994). Identification of myelin-associated glycoprotein as a major myelin-derived inhibitor of neurite growth. *Neuron* **13**, 805-11.

McMahon, S. B. and Kett-White, R. (1991). Sprouting of peripherally regenerating primary sensory neurones in the adult central nervous system. *J Comp Neurol* **304**, 307-15.

Meredith, A. and Johnson, J. E. (2000). Negative autoregulation of Mash1 expression in CNS development. *Dev Biol* **222**, 336-46.

Merkler, D., Metz, G. A., Raineteau, O., Dietz, V., Schwab, M. E. and Fouad, K. (2001). Locomotor recovery in spinal cord-injured rats treated with an antibody neutralizing the myelin-associated neurite growth inhibitor Nogo-A. *J Neurosci* **21**, 3665-73.

Molliver, D. C., Radeke, M. J., Feinstein, S. C. and Snider, W. D. (1995). Presence or absence of TrkA protein distinguishes subsets of small sensory neurons with unique cytochemical characteristics and dorsal horn projections. *J Comp Neurol* **361**, 404-16.

Molliver, D. C., Wright, D. E., Leitner, M. L., Parsadanian, A. S., Doster, K., Wen, D., Yan, Q. and Snider, W. D. (1997). IB4-binding DRG neurons switch from NGF to GDNF dependence in early postnatal life. *Neuron* **19**, 849-61.

Neumann, S. and Woolf, C. J. (1999). Regeneration of dorsal column fibers into and beyond the lesion site following adult spinal cord injury. *Neuron* **23**, 83-91.

Ng, C., Lam, K. Y., Gupta, T. S. and Ho, Y. H. (2004). Inflammatory fibroid polyp of the caecum in a patient with neurofibromatosis. *Ann Acad Med Singapore* **33**, 797-9.

Parada, L. F., Tsoulfas, P., Tessarollo, L., Blair, J., Reid, S. W. and Soppet, D. (1992). The Trk family of tyrosine kinases: receptors for NGF-related neurotrophins. *Cold Spring Harb Symp Quant Biol* **57**, 43-51.

Patel, T. D., Jackman, A., Rice, F. L., Kucera, J. and Snider, W. D. (2000). Development of sensory neurons in the absence of NGF/TrkA signaling in vivo. *Neuron* **25**, 345-57.

Patel, T. D., Kramer, I., Kucera, J., Niederkofler, V., Jessell, T. M., Arber, S. and Snider, W. D. (2003). Peripheral NT3 signaling is required for ETS protein expression and central patterning of proprioceptive sensory afferents. *Neuron* **38**, 403-16.

Pearse, D. D., Pereira, F. C., Marcillo, A. E., Bates, M. L., Berrocal, Y. A., Filbin, M. T. and Bunge, M. B. (2004). cAMP and Schwann cells promote axonal growth and functional recovery after spinal cord injury. *Nat Med* **10**, 610-6.

Pearson, A. G., Gray, C. W., Pearson, J. F., Greenwood, J. M., During, M. J. and Dragunow, M. (2003). ATF3 enhances c-Jun-mediated neurite sprouting. *Brain Res Mol Brain Res* **120**, 38-45.

Petersen, J. M. and Ferguson, D. R. (1984). Gastrointestinal neurofibromatosis. *J Clin Gastroenterol* **6**, 529-34.

Pevny, L. and Placzek, M. (2005). SOX genes and neural progenitor identity. *Curr Opin Neurobiol* **15**, 7-13.

Pindzola, R. R., Doller, C. and Silver, J. (1993). Putative inhibitory extracellular matrix molecules at the dorsal root entry zone of the spinal cord during development and after root and sciatic nerve lesions. *Dev Biol* **156**, 34-48.

Ramalho-Santos, M., Melton, D. A. and McMahon, A. P. (2000). Hedgehog signals regulate multiple aspects of gastrointestinal development. *Development* **127**, 2763-72.

Ramer, M. S., Priestley, J. V. and McMahon, S. B. (2000). Functional regeneration of sensory axons into the adult spinal cord. *Nature* **403**, 312-6.

Riccardi, V. M. (1981). Von Recklinghausen neurofibromatosis. *N Engl J Med* **305**, 1617-27.

Riccardi, V. M. (1999). In "Neurofibromatosis: Phenotype, Natural History, and Pathogenesis" (ed., pp. 1-25: Johns Hopkins Press, Baltimore.

Rico, B., Beggs, H. E., Schahin-Reed, D., Kimes, N., Schmidt, A. and Reichardt, L. F. (2004). Control of axonal branching and synapse formation by focal adhesion kinase. *Nat Neurosci* **7**, 1059-69.

Rivero-Melian, C., Rosario, C. and Grant, G. (1992). Demonstration of transganglionically transported choleragenoid in rat spinal cord by immunofluorescence cytochemistry. *Neurosci Lett* **145**, 114-7.

Romano, G., Prisco, M., Zanocco-Marani, T., Peruzzi, F., Valentinis, B. and Baserga, R. (1999). Dissociation between resistance to apoptosis and the transformed phenotype in IGF-I receptor signaling. *J Cell Biochem* **72**, 294-310.

Romero, M. I., Lin, L., Lush, M. E., Lei, L., Parada, L. F. and Zhu, Y. (2007). Deletion of Nf1 in neurons induces increased axon collateral branching after dorsal root injury. *J Neurosci* **27**, 2124-34.

Romero, M. I., Rangappa, N., Garry, M. G. and Smith, G. M. (2001). Functional regeneration of chronically injured sensory afferents into adult spinal cord after neurotrophin gene therapy. *J Neurosci* **21**, 8408-16.

Rutgeerts, P., Hendrickx, H., Geboes, K., Ponette, E., Broeckaert, L. and Vantrappen, G. (1981). Involvement of the upper digestive tract by systemic neurofibromatosis. *Gastrointest Endosc* **27**, 22-5.

Saitou, M., Furuse, M., Sasaki, H., Schulzke, J. D., Fromm, M., Takano, H., Noda, T. and Tsukita, S. (2000). Complex phenotype of mice lacking occludin, a component of tight junction strands. *Mol Biol Cell* **11**, 4131-42.

Sanapanich, K., Morrison, W. A. and Messina, A. (2002). Physiologic and morphologic aspects of nerve regeneration after end-to-end or end-to-side coaptation in a rat model of brachial plexus injury. *J Hand Surg [Am]* **27**, 133-42.

Scarff, K. L., Judd, L. M., Toh, B. H., Gleeson, P. A. and Van Driel, I. R. (1999). Gastric H(+),K(+)-adenosine triphosphatase beta subunit is required for normal function, development, and membrane structure of mouse parietal cells. *Gastroenterology* **117**, 605-18.

Schepers, G. E., Teasdale, R. D. and Koopman, P. (2002). Twenty pairs of sox: extent, homology, and nomenclature of the mouse and human sox transcription factor gene families. *Dev Cell* **3**, 167-70.

Schultheis, P. J., Clarke, L. L., Meneton, P., Harline, M., Boivin, G. P., Stemmermann, G., Duffy, J. J., Doetschman, T., Miller, M. L. and Shull, G. E. (1998). Targeted disruption of the murine Na+/H+ exchanger isoform 2 gene causes reduced viability of gastric parietal cells and loss of net acid secretion. *J Clin Invest* **101**, 1243-53.

Scott, S. (1992). Sensory Neurons: Diversity, Development, and Plasticity: Oxford University Press.

Serbedzija, G. N., Fraser, S. E. and Bronner-Fraser, M. (1990). Pathways of trunk neural crest cell migration in the mouse embryo as revealed by vital dye labelling. *Development* **108**, 605-12.

Sharp, R., Babyatsky, M. W., Takagi, H., Tagerud, S., Wang, T. C., Bockman, D. E., Brand, S. J. and Merlino, G. (1995). Transforming growth factor alpha disrupts the normal program of cellular differentiation in the gastric mucosa of transgenic mice. *Development* **121**, 149-61.

Sheu, J. Y., Kulhanek, D. J. and Eckenstein, F. P. (2000). Differential patterns of ERK and STAT3 phosphorylation after sciatic nerve transection in the rat. *Exp Neurol* **166**, 392-402.

Sims, T. J. and Gilmore, S. A. (1994). Regrowth of dorsal root axons into a radiation-induced glial-deficient environment in the spinal cord. *Brain Res* **634**, 113-26.

Smeyne, R. J., Klein, R., Schnapp, A., Long, L. K., Bryant, S., Lewin, A., Lira, S. A. and Barbacid, M. (1994). Severe sensory and sympathetic neuropathies in mice carrying a disrupted Trk/NGF receptor gene. *Nature* **368**, 246-9.

Sock, E., Rettig, S. D., Enderich, J., Bosl, M. R., Tamm, E. R. and Wegner, M. (2004). Gene targeting reveals a widespread role for the high-mobility-group transcription factor Sox11 in tissue remodeling. *Mol Cell Biol* **24**, 6635-44.

Soriano, P. (1999). Generalized lacZ expression with the ROSA26 Cre reporter strain. *Nat Genet* **21**, 70-1.

Spencer, T., Domeniconi, M., Cao, Z. and Filbin, M. T. (2003). New roles for old proteins in adult CNS axonal regeneration. *Curr Opin Neurobiol* **13**, 133-9.

Srinivas, S., Watanabe, T., Lin, C. S., William, C. M., Tanabe, Y., Jessell, T. M. and Costantini, F. (2001). Cre reporter strains produced by targeted insertion of EYFP and ECFP into the ROSA26 locus. *BMC Dev Biol* **1**, 4.

Stemple, D. L. and Anderson, D. J. (1992). Isolation of a stem cell for neurons and glia from the mammalian neural crest. *Cell* **71**, 973-85.

Sun, Y., Liang, X., Najafi, N., Cass, M., Lin, L., Cai, C. L., Chen, J. and Evans, S. M. (2007). Islet 1 is expressed in distinct cardiovascular lineages, including pacemaker and coronary vascular cells. *Dev Biol* **304**, 286-96.

Takami, T., Oudega, M., Bates, M. L., Wood, P. M., Kleitman, N. and Bunge, M. B. (2002). Schwann cell but not olfactory ensheathing glia transplants improve hindlimb locomotor performance in the moderately contused adult rat thoracic spinal cord. *J Neurosci* **22**, 6670-81.

Tanabe, K., Bonilla, I., Winkles, J. A. and Strittmatter, S. M. (2003). Fibroblast growth factor-inducible-14 is induced in axotomized neurons and promotes neurite outgrowth. *J Neurosci* **23**, 9675-86.

Tanaka, S., Kamachi, Y., Tanouchi, A., Hamada, H., Jing, N. and Kondoh, H. (2004). Interplay of SOX and POU factors in regulation of the Nestin gene in neural primordial cells. *Mol Cell Biol* **24**, 8834-46.

Tebbutt, N. C., Giraud, A. S., Inglese, M., Jenkins, B., Waring, P., Clay, F. J., Malki, S., Alderman, B. M., Grail, D., Hollande, F. et al. (2002). Reciprocal regulation of gastrointestinal homeostasis by SHP2 and STAT-mediated trefoil gene activation in gp130 mutant mice. *Nat Med* **8**, 1089-97.

Teng, Y. D., Lavik, E. B., Qu, X., Park, K. I., Ourednik, J., Zurakowski, D., Langer, R. and Snyder, E. Y. (2002). Functional recovery following traumatic spinal cord injury mediated by a unique polymer scaffold seeded with neural stem cells. *Proc Natl Acad Sci U S A* **99**, 3024-9.

Tessarollo, L., Vogel, K. S., Palko, M. E., Reid, S. W. and Parada, L. F. (1994). Targeted mutation in the neurotrophin-3 gene results in loss of muscle sensory neurons. *Proc Natl Acad Sci U S A* **91**, 11844-8.

The, I., Hannigan, G. E., Cowley, G. S., Reginald, S., Zhong, Y., Gusella, J. F., Hariharan, I. K. and Bernards, A. (1997). Rescue of a Drosophila NF1 mutant phenotype by protein kinase A. *Science* **276**, 791-4.

Traub, R. J., Allen, B., Humphrey, E. and Ruda, M. A. (1990). Analysis of calcitonin gene-related peptide-like immunoreactivity in the cat dorsal spinal cord and dorsal root ganglia provide evidence for a multisegmental projection of nociceptive C-fiber primary afferents. *J Comp Neurol* **302**, 562-74.

Trieu, M., Ma, A., Eng, S. R., Fedtsova, N. and Turner, E. E. (2003). Direct autoregulation and gene dosage compensation by POU-domain transcription factor Brn3a. *Development* **130**, 111-21.

Trieu, M., Rhee, J. M., Fedtsova, N. and Turner, E. E. (1999). Autoregulatory sequences are revealed by complex stability screening of the mouse brn-3.0 locus. *J Neurosci* **19**, 6549-58.

Uflacker, R., Alves, M. A. and Diehl, J. C. (1985). Gastrointestinal involvement in neurofibromatosis: angiographic presentation. *Gastrointest Radiol* **10**, 163-5.

Ushijima, T. and Sasako, M. (2004). Focus on gastric cancer. *Cancer Cell* **5**, 121-5.

Vogel, K. S., Brannan, C. I., Jenkins, N. A., Copeland, N. G. and Parada, L. F. (1995). Loss of neurofibromin results in neurotrophin-independent survival of embryonic sensory and sympathetic neurons. *Cell* **82**, 733-42.

Vogel, K. S., El-Afandi, M. and Parada, L. F. (2000). Neurofibromin negatively regulates neurotrophin signaling through p21ras in embryonic sensory neurons. *Mol Cell Neurosci* **15**, 398-407.

Vogelbaum, M. A., Tong, J. X. and Rich, K. M. (1998). Developmental regulation of apoptosis in dorsal root ganglion neurons. *J Neurosci* **18**, 8928-35.

Waite, P. (1995). Trigeminal Sensory system. In The Rat Nervous System. San Diego, CA: Academic Press.

Wallace, M. R., Marchuk, D. A., Andersen, L. B., Letcher, R., Odeh, H. M., Saulino, A. M., Fountain, J. W., Brereton, A., Nicholson, J., Mitchell, A. L. et al. (1990). Type 1 neurofibromatosis gene: identification of a large transcript disrupted in three NF1 patients. *Science* **249**, 181-6.

Wang, K. C., Koprivica, V., Kim, J. A., Sivasankaran, R., Guo, Y., Neve, R. L. and He, Z. (2002). Oligodendrocyte-myelin glycoprotein is a Nogo receptor ligand that inhibits neurite outgrowth. *Nature* **417**, 941-4.

Wang, T. C., Dangler, C. A., Chen, D., Goldenring, J. R., Koh, T., Raychowdhury, R., Coffey, R. J., Ito, S., Varro, A., Dockray, G. J. et al. (2000). Synergistic interaction between hypergastrinemia and Helicobacter infection in a mouse model of gastric cancer. *Gastroenterology* **118**, 36-47.

Wegner, M. and Stolt, C. C. (2005). From stem cells to neurons and glia: a Soxist's view of neural development. *Trends Neurosci* **28**, 583-8.

White, F. A., Keller-Peck, C. R., Knudson, C. M., Korsmeyer, S. J. and Snider, W. D. (1998). Widespread elimination of naturally occurring neuronal death in Bax-deficient mice. *J Neurosci* **18**, 1428-39.

White, F. A., Silos-Santiago, I., Molliver, D. C., Nishimura, M., Phillips, H., Barbacid, M. and Snider, W. D. (1996). Synchronous onset of NGF and TrkA survival dependence in developing dorsal root ganglia. *J Neurosci* **16**, 4662-72.

Xu, G. F., Lin, B., Tanaka, K., Dunn, D., Wood, D., Gesteland, R., White, R., Weiss, R. and Tamanoi, F. (1990a). The catalytic domain of the neurofibromatosis type 1 gene product stimulates ras GTPase and complements ira mutants of S. cerevisiae. *Cell* **63**, 835-41.

Xu, G. F., O'Connell, P., Viskochil, D., Cawthon, R., Robertson, M., Culver, M., Dunn, D., Stevens, J., Gesteland, R., White, R. et al. (1990b). The neurofibromatosis type 1 gene encodes a protein related to GAP. *Cell* **62**, 599-608.

Xu, J., Ismat, F. A., Wang, T., Yang, J. and Epstein, J. A. (2007). NF1 regulates a Ras-dependent vascular smooth muscle proliferative injury response. *Circulation* **116**, 2148-56.

Xu, X., Brodie, S. G., Yang, X., Im, Y. H., Parks, W. T., Chen, L., Zhou, Y. X., Weinstein, M., Kim, S. J. and Deng, C. X. (2000). Haploid loss of the tumor suppressor Smad4/Dpc4 initiates gastric polyposis and cancer in mice. *Oncogene* **19**, 1868-74.

Yang, F. C., Chen, S., Clegg, T., Li, X., Morgan, T., Estwick, S. A., Yuan, J., Khalaf, W., Burgin, S., Travers, J. et al. (2006). Nf1+/- mast cells induce neurofibroma like phenotypes through secreted TGF-beta signaling. *Hum Mol Genet* **15**, 2421-37.

Yang, F. C., Ingram, D. A., Chen, S., Hingtgen, C. M., Ratner, N., Monk, K. R., Clegg, T., White, H., Mead, L., Wenning, M. J. et al. (2003). Neurofibromin-deficient Schwann cells secrete a potent migratory stimulus for Nf1+/- mast cells. *J Clin Invest* **112**, 1851-61.

Yiu, G. and He, Z. (2006). Glial inhibition of CNS axon regeneration. *Nat Rev Neurosci* **7**, 617-27.

Zavros, Y., Eaton, K. A., Kang, W., Rathinavelu, S., Katukuri, V., Kao, J. Y., Samuelson, L. C. and Merchant, J. L. (2005). Chronic gastritis in the hypochlorhydric gastrin-deficient mouse progresses to adenocarcinoma. *Oncogene* **24**, 2354-66.

Zhong, J., Li, X., McNamee, C., Chen, A. P., Baccarini, M. and Snider, W. D. (2007). Raf kinase signaling functions in sensory neuron differentiation and axon growth in vivo. *Nat Neurosci* **10**, 598-607.

Zhou, F. Q., Zhou, J., Dedhar, S., Wu, Y. H. and Snider, W. D. (2004). NGF-induced axon growth is mediated by localized inactivation of GSK-3beta and functions of the microtubule plus end binding protein APC. *Neuron* **42**, 897-912.

Zhou, L., Nepote, V., Rowley, D. L., Levacher, B., Zvara, A., Santha, M., Mi, Q. S., Simonneau, M. and Donovan, D. M. (2002). Murine peripherin gene sequences direct Cre recombinase expression to peripheral neurons in transgenic mice. *FEBS Lett* **523**, 68-72.

Zhu, Y. and Parada, L. F. (2001a). Neurofibromin, a tumor suppressor in the nervous system. *Exp Cell Res* **264**, 19-28.

Zhu, Y. and Parada, L. F. (2001b). A particular GAP in mind. *Nat Genet* **27**, 354-5.

Zhu, Y., Richardson, J. A., Parada, L. F. and Graff, J. M. (1998). Smad3 mutant mice develop metastatic colorectal cancer. *Cell* **94**, 703-14.

Zhu, Y., Romero, M. I., Ghosh, P., Ye, Z., Charnay, P., Rushing, E. J., Marth, J. D. and Parada, L. F. (2001). Ablation of NF1 function in neurons induces abnormal development of cerebral cortex and reactive gliosis in the brain. *Genes Dev* **15**, 859-76.

Zong, W. X., Lindsten, T., Ross, A. J., MacGregor, G. R. and Thompson, C. B. (2001). BH3-only proteins that bind pro-survival Bcl-2 family members fail to induce apoptosis in the absence of Bax and Bak. *Genes Dev* **15**, 1481-6.